

## CHAPTER FOUR

### RESULTS AND DISCUSSION - LARVICIDAL PRINCIPLES

#### 4.1 Isolation of larvicidal principles from the stem bark of the various species studied

Table 4.1 below summarises the larvicidal principles present in the stem bark of the various species studied.

**Table 4. 1: Larvicidal principles present in the stem bark of various plant species studied**

Natural products	Plant species studied													
	1	2	3	4	5	6	7	8	9	10	11	12	13	14
(+)-Goniothalamine	√	√	√	√			√	√	√		√	√		
(+)-Goniothalamine epoxide	√	√					√	√	√		√		√	√
(+)-Goniodiol	√	√										√		
(+)-Goniodiol diacetate									√		√	√		√
(-)-Naringenin		√									√	√		√
(-)-Pinocembrin		√						√	√		√	√		
(-)-Iso-5-deoxygoniopypyrone	√	√										√	√	
(+)-5β-Hydroxygoniothalamine		√												
(+)-Annonacin		√	√	√	√					√				
(+)-Goniothalamine		√	√	√	√									
Aristolactam BII			√	√	√					√				
Ouregidione			√	√						√				
Liriodenine						√								
(+)-Goniothalenol	√		√	√						√				
Disepalin						√								
Sesquiterpene mixtures	√	√		√			√	√		√			√	√

Legend: (√) denotes the presence of the natural product. Plant species studied include: 1 = *Goniothalamus andersonii*, 2 = *G. dolichocarpus*, 3 = *G. malayanus*, 4 = *G. velutinus*, 5 = *Mezzetia umbellata*, 6 = *Disepalum anomalum*, 7 = *G. ridleyi*, 8 = *G. macrophyllus*, 9 = *G. uvarioides*, 10 = *G. macranii*, 11 = *G. sinclairianus*, 12 = *G. gigantifolius*, 13 = *G. umbrosus*, 14 = *G. montanus*.

## 4.2 Isolation of larvicidal principles from the stem bark of various insecticidal plants from the Annonaceae family

Table 4.1 shows the various larvicidal principles present in twelve *Goniothalamus* species, one *Disepalum* and one *Mezzetia* species. Six species (*Goniothalamus andersonii*, *G. dolichocarpus*, *G. malayanus*, *G. velutinus*, *Mezzetia umbellata* and *Disepalum anomalum*) were studied in detail whereas the other eight species (*G. ridleyi*, *G. macrophyllus*, *G. uvarioides*, *G. macranii*, *G. sinclairinius*, *G. gigantifolius*, *G. umbrosus* and *G. montanus*) were screened for their various bioactive principles by means of thin layer chromatography and gas chromatography.

### 4.2.1 *Goniothalamus andersonii*

The hexane extract of the stem bark of *G. andersonii* after vacuum evaporation in a rotary evaporator to remove solvent was redissolved in ethanol and cooled to provide crude (+)-goniothalamine crystals. The crude (+)-goniothalamine was recrystallised in ethanol to give colourless crystals. The mother liquor when subjected to SiO<sub>2</sub> column chromatography (Merck, Kieselgel 60) gave a complex inseparable mixture of essential oils of very high R<sub>f</sub> (0.78, 5% ethyl acetate/hexane) value. The mixture after partial separation by gas chromatography (OV-17) was further analysed by gas chromatography-mass spectrometry (OV-17). The presence of a complex mixture of sesquiterpenes was noted but not investigated in detail.

The ethyl acetate extract of the same plant material when subjected to column chromatography gave (+)-goniothalamine, (+)-goniothalamine epoxide, (+)-goniodiol and (-)-iso-5-deoxygonioppyrone. The ethanol extract gave a minor amount of (+)-goniothalenol.



#### 4.2.2 *Goniiothalamus dolichocarpus*

The hexane extract of the stem bark of *Goniiothalamus dolichocarpus* was similarly treated as for *G. andersonii* and was found to contain goniiothalamine which could be crystallised out. Again, the mother liquor showed a complex mixture of essential oils of very high  $R_f$  value (0.79, 5% ethyl acetate/hexane), when subjected to  $SiO_2$  column chromatography (Merck, Kieselgel 60). This mixture was also subjected to partial separation by gas chromatography (OV-17) and then analysed by gas chromatography-mass spectrometry (OV-17 column). GC-MS indicated the presence of a complex mixture of sesquiterpenes.

The ethyl acetate extract of this same bark when separated by  $SiO_2$  column chromatography gave (+)-goniiothalamine, (-)-pinocembrin, (-)-naringenin, (+)-5 $\beta$ -hydroxygoniiothalamine, (+)-goniiothalamine epoxide, (-)-iso-5-deoxygoniopyrone and (+)-goniodiol.

The ethanol extract of the same bark after being subjected to a partitioning between (i)  $CHCl_3$  and water (ii) 90% aqueous methanol and hexane gave the annonaceous acetogenin annonacin and a very minor amount (not isolated) of an acetogenin containing twenty-eight mass unit more than annonacin.

#### 4.2.3 *Goniiothalamus malayanus*

The ethanol extract of the stem bark of *Goniiothalamus malayanus* after being subjected to the usual partitioning process, and separation by column chromatography (Merck, Kieselgel 60) gave (+)-annonacin, (+)-goniiothalamine (not separated from annonacin), (+)-goniiothalenol, ouregidione, (+)-goniiothalamine and aristolactam BII. No sesquiterpenes were detected in the hexane soluble extract of *G. malayanus*.

#### 4.2.4 *Goniiothalamus velutinus*

The hexane extract of the stem bark of *Goniiothalamus velutinus* gave a complex mixture of essential oils which are mainly sesquiterpenes as analysed by GC-MS.

The ethanol extract after the two-step partitioning process gave the methanol soluble fraction which contained (+)-goniothalamine, (+)-goniothalenol, aristolactam BII, ouregidione, (+)-annonacin and a very minor amount of another acetogenin of molecular weight 596, probably goniiothalamine (HPLC). The acetogenins were purified by high performance liquid chromatography (HPLC) using a reverse phase column and 90:10 methanol:water as the mobile phase.

#### 4.2.5 *Mezzettia umbellata*

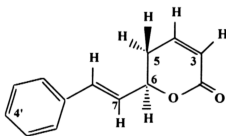
The ethanol extract of the stem bark of *Mezzettia umbellata* was partitioned in the usual manner to provide the methanol soluble fraction. Thin layer chromatography (TLC) indicated the presence of a few compounds as shown by the number of spots on the silica gel plate. Aristolactam BII was detected, together with the polar acetogenins (+)-annonacin and (+)-goniothalamine (not separated from annonacin). Column chromatography and multiple preparative layer chromatography (PLC) gave a very bioactive fraction which contains (+)-annonacin.

#### 4.2.6 *Disepalum anomalum*

The ethanol extract of the stem bark of *Disepalum anomalum* was also partitioned in the usual manner and provided the methanol soluble fraction. Again, thin layer chromatography indicated that only a few compounds were present. However, after column chromatography, one major and a minor compound were obtained. Multiple preparative layer chromatography furnished the minor alkaloid

liriodenine. Fractions 18-22 gave the crude acetogenin which could not be purified by preparative layer chromatography. HPLC using a normal phase column and mobile phase of 1% methanol: 99% chloroform was able to give the pure acetogenin. This acetogenin is a new compound containing a mono-THF ring with an adjacent acetate group and a total of thirty nine carbons. The pure compound was silylated by reacting a small amount (3 mg) of the pure acetogenin with BSTFA at 80 °C in a sealed ampoule over 24 hours. The crude acetogenin was acetylated using acetic anhydride and pyridine overnight at room temperature. The acetate derivative was purified using HPLC (normal phase column, chloroform as the mobile phase).

#### 4.2.7 Characterisation of GA-1 as goniotalamin



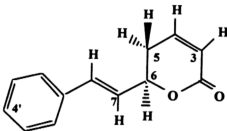
(+)-Goniotalamin

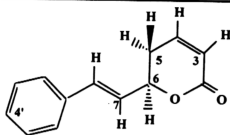
Figure 4. 1: Structure of (+)-goniotalamin

Goniotalamin was recrystallised from ethanol as colourless crystals with a melting point of 83-84 °C (Lit. 85 °C) (Jewers *et al.*, 1972) and  $[\alpha]_D^{20} = 193.2$  (c 1.0, CHCl<sub>3</sub>) (Lit. +170.3) (Jewers *et al.*, 1972). Mass spectral data showed a molecular ion at  $m/z$  200 expected for C<sub>13</sub>H<sub>12</sub>O<sub>2</sub>. Strong IR absorptions were observed at 1721 cm<sup>-1</sup> (C = O of the pyrone ring), 1249 cm<sup>-1</sup> (also for the 2-pyrone ring), 1495 cm<sup>-1</sup> and

spectra include 2-D experiments such as  $^1\text{H}$ - $^1\text{H}$  COSY and  $^1\text{H}$ - $^{13}\text{C}$  HETCOR. The  $^1\text{H}$  NMR (270 MHz,  $\text{CDCl}_3$ ) gave a doublet at  $\delta$  6.73 ( $J$  15.6 Hz) and a doublet of doublet at  $\delta$  6.28 ( $J$  15.6 Hz, 6.3 Hz). These were assigned to H-8 and H-7 of the styryl group respectively. The large coupling constant value of 15.6 Hz between H-7 and H-8 indicates the two protons to be *trans*. A ddd at  $\delta$  6.92 ( $J$  9.8 Hz, 4.2 Hz and 1.5 Hz) and a dt at  $\delta$  6.08 ( $J$  9.8 Hz, 1.9 Hz) were assigned to the H-4 and H-3 of the olefinic group in the  $\alpha,\beta$ -unsaturated  $\delta$ -lactone moiety. The two proton multiplet at  $\delta$  2.55 and the ddd at  $\delta$  5.11 were assigned to H-5 and H-6 respectively. Another multiplet at  $\delta$  7.35 was assigned to the protons of the phenyl ring. The  $^{13}\text{C}$  NMR (67.8 MHz,  $\text{CDCl}_3$ ) indicated a total of thirteen carbons. Electron-impact mass spectrometry gave an  $M^+$  of 200 (61%) and a base peak of 104 which results from fragmentation at the C-6-C-7 bond. Other fragments are as shown in Figure 4.7. The  $^{13}\text{C}$  NMR were assigned by DEPT and HETCOR ( $^1\text{H}$ - $^{13}\text{C}$ ). The  $^1\text{H}$  and  $^{13}\text{C}$  NMR assignments are shown in Tables 4.2 and 4.5; their connectivities in Table 4.3 for  $^1\text{H}$ - $^1\text{H}$  and Table 4.4 for  $^1\text{H}$ - $^{13}\text{C}$  (also see Figures 4.2-4.5).

**Table 4. 2:**  $^1\text{H}$  NMR ( $\delta$ ) assignments and  $J(\text{Hz})$  values for goniotalamin (270 MHz,  $\text{CDCl}_3$ )

Proton	$\delta$	$J$ (Hz)	 <p>(+)-Goniotalamin</p>
H-3	6.08, dt	9.8, 1.9	
H-4	6.92, ddd	9.8, 4.2, 1.5	
H-5a	2.55, m	-	
H-5b	2.55, m	-	
H-6	5.11, ddd	6.3, 8.0, 2.9	
H-7	6.28 dd	15.6, 6.3	
H-8	6.73 d	15.6	
Ph	7.35, m	-	



(+)-Goniothalamine

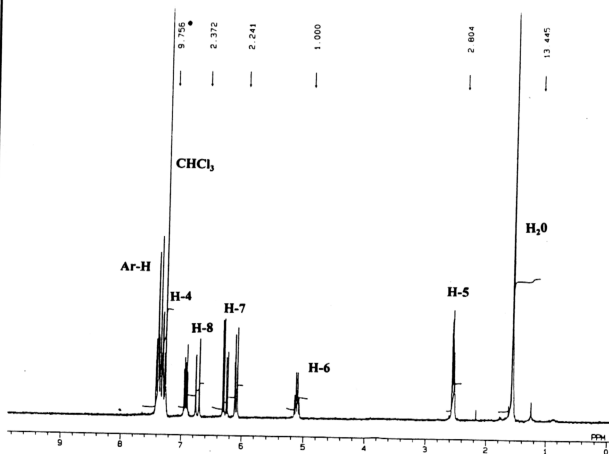
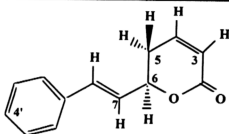


Figure 4. 2:  $^1\text{H}$  NMR spectrum of (+)-goniothalamine (270 MHz,  $\text{CDCl}_3$ )



(+)-Goniothalamine

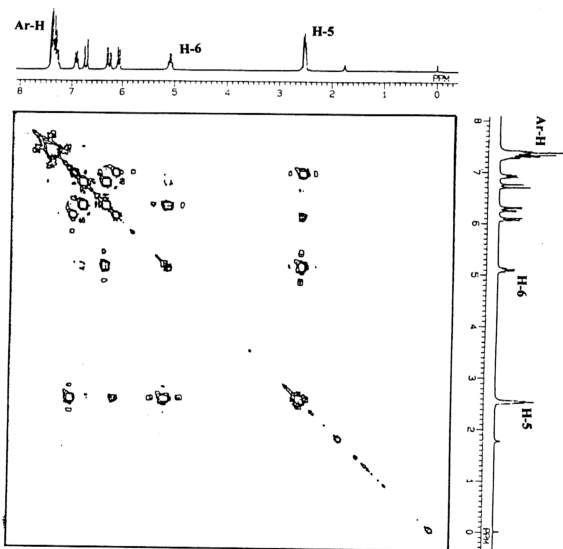
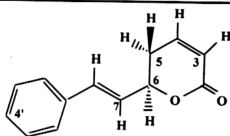


Figure 4. 3:  $^1\text{H}$  -  $^1\text{H}$  COSY spectrum of (+)-goniothalamine



(+)-Goniothalamine

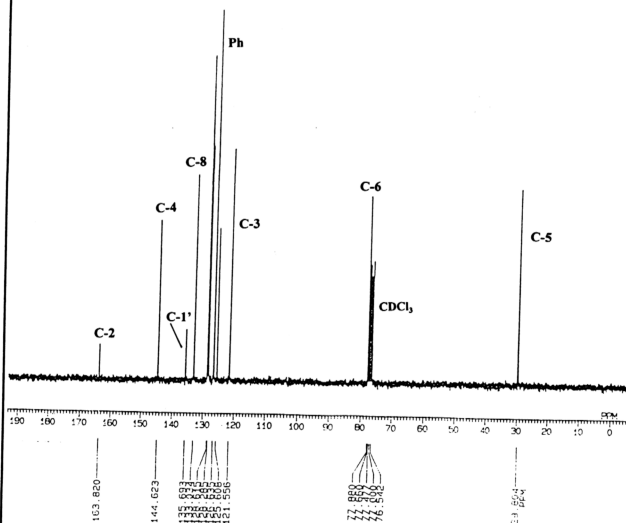
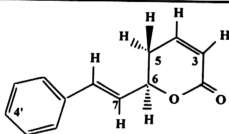


Figure 4. 4:  $^{13}\text{C}$  NMR spectrum of (+)-goniothalamine (67.8 MHz,  $\text{CDCl}_3$ )



(+)-Goniothalamine

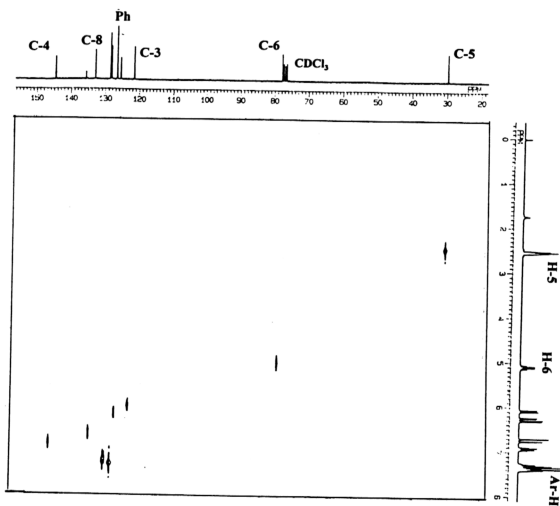


Figure 4. 5:  $^1\text{H}$  -  $^{13}\text{C}$  HETCOR spectrum of (+)-goniothalamine



**Table 4. 3: Proton-proton connectivities obtained from  $^1\text{H}$ - $^1\text{H}$  COSY experiment for (+)-goniothalamine (270 MHz and 67.8 MHz)**

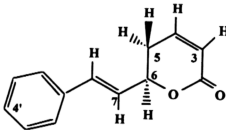
Proton resonance	Connectivity
6.08 (H-3)	6.92 (H-4), 2.55 (LR) (H-5)
6.92 (H-4)	2.55 (H-5), 6.08 (H-3)
2.55 (H-5)	6.92 (H-4), 5.11 (H-6), 6.08 (LR) (H-3)
5.11 (H-6)	2.55 (H-5), 6.28 (H-7)
6.28 (H-7)	5.11 (H-6), 6.73 (H-8)
6.73 (H-8)	6.28 (H-7)

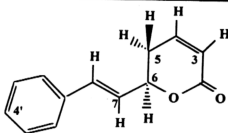
LR refers to long range coupling

**Table 4. 4: Proton and carbon connectivities obtained from  $^1\text{H}$ - $^{13}\text{C}$  HETCOR experiment for (+)-goniothalamine (270 MHz and 67.8 MHz)**

Proton resonance	Connectivity
6.08 (H-3)	120.1
6.92 (H-4)	144.6
2.55 (H-5)	28.7
5.11 (H-6)	77.0
6.28 (H-7)	125.0
6.73 (H-8)	131.9

**Table 4. 5:  $^{13}\text{C}$  NMR ( $\delta$ ) assignments for goniothalamine (67.8 MHz,  $\text{CDCl}_3$ )**

Carbon	$\delta$	 <p>(+)-Goniothalamine</p>
C-2	163.0	
C-3	120.1	
C-4	144.6	
C-5	28.7	
C-6	77.0	
C-7	125.0	
C-8	131.9	
C-1'	134.9	
C-2', C-6'	125.8	
C-3', C-5'	127.8	
C-4	127.4	



(+)-Goniothalamine

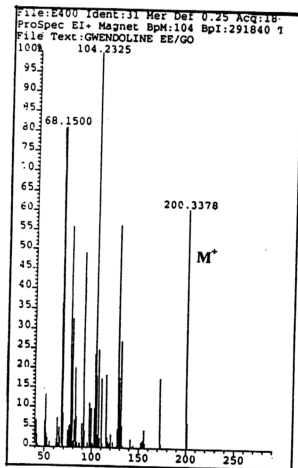


Figure 4. 6: EIMS spectrum of (+)-goniothalamine

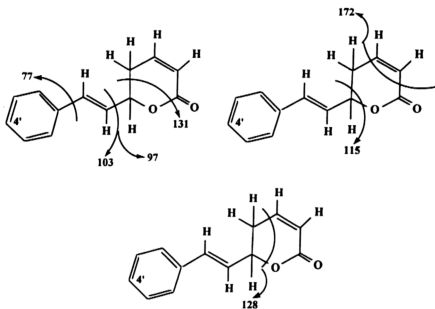
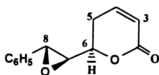


Figure 4. 7: EIMS fragmentation of (+)-goniothalamin

#### 4.2.8 Characterisation of GA-2 as (+)-goniothalamin epoxide



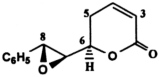
(+)-Goniothalamine epoxide

Figure 4. 8: Structure of (+)-goniothalamine epoxide

Goniothalamine epoxide was isolated as plates of melting point 88-89 °C (Lit. 90-94 °C) (Sam *et al.*, 1987) and  $[\alpha]_D^{20} = +120.5$  (c 1.0, CHCl<sub>3</sub>) (Lit. +100.7) (Sam *et al.*, 1987). EIMS gave an  $M^+$  of 216 indicating a molecular formula C<sub>13</sub>H<sub>12</sub>O<sub>3</sub>. The IR spectrum showed the loss of the styryl band at 1495 and 970 cm<sup>-1</sup>. The 2-pyrone bands show up as in goniothalamine at 1727 cm<sup>-1</sup> for C = O and 1248 cm<sup>-1</sup>. <sup>1</sup>H NMR values were assigned using <sup>1</sup>H-<sup>1</sup>H COSY (see Table 4.7 and Figure 4.10). Also the <sup>1</sup>H NMR spectrum indicated the loss of the H-7 dd at  $\delta$  6.28 and the H-8 doublet at  $\delta$

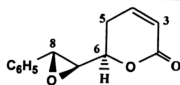
6.73. This implied the disappearance of the H-7 and H-8 styryl double bond. Instead, the H-7 signal showed up as a dd at  $\delta$  3.20 with coupling constant values of 2.0 Hz and 5.4 Hz; the H-8 signal appeared as a doublet at  $\delta$  3.82 with a  $J$  value of 2.0. H-5 appeared as a multiplet at  $\delta$  2.55 while H-6 showed up as a dt at  $\delta$  4.37 due to coupling with H-5 and H-7 respectively. H-3 and H-4 signals were unchanged when compared with that of goniothalamine. H-3 showed up as a dd at  $\delta$  5.99 with coupling constant values of 1.5 Hz and 9.8 Hz for long range coupling with one H-5 and coupling with H-4, respectively. H-4 appeared at  $\delta$  6.86 as a ddd with coupling constant values of 1.5 Hz and 4.9 Hz for coupling between H-5a and H-5b and 9.8 Hz with H-3 (see Table 4.6 and Figure 4.9).  $^{13}\text{C}$  NMR assignments are shown in Table 4.9 (see also Figure 4.15).

**Table 4. 6:  $^1\text{H}$  NMR ( $\delta$ ) assignments and coupling constant values (Hz) for goniothalamine epoxide**

Proton	$\delta$	$J(\text{Hz})$	 <p>(+)-Goniothalamine epoxide</p>
H-3	5.99, dd	1.5, 9.8	
H-4	6.86, ddd	1.5, 4.9, 9.8	
H-5	2.55, m		
H-6	4.37 dt	8.8, 5.4	
H-7	3.20 dd	2.0, 5.4	
H-8	3.82 d	2.0	
Ph	7.23, m	-	

**Table 4. 7:  $^1\text{H}$  -  $^1\text{H}$  connectivities ( $^1\text{H}$  -  $^1\text{H}$  COSY) for goniothalamine epoxide**

Proton resonance	Connectivity
5.99 (H-3)	6.86 (H-4), 2.55 (LR) (H-5)
6.86 (H-4)	2.55 (H-5), 5.99 (H-3)
2.55 (H-5)	6.86 (H-4), 4.37 (H-6), 5.99 (LR) (H-3)
4.37 (H-6)	2.55 (H-5), 3.20 (H-7)
3.20 (H-7)	4.37 (H-6), 3.82 (H-8)
3.82 (H-8)	3.20 (H-7)



(+)-Goniothalamine epoxide

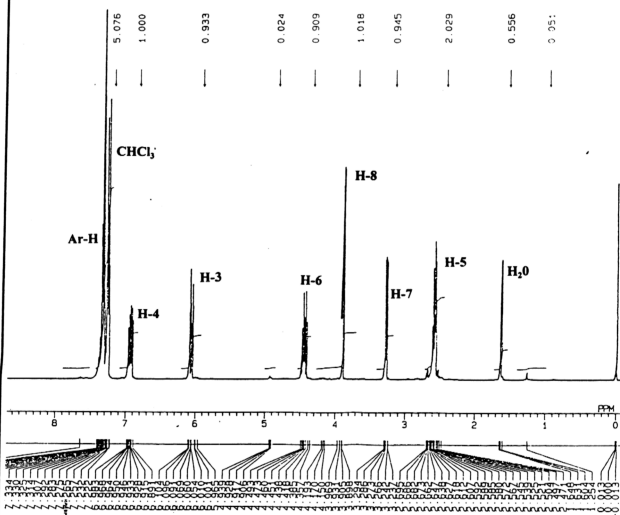
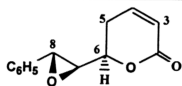


Figure 4. 9: <sup>1</sup>H NMR spectrum of (+)-goniothalamine epoxide (270 MHz, CDCl<sub>3</sub>)



(+)-Goniothalamine epoxide

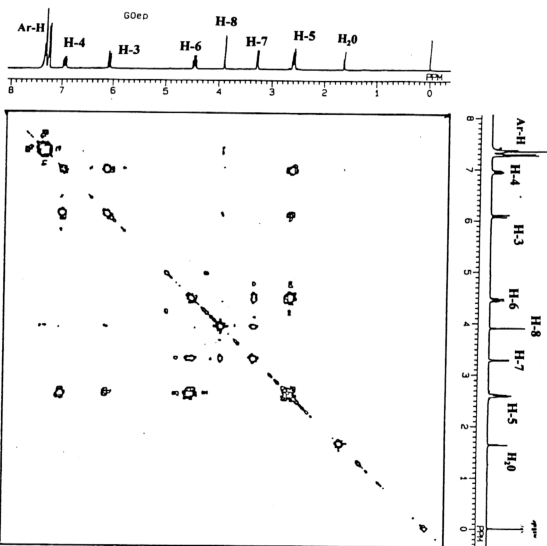
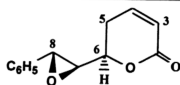


Figure 4. 10:  $^1\text{H} - ^1\text{H}$  COSY spectrum of (+)-goniothalamine epoxide



(+)-Goniothalamin epoxide

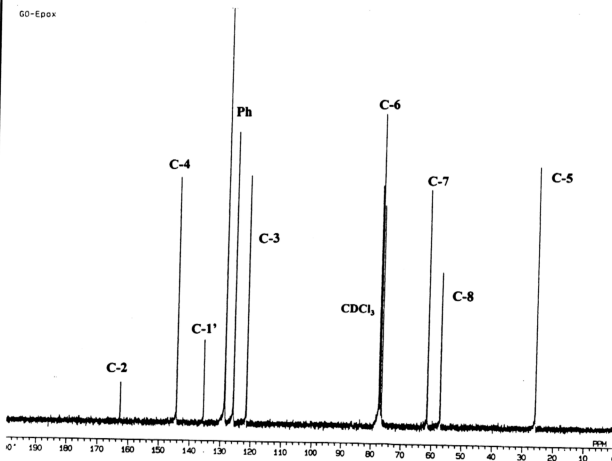
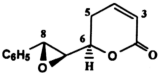


Figure 4. 11: <sup>13</sup>C NMR spectrum of (+)-goniothalamin epoxide

**Table 4. 8:**  $^1\text{H}$  -  $^{13}\text{C}$  connectivities obtained from  $^1\text{H}$  -  $^{13}\text{C}$  HETCOR experiment for goniiothalamine epoxide.

Proton resonance	Connectivity
5.99 (H-3)	121.4
6.86 (H-4)	144.3
2.55 (H-5)	25.8
4.37 (H-6)	77.0
3.20 (H-7)	61.4
3.82 (H-8)	57.1

**Table 4. 9:**  $^{13}\text{C}$  NMR ( $\delta$ ) assignments for goniiothalamine epoxide

Carbon	$\delta$	 <p>(+)-Goniiothalamine epoxide</p>
C-2	162.7	
C-3	121.4	
C-4	144.3	
C-5	25.8	
C-6	77.0	
C-7	61.4	
C-8	57.1	
C-1'	135.6	
C-2', C-6'	125.6	
C-3', C-5'	128.6	
C-4'	128.5	

#### 4.2.9 Characterisation of (+)-isogoniiothalamine epoxide

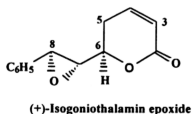


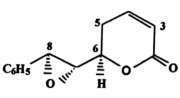
**Figure 4. 12:** Structure of (+)-isogoniiothalamine epoxide

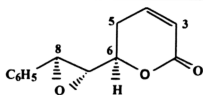
Synthetic isogoniiothalamine epoxide was crystallised as needles of melting point 108-110  $^{\circ}\text{C}$  and  $[\alpha]_{\text{D}}^{20} = +110$  (c, 1.0,  $\text{CHCl}_3$ ). EIMS gave an  $\text{M}^{+}$  of 216



indicating a molecular formula  $C_{13}H_{12}O_3$ . The IR spectrum is similar to that of goniothalamine epoxide. The  $^1H$  NMR (270 MHz,  $CDCl_3$ ) was almost similar to that for GA-2 (goniothalamine epoxide). H-7 appeared at  $\delta$  3.24 as a dd with coupling constant values of 2.0 and 4.0 Hz for coupling with H-8 and H-6, respectively. H-8 appeared at  $\delta$  4.07 as a doublet with a coupling constant value of 2.0 Hz for coupling with H-7. H-3 still appeared at  $\delta$  6.02 as a dt with  $J$  values 9.8 and 1.5 Hz for coupling with H-4 and long range coupling with one H-5. H-4 appeared at  $\delta$  6.93 as a ddd with coupling constant values of 9.8, 2.9 and 5.4 Hz for coupling with H-3, H-5a and H-5b respectively. H-5 appeared as a multiplet at  $\delta$  2.65 while H-6 showed up at  $\delta$  4.66 as a ddd with coupling constant values of 4 Hz for coupling with H-7, 10 and 3 Hz for coupling with the two protons at position 5 (see Tables 4.10 and 4.11, also Figures 4.13 and 4.14). The  $^{13}C$  NMR (67.8 MHz,  $CDCl_3$ ) values are shown in Table 4.13 (also see Figure 4.15).

**Table 4. 10:**  $^1H$  NMR ( $\delta$ ) assignments and  $J(Hz)$  values for (+)-isogoniothalamine epoxide

Proton	$\delta$	$J(Hz)$	 <p>(+)-Isogoniothalamine epoxide</p>
H-3	6.02, dt	9.8, 1.5	
H-4	6.93, ddd	9.8, 2.9, 5.4.	
H-5	2.65, m	-	
H-6	4.66, ddd	4.0, 10.0, 3.0	
H-7	3.24, dd	2.0, 4.0	
H-8	4.07, d	2.0	
Ph	7.31, m		



(+)-Isogoniothalamine epoxide

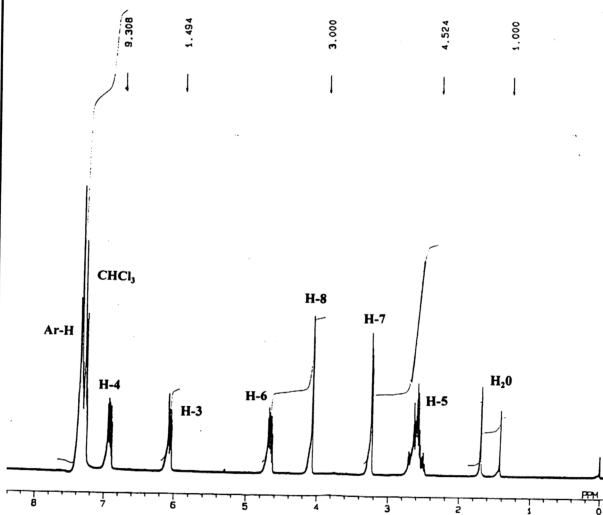
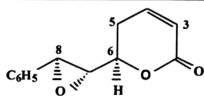


Figure 4. 13:  $^1\text{H}$  NMR spectrum of (+)-isogoniothalamine epoxide (270 MHz,  $\text{CDCl}_3$ )



(+)-Isogoniothalamine epoxide

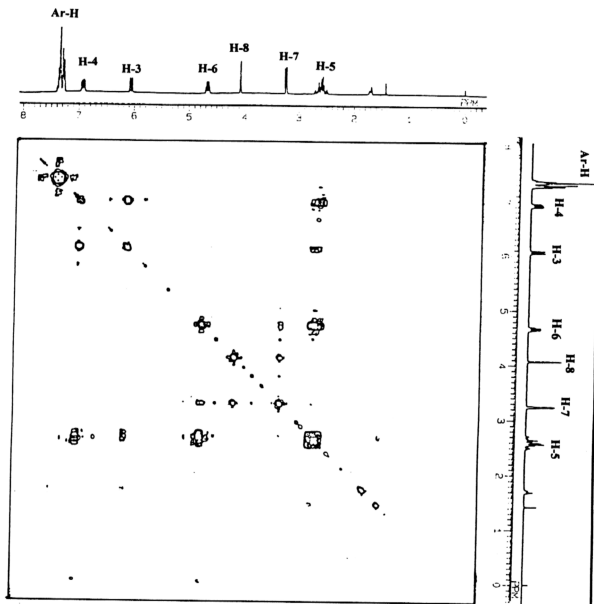
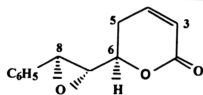


Figure 4. 14:  $^1\text{H} - ^1\text{H}$  COSY spectrum of (+)-isogoniothalamine epoxide



(+)-Isogoniothalamine epoxide

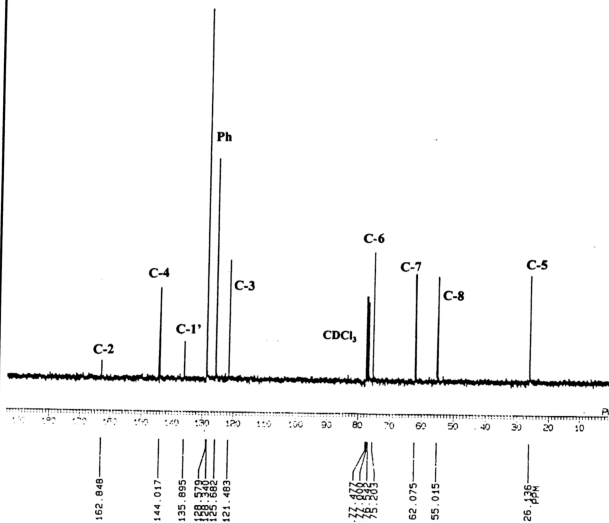
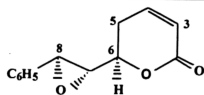


Figure 4. 15:  $^{13}\text{C}$  NMR spectrum of (+)-isogoniothalamine epoxide (67.8 MHz,  $\text{CDCl}_3$ )



(+)-Isogoniothalamine epoxide

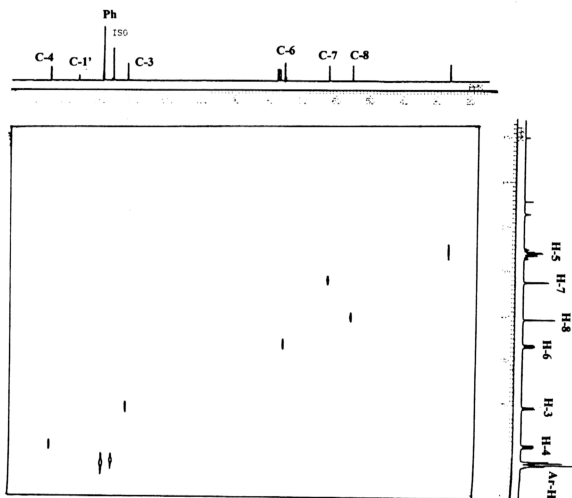
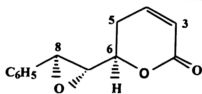


Figure 4. 16:  $^1\text{H} - ^{13}\text{C}$  HETCOR spectrum of (+)-isogoniothalamine epoxide



(+)-Isogoniothalamin epoxide

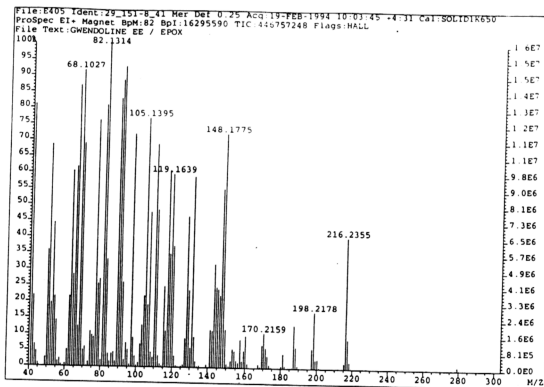


Figure 4. 17: EIMS spectrum of (+)-isogoniothalamin epoxide

**Table 4. 11:  $^1\text{H}$  -  $^1\text{H}$  connectivities ( $^1\text{H}$  -  $^1\text{H}$  COSY) for (+)-isogoniothalamine epoxide**

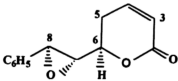
Proton resonance	Connectivity
6.02 (H-3)	6.93 (H-4), 2.65 (LR) (H-5)
6.93 (H-4)	6.02 (H-3), 2.65 (H-5a), 2.65 (H-5b)
2.65 (H-5)	6.93 (H-4), 4.66 (H-6)
4.66 (H-6)	2.65 (H-5a), 3.24 (H-7), 2.65 (H-5b)
3.24 (H-7)	4.66 (H-6), 4.07 (H-8)
4.07 (H-8)	3.24 (H-7)

LR refers to long range coupling

**Table 4. 12:  $^1\text{H}$  -  $^{13}\text{C}$  connectivities ( $^1\text{H}$  -  $^{13}\text{C}$  HETCOR) for (+)-isogoniothalamine epoxide**

Proton resonance	Connectivity
6.02 (H-3)	121.5
6.93 (H-4)	144.1
2.65 (H-5)	26.1
4.66 (H-6)	75.2
3.24 (H-7)	62.1
4.07 (H-8)	55.0

**Table 4. 13:  $^{13}\text{C}$  NMR ( $\delta$ ) assignments for isogoniothalamine epoxide**

Carbon	$\delta$	 <p>(+)-Isogoniothalamine epoxide</p>
C-2	162.9	
C-3	121.5	
C-4	144.1	
C-5	26.1	
C-6	75.2	
C-7	62.1	
C-8	55.0	
C-1'	135.9	
C-2', C-6'	125.7	
C-3', C-5'	128.6	
C-4'	128.3	

(+)-Isogoniothalamine epoxide was subjected to single crystal X-ray crystallographic structure analysis for stereochemical determination. The crystal

selected was a colourless needle, 0.1 by 0.18 by 0.2 mm and the refracted intensities were from  $M_oK_\alpha$  radiation ( $\lambda$  0.71073 Å). The space group is  $P2_12_12_1$ ,  $M_r$  216.24,  $a$  6.1158(4),  $b$  7.3408(4),  $c$  24.91(2) Å,  $R_f$  0.029,  $Z$  4,  $F(000)$  456,  $D_c$  1.284 g cm<sup>-3</sup>. The scan type was  $\omega$ -2 $\theta$ . 1139 unique data were measured; 449 observed data with  $I > 3\sigma(I)$  were used for the structure analysis. The number of reflections measured was 4342; number of independent reflections 4342; number of independent reflections 1139; number of observed reflection 449 [ $>3\sigma(I)$ ];  $R$  0.029;  $R_w$  ( $w = [\sigma(F)^2]^{-1}$ ) 0.034; (shift/e.s.d.)<sub>max</sub> 0.01;  $\Delta\rho_{max}$  0.124 e/Å<sup>3</sup> (see Appendix 6 for detailed X-ray data). Hydrogen atoms were generated geometrically and refined isotropically. The lengths of the molecules are packed running parallel to the  $c$ -axis. The structure was solved by the direct method MULTAN (see Figure 4.18).

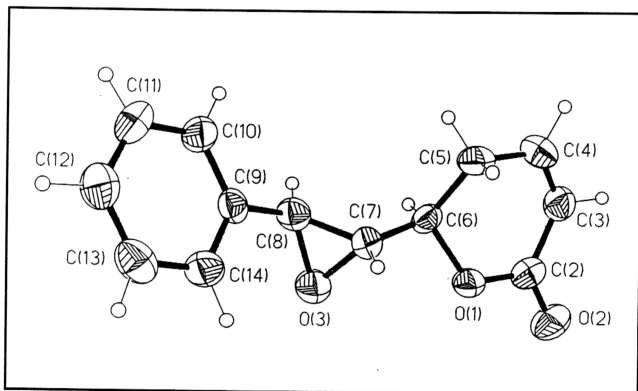


Figure 4. 18: A perspective view of (+)-isogoniothalamine epoxide



#### 4.2.10 Synthesis of goniiothalamine epoxide and isogoniiothalamine epoxide

(+)-Goniiothalamine was epoxidised with *m*-chloroperoxybenzoic acid. A mixture of approximately 1.8:1.0 goniiothalamine epoxide and isogoniiothalamine epoxide was obtained, from  $\beta$ -epoxidation to give (+)-goniiothalamine epoxide and to  $\alpha$ -epoxidation isogoniiothalamine epoxide.

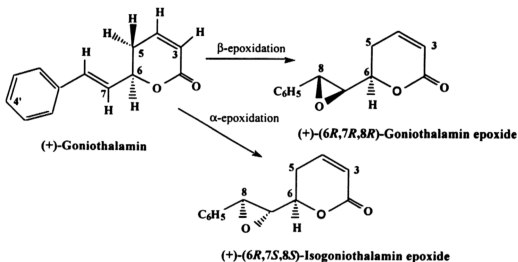


Figure 4. 19: Synthesis of goniiothalamine epoxide

#### 4.2.11 Characterisation of GA-4 as (+)-goniiodiol

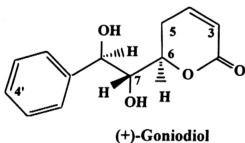
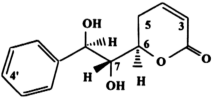


Figure 4. 20: Structure of (+)-goniiodiol

(+)-Goniodiol was isolated as an oil with an  $[\alpha]_D^{20} = +70.0$  (c, 1.0,  $\text{CHCl}_3$ ) (Lit. +74.4; c, 0.3,  $\text{CDCl}_3$ ) (Fang *et al.*, 1991). EIMS gave an  $m/z$  of 217 ( $\text{MH}^+ - 2\text{H}_2\text{O}$ ).  $^1\text{H}$  NMR gave a coupling constant value between H-7 and H-8 of 7.3 Hz indicating 7-OH and 8-OH to be in a diaxial position. Hence, the natural product goniodiol is of *erythro* configuration. Coupling constant and chemical shift values for H-3 and H-4 remain as in goniothalamine whereas H-5 and H-6 were better resolved than in goniothalamine. A large coupling constant value of 12.8 Hz between H-6 and H-5b and a smaller coupling constant value of 3.9 Hz between H-6 and H-5a is consistent with the structure. A coupling constant value of 2.5 Hz between H-7 and H-6 is consistent with an *erythro* configuration and a preferential conformation shown. NMR assignments were made using  $^1\text{H}$ - $^1\text{H}$  COSY and  $^1\text{H}$ - $^{13}\text{C}$  HETCOR experiments (see Tables 4.14-4.17 and Figures 4.21-4.24).

**Table 4. 14:**  $^1\text{H}$  NMR ( $\delta$ ) assignments and  $J(\text{Hz})$  values for (+)-goniodiol (270 MHz,  $\text{CDCl}_3$ )

Proton	$\delta$	$J(\text{Hz})$	 <p>(+)-Goniodiol</p>
H-3	6.00, dd	9.8, 2.4 (LR)	
H-4	6.93, ddd	9.8, 6.6, 2.4	
H-5a	2.80 ddd	18.6, 6.6, 39	
H-5b	2.18 dddd	18.6, 12.8, 2.4, 2.4 (LR)	
H-6	4.80 ddd	12.8, 2.5, 3.9	
H-7	3.73, brd	7.3	
H-8	4.95, d	7.3	
7-OH, 8-OH	2.39, br s	-	
ArH	7.37, m	-	

LR refers to long range coupling

Table 4. 15:  $^1\text{H}$  -  $^1\text{H}$  connectivities ( $^1\text{H}$  -  $^1\text{H}$  COSY) for (+)-goniodiol

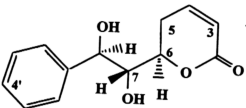
Proton resonance	Connectivity
6.00 (H-3)	6.93 (H-4), 2.18 (LR) (H-5b)
6.93 (H-4)	6.00 (H-3), 2.80 (H-5a), 2.18 (H-5b)
2.80 (H-5a)	2.18 (H-5b), 6.93 (H-4), 4.80 (H-6)
2.18 (H-5b)	2.80 (H-5a), 4.80 (H-6), 6.00 (H-3), 6.93 (H-4)
4.80 (H-6)	2.18 (H-5b), 2.80 (H-5a), 3.73 (H-7)
3.73 (H-7)	4.80 (H-6), 4.95 (H-8)
4.95 (H-8)	3.73 (H-7)
2.39 (7-OH)	3.73 (H-7)
2.39 (8-OH)	4.95 (H-8)

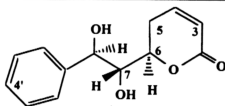
LR refers to long range coupling

Table 4. 16:  $^1\text{H}$ - $^{13}\text{C}$  connectivities ( $^1\text{H}$ - $^{13}\text{C}$  HETCOR) for (+)-goniodiol

Proton resonance	Connectivity
6.00 (H-3)	120.62
6.93 (H-4)	146.13
2.80 (H-5a)	26.07
2.18 (H-5b)	26.07
4.80 (H-6)	76.77
3.73 (H-7)	73.76
4.95 (H-8)	75.01

Table 4. 17:  $^{13}\text{C}$  NMR ( $\delta$ ) assignments for (+)-goniodiol (67.8 MHz,  $\text{CDCl}_3$ )

Carbon	$\delta$	 <p>(+)-Goniodiol</p>
C-2	163.64	
C-3	120.62	
C-4	146.13	
C-5	26.07	
C-6	76.77	
C-7	73.76	
C-8	75.01	
C-1'	140.70	
C-2', C-6'	126.54	
C-3', C-5'	128.78	
C-4'	128.34	



(+)-Goniodiol

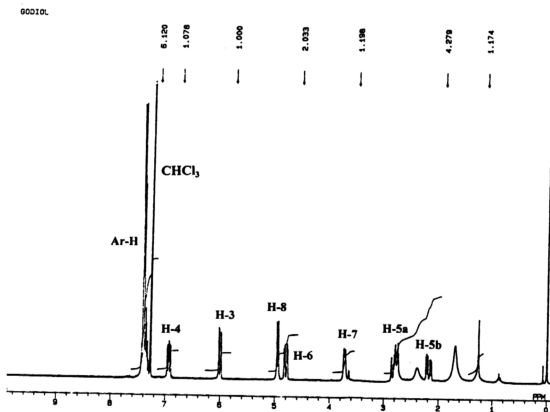
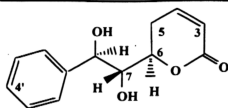


Figure 4. 21: <sup>1</sup>H NMR spectrum of (+)-goniodiol (270 MHz, CDCl<sub>3</sub>)



(+)-Goniodiol

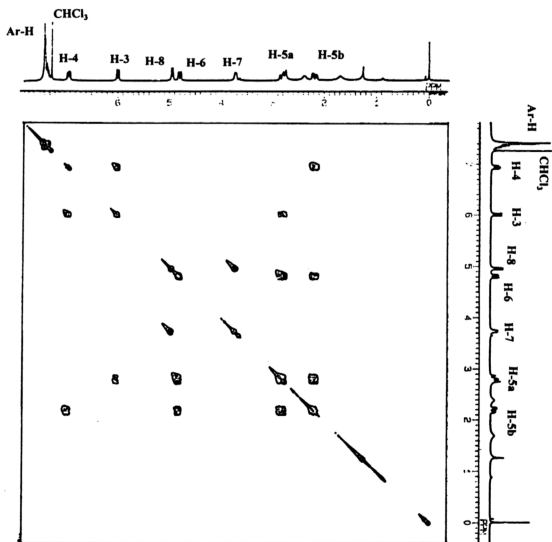
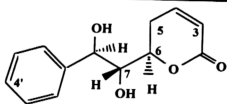


Figure 4. 22:  $^1\text{H}$ - $^1\text{H}$  COSY spectrum of (+)-goniodiol



(+)-Goniodiol

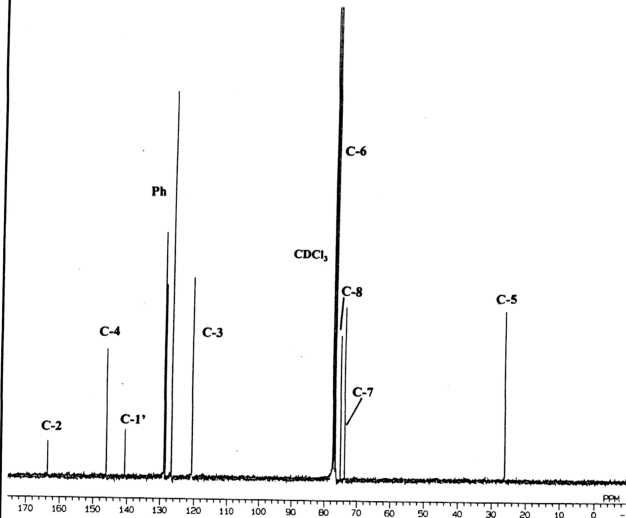


Figure 4. 23:  $^{13}\text{C}$  NMR spectrum of (+)-goniodiol

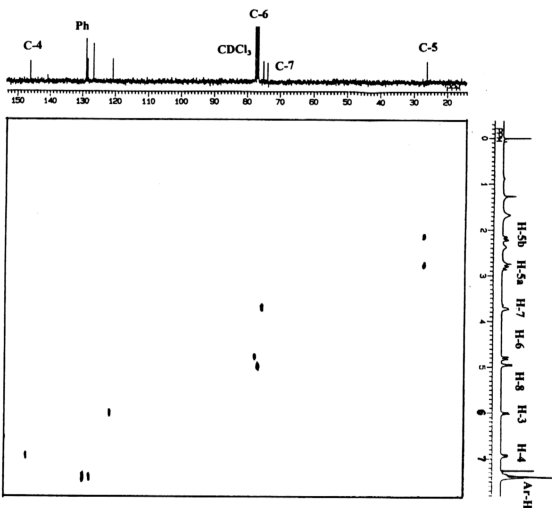
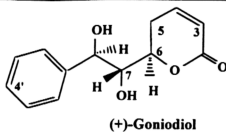


Figure 4. 24:  $^1\text{H}$ - $^{13}\text{C}$  HETCOR spectrum of (+)-goniodiol

#### 4.2.11.1 Synthesis of goniodiol

Goniodiol could be synthesised starting from (2*S*, 3*R*)-1,2-*O*-isopropylidene-3-(-2-furyl)glycerol (Tsubuki *et al.*, 1992,). This gave the (+)-goniodiol which was similar to the natural product isolated from *Goniiothalamus giganteus*. In this work, (+)-goniodiol was synthesised from the stereoisomer of the natural product (+)-goniothalamine epoxide, isogoniothalamine epoxide by reacting it with 1M perchloric acid.

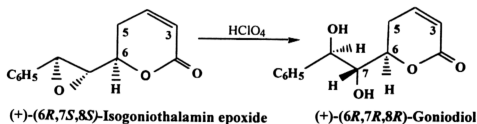


Figure 4. 25: Synthesis of (+)-goniodiol

The regiospecific opening up of the epoxide ring by acid hydrolysis follows the following mechanism:

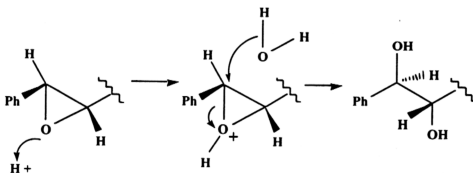


Figure 4. 26: Mechanism for the synthesis of (+)-goniodiol



This means that the natural (+)-goniodiol may be derived from an alternative regiospecific opening of the naturally occurring (+)-goniothalamine epoxide.

However, goniothalamine when reacted with osmium tetroxide provided other diastereomeric mixture of goniodiols.

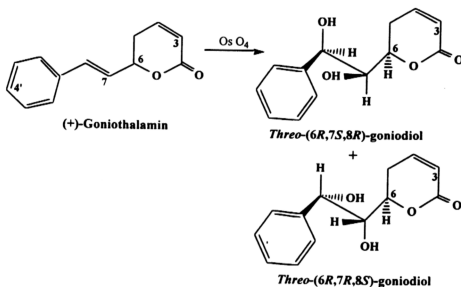


Figure 4. 27: Synthesis of *threo*-goniodiol

The  $^1\text{H}$  NMR shows the disappearance of olefinic peaks at  $\delta$  6.28 and  $\delta$  6.73 due to hydroxylation at C-7 and C-8. The mixture could be separated by preparative layer chromatography using a solvent mixture of 50:50 ethyl acetate:chloroform as the mobile phase. The product obtained was *threo*-goniodiol, a white solid. The proton NMR spectrum has the same pattern as that of the *erythro*-goniodiol except for a different coupling constant value between H-7 and H-8 (5.2 Hz). Also, a large coupling constant value of 10.3 Hz between H-7 and H-6 was observed compared to a smaller  $J_{7,6}$  value of 2.5 Hz in the *erythro*-diol (see Tables 4.18 and 4.19, also Figures



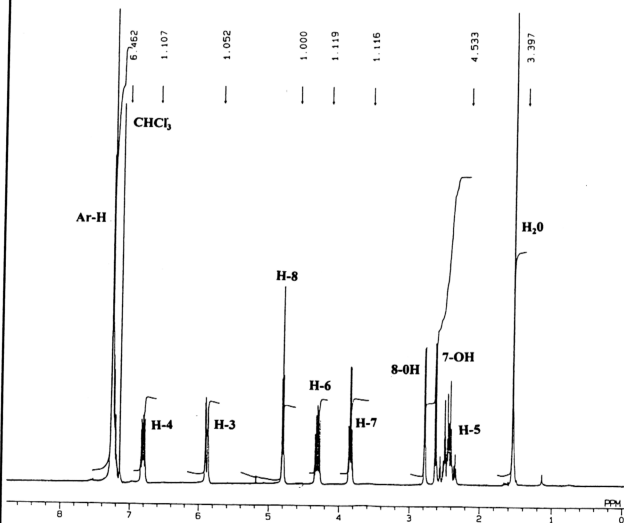
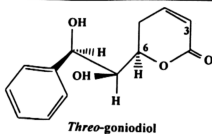


Figure 4. 28:  $^1\text{H}$  NMR spectrum of *threo*-goniodiol (270 MHz,  $\text{CDCl}_3$ )

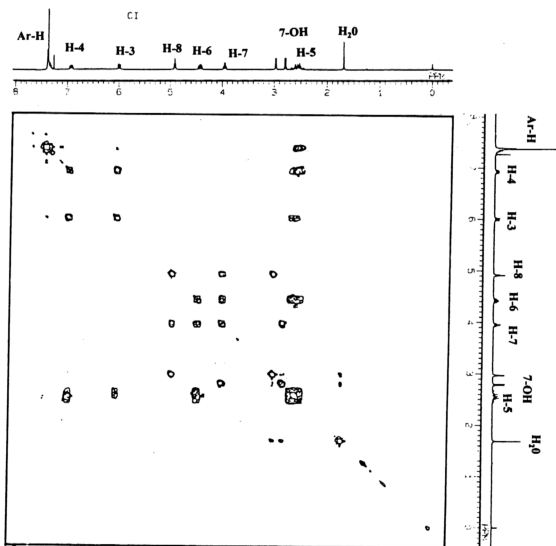
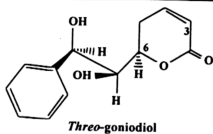


Figure 4. 29:  $^1\text{H}$ - $^1\text{H}$  COSY spectrum of *threo*-goniodiol

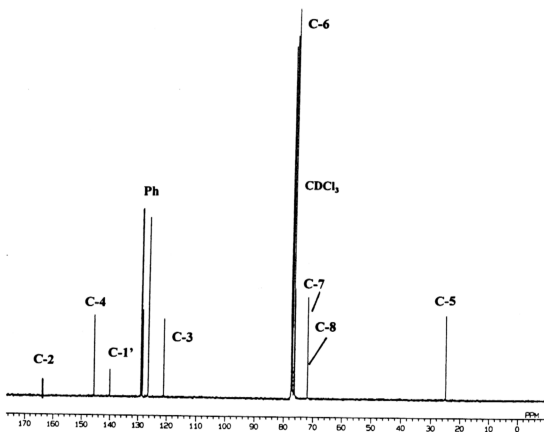
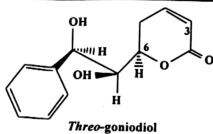


Figure 4. 30:  $^{13}\text{C}$  NMR spectrum of *threo*-goniodiol (67.8 MHz,  $\text{CDCl}_3$ )

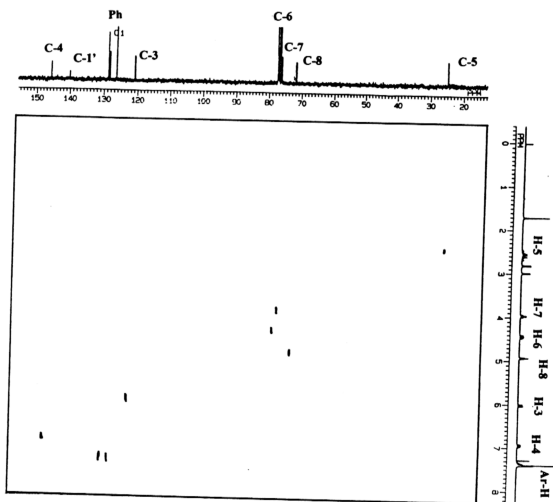
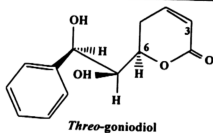
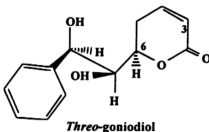


Figure 4.  $^{31}\text{H}-^{13}\text{C}$  HETCOR spectrum of *threo*-goniodiol

Table 4. 21:  $^{13}\text{C}$  NMR assignments ( $\delta$ ) for *threo*-goniodiol (67.8 MHz,  $\text{CDCl}_3$ )

Carbon	$\delta$
C-2	163.7
C-3	120.9
C-4	145.6
C-5	24.8
C-6	77.3
C-7	76.1
C-8	71.9
C-1'	140.1
C-2', 6'	126.4
C-3', 5'	128.8
C-4'	128.4



It is postulated that *threo*-goniodiol could be cyclised by a catalytic amount of DBU in THF to give (+)-5-deoxygonioppyrone whereas the *erythro*-diol could be cyclised by the same reagent to give (-)-iso-5-deoxygonioppyrone.

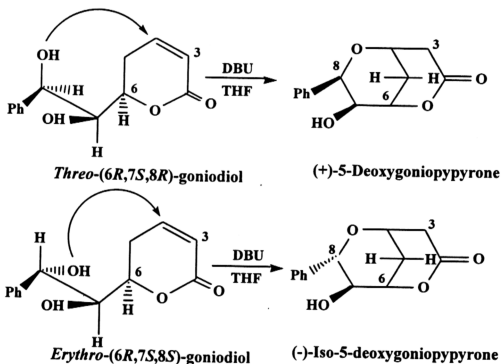
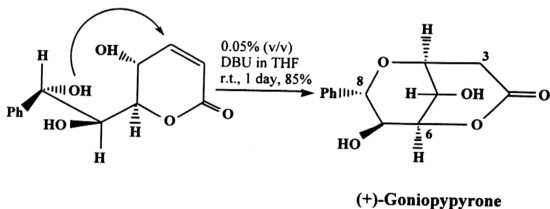


Figure 4. 32: Cyclisation of *threo*-goniodiol and *erythro*-goniodiol

Zhou and Yang (1993) were successful in synthesising (+)-goniopypyrone from methyl cinnamate. The reaction occurs via  $\text{OsO}_4$  catalytic asymmetric dihydroxylation of methyl cinnamate and highly stereoselective 2-furycopper addition in eight steps with an overall yield of 20% of goniopypyrone. In the final step of the reported synthesis (+)-(6*R*, 7*S*, 8*S*)-goniotriol was cyclised to give goniopypyrone using a catalytic amount of DBU in THF at room temperature.



**Figure 4. 33: Synthesis of (+)-goniopypyrone**

In relation to this discovery, an attempt was made in our laboratory to synthesise (-)-iso-5-deoxygoniopypyrone by reacting (+)-*erythro*-goniodiol with a catalytic amount of DBU in THF under nitrogen atmosphere.



#### 4.2.12 Characterisation of GA-5 as (+)-goniodiol diacetate

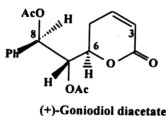


Figure 4. 34: Structure of (+)-goniodiol diacetate

Goniodiol was acetylated with acetic anhydride/pyridine to give the goniodiol diacetate. It had a melting point of 140°C ( Lit. 141-143 °C) (Fang *et al.*, 1991),  $[\alpha]_D^{20} +51.6$  (c, 1.0, CHCl<sub>3</sub>). The <sup>1</sup>H NMR ( CDCl<sub>3</sub>, 270 MHz) spectrum showed two acetoxy singlets at  $\delta$  1.83 and  $\delta$  2.09. The signals for H-3 was maintained at  $\delta$  6.05 as a broad doublet with a coupling constant value of 8.3 Hz and for H-4 at  $\delta$  6.87 as a ddd with coupling constants of 3.2, 5.1 and 8.3 Hz. H-5a and H-5b appeared as a 2-proton multiplet at  $\delta$  2.36. H-6 appeared more or less in the same field as that for goniodiol that is, at  $\delta$  4.77 as a ddd with coupling constant values of 2.9, 6.1 and 9.8 Hz for coupling with H-7, H-5a and H-5b. Splitting was seen quite clearly for H-7 which appeared at  $\delta$  5.36 as a dd with coupling constant values of 8.3 and 2.9 Hz for coupling between H-7 and H-8 and coupling between H-7 and H-6, respectively. H-8 appears as a broad doublet at  $\delta$  6.05 with a coupling of 8.3 Hz. The aromatic protons appeared at  $\delta$  7.35 as a multiplet (see Tables 4.22 and 4.24, and Figures 4.35 and 4.36). <sup>13</sup>C NMR shift values assigned by the <sup>1</sup>H-<sup>13</sup>C HETCOR (Table 4.24 and Figure 4.38) are shown in Table 4.25 (see Figure 4.37).

**Table 4. 22:  $^1\text{H}$  NMR ( $\delta$ ) assignments and  $J$  values (Hz) for goniodiol diacetate**

Proton	$\delta$	$J(\text{Hz})$
H-3	6.05, brd	8.3
H-4	6.87, ddd	3.2, 5.1, 8.3
H-5	2.36, m	-
H-6	4.77, ddd	2.9, 6.1, 9.8
H-7	5.36, dd	2.9, 8.3
H-8	6.05, brd	8.3
Ph	7.35, m	

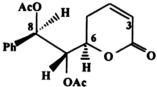
**Table 4. 23:  $^1\text{H}$  -  $^1\text{H}$  connectivities ( $^1\text{H}$  -  $^1\text{H}$  COSY) for goniodiol diacetate**

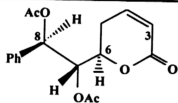
Proton resonance	Connectivity
6.05 (H-3)	6.87 (H-4)
6.87 (H-4)	6.05 (H-3), 2.36 (H-5a), 2.36 (H-5b)
2.36 (H-5)	6.87 (H-4), 4.77 (H-6)
4.77 (H-6)	2.36 (H-5b), 2.36 (H-5a), 5.36 (H-7)
5.36 (H-7)	4.77 (H-6), 6.05 (H-8)
6.05 (H-8)	5.36 (H-7)

**Table 4. 24:  $^1\text{H}$  -  $^{13}\text{C}$  connectivities ( $^1\text{H}$  -  $^{13}\text{C}$  HETCOR) for goniodiol diacetate**

Proton resonance	Connectivity
6.05 (H-3)	121.42
6.87 (H-4)	144.22
2.36 (H-5)	26.06
4.77 (H-6)	74.59
5.36 (H-7)	73.46
6.05 (H-8)	72.31

**Table 4. 25:  $^{13}\text{C}$  NMR ( $\delta$ ) assignments for goniodiol diacetate (67.8 MHz,  $\text{CDCl}_3$ )**

Carbon	$\delta$	 <p>(+)-Goniodiol diacetate</p>
OAc	20.31	
OAc	21.03	
C-2	162.90	
C-3	121.42	
C-4	144.22	
C-5	26.06	
C-6	74.59	
C-7	73.46	
C-8	72.31	
C-2', C-6'	127.42	
C-3', C-5'	128.42	
C-4'	128.69	
C-1'	136.45	
C-OAc	168.99	
C-OAc	169.76	



(+)-Goniodiol diacetate

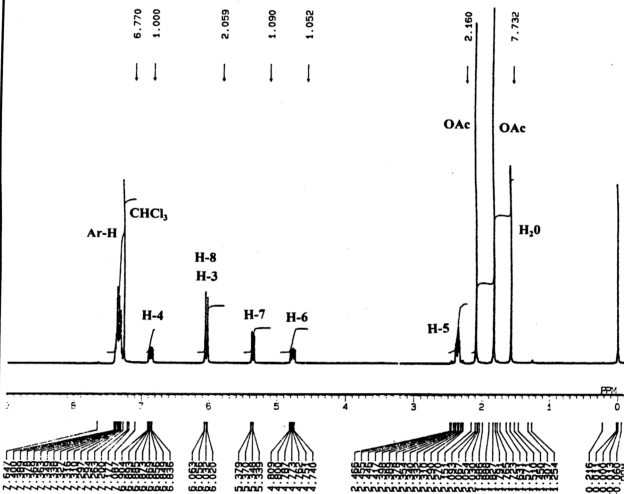
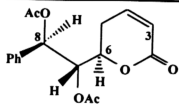


Figure 4. 35: <sup>1</sup>H NMR spectrum of (+)-goniodiol diacetate (270 MHz, CDCl<sub>3</sub>)



(+)-Goniodiol diacetate

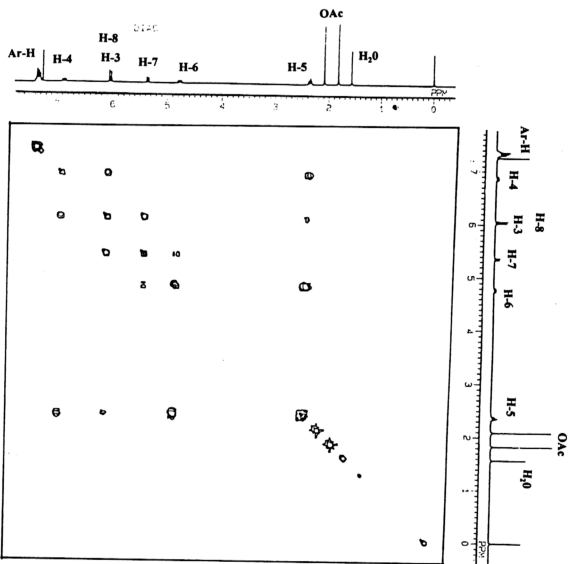
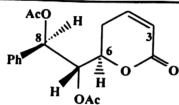


Figure 4. 36:  $^1\text{H}$ - $^1\text{H}$  COSY spectrum of (+)-goniodiol diacetate



(+)-Goniodiol diacetate

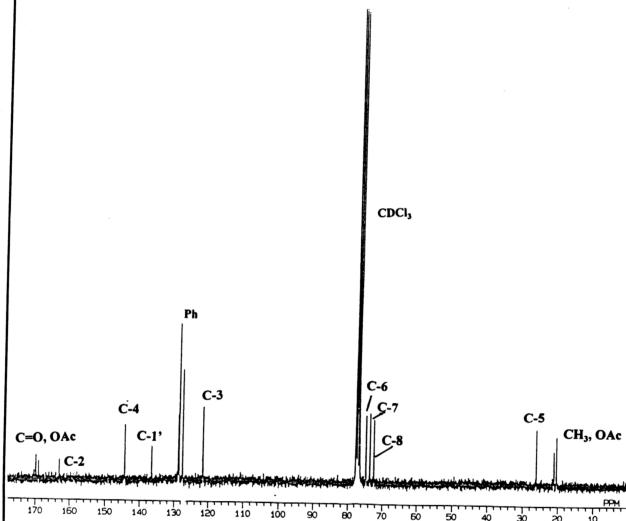


Figure 4. 37:  $^{13}\text{C}$  NMR spectrum of (+)-goniodiol diacetate (67.8 MHz,  $\text{CDCl}_3$ )

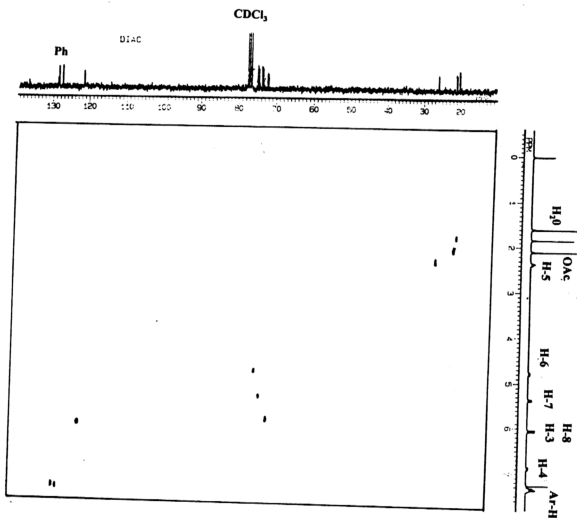
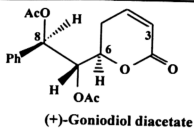


Figure 4. 38:  $^1\text{H}$ - $^{13}\text{C}$  HETCOR spectrum of (+)-goniodiol diacetate

#### 4.2.13 Characterisation of LB5 as pinocembrin

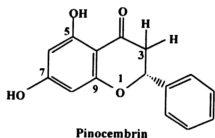
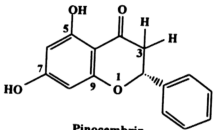


Figure 4. 39: Structure of pinocembrin

LB5 was isolated from the ethyl acetate extract of *Goniiothalamus dolichocarpus* as white crystals with melting point of 190-191 °C (Lit. 192-193 °C) (Buckingham, 1994) and  $[\alpha]_D^{20} = -44.0$  (c, 1.0, CH<sub>3</sub>COCH<sub>3</sub>) (Lit. = -45.3 (c, 0.9, CH<sub>3</sub>COCH<sub>3</sub>)) (Buckingham, 1994). It gave a pink colouration on the TLC plate when stained with vanillin/H<sub>2</sub>SO<sub>4</sub>. EIMS gave an M<sup>+</sup> of 256 which is consistent with the molecular formula C<sub>15</sub>H<sub>12</sub>O<sub>4</sub> (see Figure 4.44). Loss of one water molecule gave the fragment 238 which implied the existence of one hydroxyl group in the molecule. Other fragments were 179 (M<sup>+</sup> - 77), 152 (C<sub>7</sub>H<sub>4</sub>O<sub>4</sub>), 124 (C<sub>6</sub>H<sub>4</sub>O<sub>3</sub>), 104 (C<sub>8</sub>H<sub>8</sub>) and 77 (C<sub>6</sub>H<sub>5</sub>) (see Figure 4.45). The <sup>1</sup>H NMR values were assigned using <sup>1</sup>H - <sup>1</sup>H COSY. The <sup>1</sup>H NMR spectrum of LB5 (270 MHz, CD<sub>3</sub>COCD<sub>3</sub>) gave a multiplet at δ 7.57 of five protons implying a phenyl ring. Other signals were a one-proton sharp singlet at δ 12.25 for hydrogen bonded OH, a two-proton sharp singlet at δ 6.09 for two non-equivalent protons at positions C-6 and C-8, a dd at δ 5.62 with coupling constant values of 3.3 and 12.8 Hz for the proton at C-2 which is coupled to H-3a and H-3b, respectively. The signal for H-3a appeared at δ 2.87 as a dd with coupling constant

values of 3.3 Hz ( $J_{H_{3a-2}}$ ) and 17.2 Hz ( $J_{H_{3a-3b}}$ ) (see Tables 4.26 and 4.27). H-3b gave a signal at  $\delta$  3.22 with coupling constant values of 12.8 Hz ( $J_{H_{3b-2}}$ ) and 17.2 Hz ( $J_{H_{3b-3a}}$ ). The  $^{13}\text{C}$  values were assigned from  $^1\text{H} - ^{13}\text{C}$  connectivities obtained from  $^1\text{H} - ^{13}\text{C}$  HETCOR experiment and by comparisons with literature values (see Tables 4.28 and 4.29, and Figures 4.42 and 4.43) (Breitmaier and Voelter, 1987).

**Table 4. 26:**  $^1\text{H}$  NMR ( $\delta$ ) assignments and  $J(\text{Hz})$  values for pinocembrin (270 MHz,  $\text{CD}_3\text{COCD}_3$ )

Proton	$\delta$	$J(\text{Hz})$	 <p style="text-align: center;">Pinocembrin</p>
H-2	5.62 dd	3.3, 12.8	
H-3a	2.87 dd	3.3, 17.2	
H-3b	3.22 dd	12.8, 17.2	
H-6	6.09 s (2H)	-	
H-8	6.09 s (2H)	-	
Ph	7.57, m	-	
5-OH	12.25 s	-	

**Table 4. 27:**  $^1\text{H} - ^1\text{H}$  connectivities obtained from  $^1\text{H} - ^1\text{H}$  COSY experiment for pinocembrin

Proton resonance	Connectivity
5.62 (H-2)	2.87 (H-3a), 3.22 (H-3b)
2.87 (H-3a)	5.62 (H-2), 3.22 (H-3b)
3.22 (H-3b)	5.62 (H-2), 2.87 (H-3a)

**Table 4. 28:**  $^1\text{H} - ^{13}\text{C}$  connectivities obtained from  $^1\text{H} - ^{13}\text{C}$  HETCOR experiment for pinocembrin

Proton resonance	Connectivity
5.62 (H-2)	79.8
2.87 (H-3a)	43.5
3.22 (H-3b)	43.5
6.09 (H-6)	95.9
6.09 (H-8)	96.9



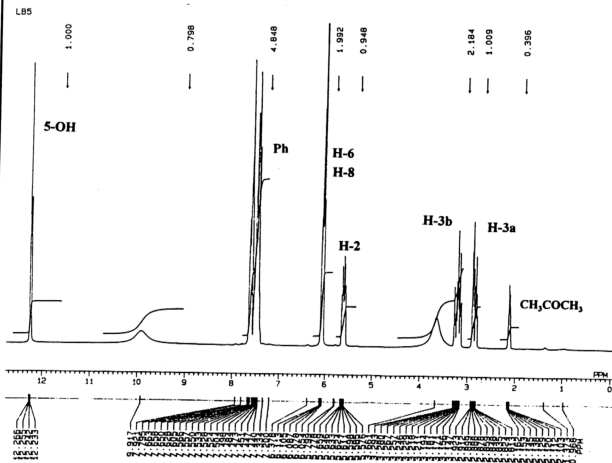
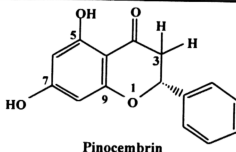
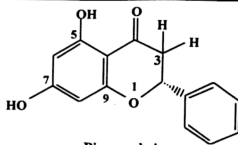


Figure 4. 40:  $^1\text{H}$  NMR spectrum of pinocembrin (270 MHz,  $\text{CD}_3\text{COCD}_3$ )



Pinocembrin

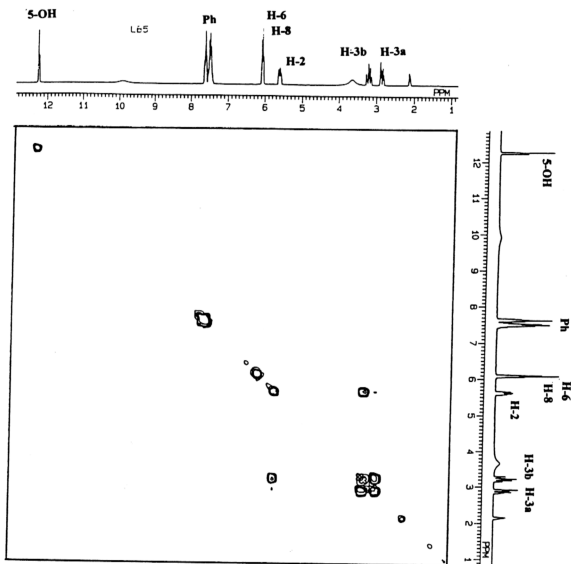


Figure 4. 41:  $^1\text{H}$ - $^1\text{H}$  COSY spectrum of pinocembrin

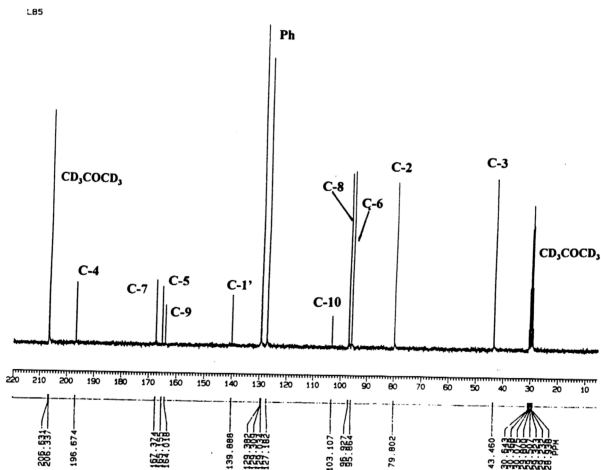
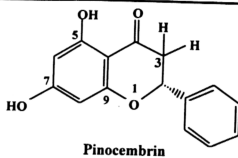


Figure 4. 42: <sup>13</sup>C NMR spectrum of pinocembrin (67.8 MHz, CD<sub>3</sub>COCD<sub>3</sub>)

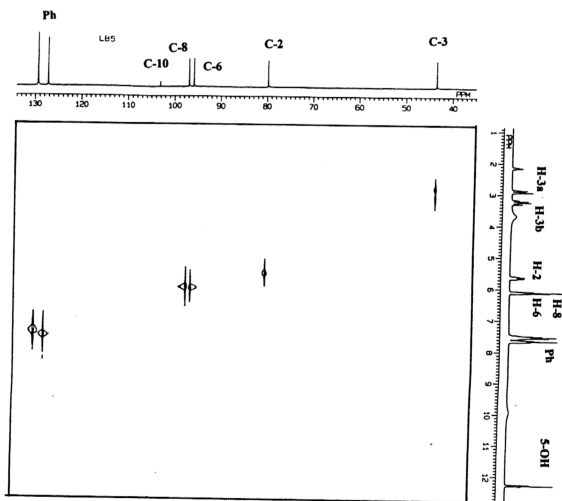
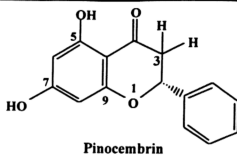


Figure 4. 43:  $^1\text{H}$ - $^{13}\text{C}$  HETCOR spectrum of pinocembrin

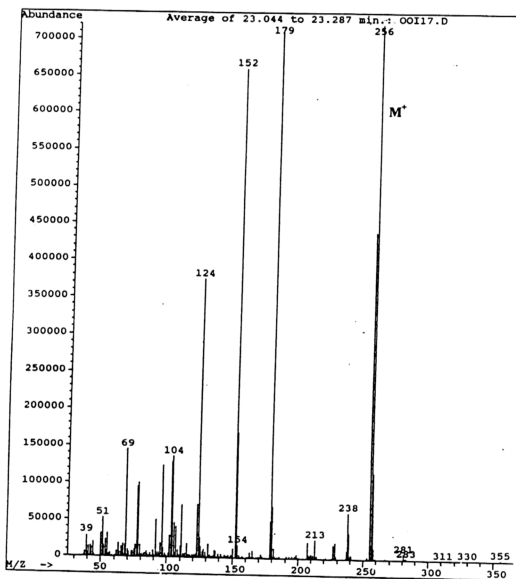
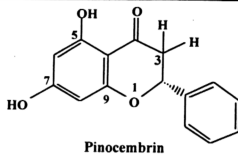


Figure 4. 44: EIMS spectrum of pinocembrin

Table 4. 29:  $^{13}\text{C}$  NMR assignments for pinocembrin (67.8 MHz,  $\text{CD}_3\text{COCD}_3$ )

Carbon	$\delta$
C-2	79.8
C-3	43.5
C-4	196.7
C-5	165.2
C-6	95.9
C-7	167.4
C-8	96.9
C-9	164.0
C-10	103.1
C-1'	138.9
C-2', 6'	127.2
C-3', 5'	129.4
C-4'	129.4

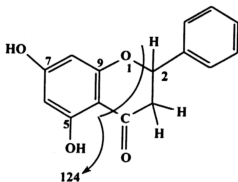
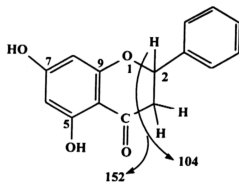
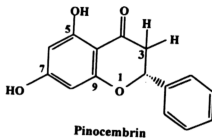


Figure 4. 45: EIMS fragmentations of pinocembrin

#### 4.2.14 Characterisation of LB6 as naringenin

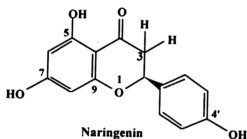


Figure 4. 46: Structure of naringenin

LB6 was isolated from the ethyl acetate extract of *Goniiothalamus dolichocarpus* as white needles; m.p. 249 °C (Lit. 250-251 °C) (Buckingham, 1994)  $[\alpha]_D^{20} = -24.5$  (c, 1.0,  $\text{CHCl}_3$ ) (Lit. -22.5, MeOH) (Buckingham, 1994). EIMS gave an  $M^+$  of 272 which is 16 units more than that of pinocembrin (see Figure 4.52). This is consistent with the presence of an extra hydroxyl group and a molecular formula of  $\text{C}_{15}\text{H}_{12}\text{O}_5$ . Other fragments were 255 ( $M^+ - \text{H}_2\text{O}$ ), 153 ( $\text{C}_7\text{H}_5\text{O}_4$ ), 179 ( $M^+ - \text{C}_6\text{H}_4\text{OH}$ ), 166 ( $\text{C}_9\text{H}_{10}\text{O}_2$ ), 93 ( $\text{C}_6\text{H}_5\text{O}_4$ ). The  $^1\text{H}$  NMR spectrum was almost similar to that of pinocembrin except for two additional signals at  $\delta$  7.16 (dd,  $J = 6.5$  Hz, 2.0 Hz) and  $\delta$  7.66 (dd,  $J = 6.5$  Hz, 2.0 Hz) for a para-substituted benzene ring. The hydroxyl group at the para position in the phenyl ring appeared at  $\delta$  9.4 as a broad singlet. The  $^1\text{H}$  NMR assignments are as shown in Table 4.30.  $^{13}\text{C}$  NMR assignments were carried out using  $^1\text{H}$ - $^{13}\text{C}$  HETCOR and by comparing with values assigned for pinocembrin (see Tables 4.32 and 4.33, and Figures 4.49 and 4.50). GC-MS and library search

(NIST) provided a matching spectrum as naringenin (see Figure 4.53). The assignments were verified by  $^1\text{H}$  and  $^{13}\text{C}$  NMR spectra.

**Table 4. 30:**  $^1\text{H}$  NMR ( $\delta$ ) assignments and  $J(\text{Hz})$  values for naringenin (270 MHz,  $\text{CD}_3\text{COCD}_3$ )

Proton	$\delta$	$J(\text{Hz})$
H-2	5.72 dd	12.5, 3.0
H-3a	3.04, dd	17.3, 3.0
H-3b	3.48 dd	17.3, 12.5
H-6	6.22, s	-
H-8	6.22, s	-
H-2', H-6'	7.16, dd	6.5, 2.0
H-3', H-5'	7.66, dd	6.5, 2.0
5-OH	12.45, s	-
4'-OH	9.4, brs	-

**Table 4. 31:**  $^1\text{H}$  -  $^1\text{H}$  connectivities obtained from  $^1\text{H}$  -  $^1\text{H}$  COSY experiment for naringenin

Proton resonance	Connectivity
5.72 (H-2)	3.04 (H-3a), 3.48 (H-3b)
3.04 (H-3a)	5.72 (H-2), 3.48 (H-3b)
3.48 (H-3b)	5.72 (H-2), 3.04 (H-3a)
7.16 (H-2')	7.66 (H-3')
7.66 (H-3')	7.16 (H-2')
7.66 (H-5')	7.16 (H-6')
7.16 (H-6')	7.66 (H-5')

**Table 4. 32:**  $^1\text{H}$  -  $^{13}\text{C}$  connectivities obtained from  $^1\text{H}$  -  $^{13}\text{C}$  HETCOR experiment for naringenin

Proton resonance	Connectivity
5.72 (H-2)	79.4
3.04 (H-3a)	43.0
3.48 (H-3b)	43.0
6.22 (H-6)	95.8
6.22 (H-8)	96.8
7.16 (H-2', H-6')	129.0
7.66 (H-3', H-5')	116.1



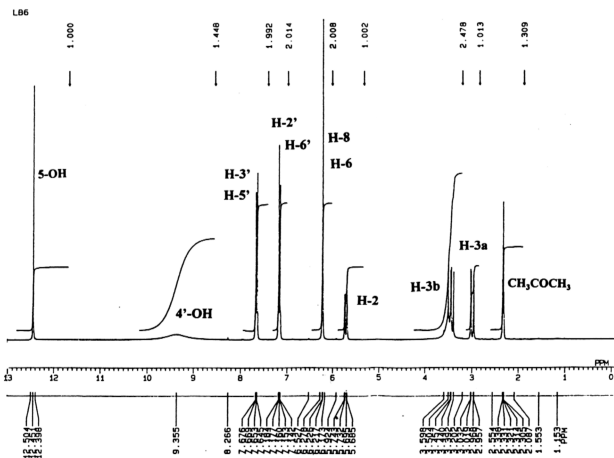
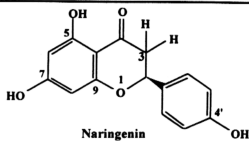


Figure 4. 47: <sup>1</sup>H NMR spectrum of naringenin (270 MHz, CD<sub>3</sub>COCD<sub>3</sub>)

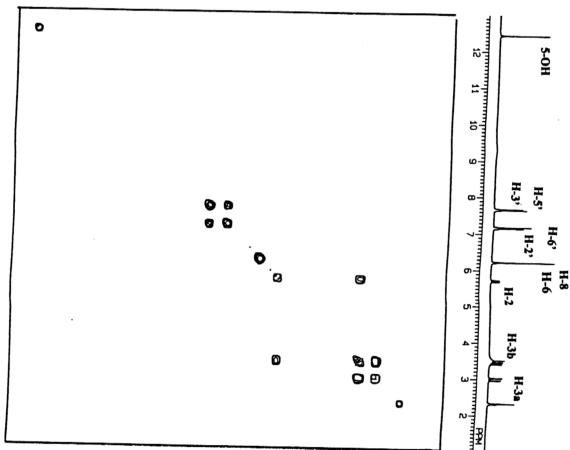
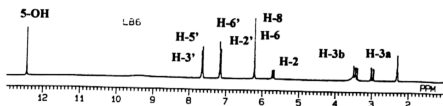
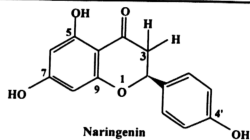


Figure 4. 48:  $^1\text{H}$ - $^1\text{H}$  COSY spectrum of naringenin

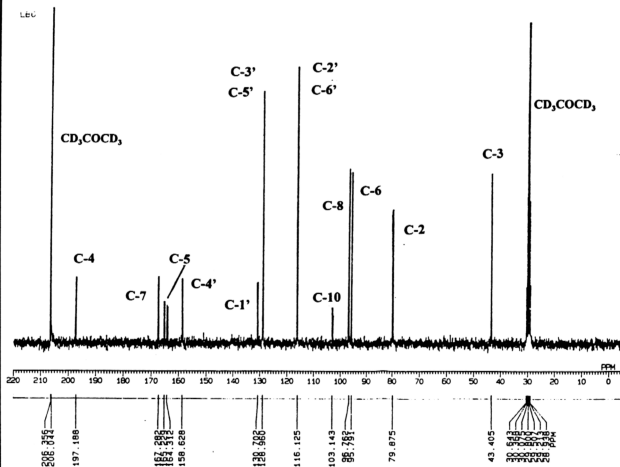
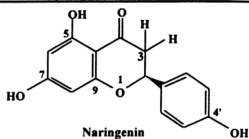


Figure 4. 49:  $^{13}\text{C}$  NMR spectrum of naringenin (67.8 MHz,  $\text{CD}_3\text{COCD}_3$ )

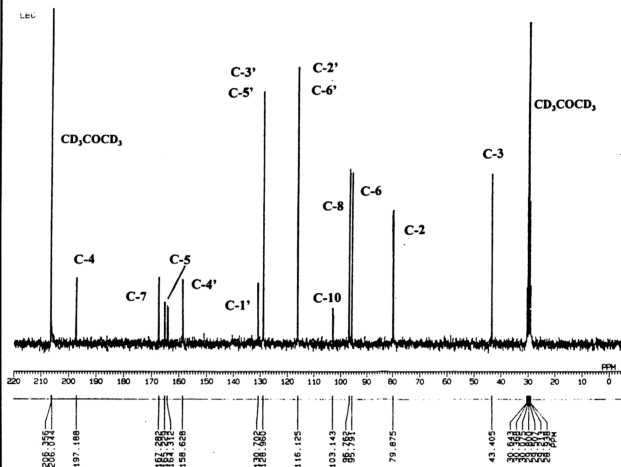
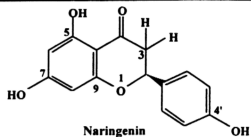


Figure 4. 49:  $^{13}\text{C}$  NMR spectrum of naringenin (67.8 MHz,  $\text{CD}_3\text{COCD}_3$ )

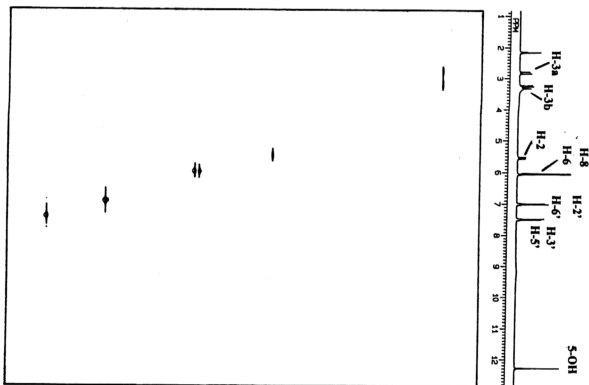
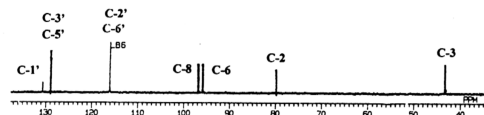
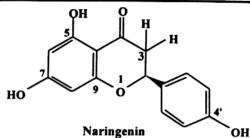
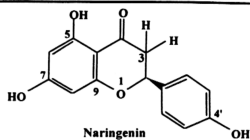
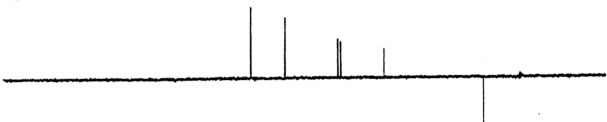


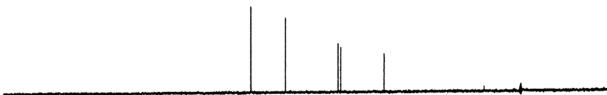
Figure 4. 50:  $^1\text{H}$ - $^{13}\text{C}$  HETCOR spectrum of naringenin



CH, CH<sub>3</sub>--->UP, CH<sub>2</sub>--->DOWN



CH



COH

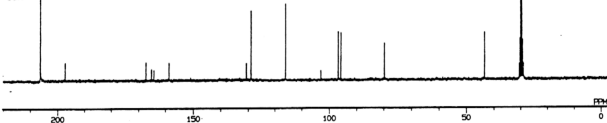
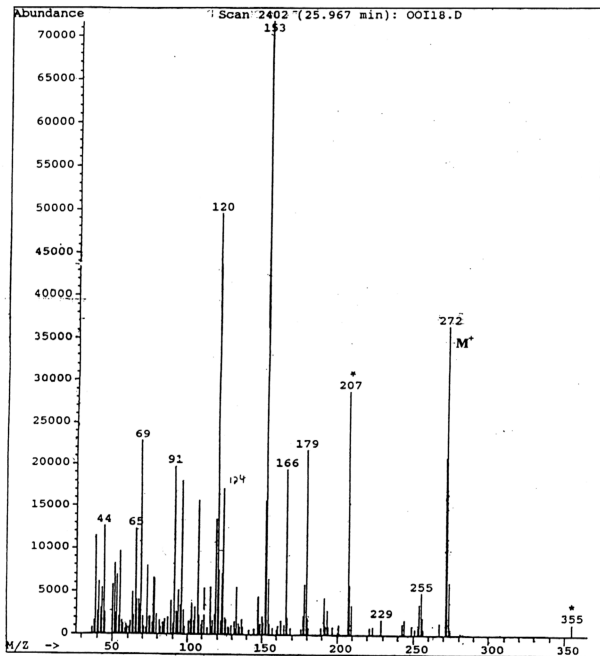
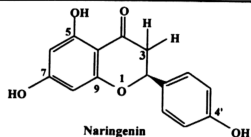
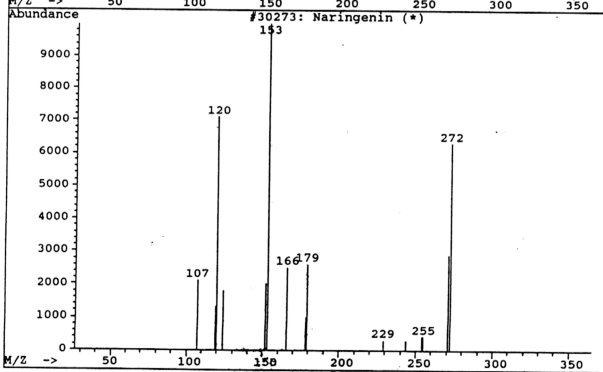
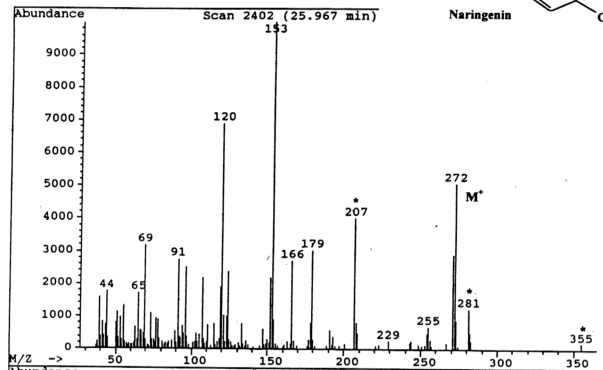
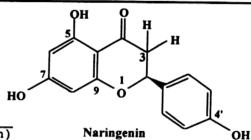


Figure 4. 51: DEPT spectra of naringenin



\* = background

Figure 4. 52: EIMS spectrum of naringenin




\* = column

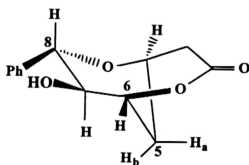
Figure 4. 53: GC-MS spectrum of naringenin



Table 4. 33:  $^{13}\text{C}$  NMR assignments for naringenin (67.8 MHz,  $\text{CD}_3\text{COCD}_3$ )

Carbon	$\delta$	
C-2	79.4	 <p>Naringenin</p>
C-3	43.0	
C-4	197.2	
C-5	165.2	
C-6	95.8	
C-7	167.3	
C-8	96.8	
C-9	164.3	
C-10	103.1	
C-1'	130.7	
C-2', C-6'	116.1	
C-3', C-5'	129.0	
C-4'	158.6	

#### 4.2.15 Characterisation of EELA 25 as (-)-iso-5-deoxygoniopypyrone



(-)-Iso-5-deoxygoniopypyrone

Figure 4. 54: Structure of (-)-iso-5-deoxygoniopypyrone

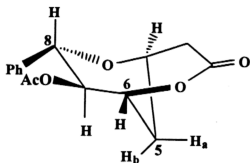
EELA 25 was isolated as an oil from the ethyl acetate extracts of the stem bark of *Goniiothalamus dolichocarpus* as well as the stem bark of *Goniiothalamus andersonii*. The mass spectrum gave a prominent peak at  $m/z$  234 ( $M^+$ ) indicating a molecular formula of  $\text{C}_{13}\text{H}_{14}\text{O}_4$  (see Figure 4.62). The presence of the carbonyl group

was confirmed by the presence of a band at  $1736\text{ cm}^{-1}$  in the infrared spectrum and a resonance at  $\delta\ 168.3$  in the  $^{13}\text{C}$  NMR spectrum (see Figure 4.60).

The compound was acetylated using acetic anhydride and pyridine. The acetylated product crystallised as needles which melted at  $140\text{--}142\text{ }^{\circ}\text{C}$  and gave an  $[\alpha]_{\text{D}}^{20} -170.47$  (c, 1.0,  $\text{CHCl}_3$ ).  $^1\text{H}\text{--}^1\text{H}$  COSY experiment was carried out to assign the  $^1\text{H}$  NMR values (see Table 4.35 and Figure 4.64). The  $^1\text{H}$  NMR gave a doublet of doublet at  $\delta\ 4.82$  with coupling constant values of 10.4 and 2.0 Hz for coupling with H-8 and H-6, respectively. This dd was assigned to H-7. A doublet at  $\delta\ 4.68$  with a coupling constant value of 10.4 Hz was assigned to H-8. A ddd at  $\delta\ 5.02$  was assigned to H-6 with coupling of 2.0, 4.4, and 3.9 Hz to H-7, H-5a and H-5b, respectively. H-5b appeared as a dddd at  $\delta\ 2.33$  with coupling constant values of 14.2 Hz for coupling with H-5a, 3.9 Hz for coupling with H-6, 2 Hz for coupling with H-3a and 2.0 Hz for coupling with H-4. A ddd at  $\delta\ 2.20$  which was assigned to H-5a had coupling constant values of 14.2, 4.4 and 2.0 Hz for coupling with H-5b, H-6 and H-4 respectively. A  $\delta\ 2.95$  doublet with a coupling constant value of 19.5 Hz was assigned to H-3b. This proton is coupled to H-3a. H-3a, however, gave a signal at  $\delta\ 3.06$  as a ddd with coupling constant values of 19.5 Hz for coupling with H-3b, 2 Hz for coupling with H-4 and another 2 Hz for coupling with H-5b. A quartet at  $\delta\ 4.52$  with coupling constant values of 2 Hz was assigned to H-4. H-4 coupled with H-3a, H-5b and H-5a to give coupling constant values of 2 Hz each. The acetate signal appeared at  $\delta\ 1.94$  as a sharp singlet while the phenyl protons gave a multiplet at  $\delta\ 7.34$  (see Table 4.34 and Figure 4.63).

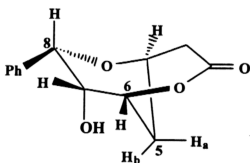
The  $^{13}\text{C}$  NMR spectrum gave a total of fifteen carbons with a carbonyl group at  $\delta$  168.3.  $^{13}\text{C}$  NMR values were assigned using the DEPT and  $^1\text{H}$ - $^{13}\text{C}$  HETCOR experiments. DEPT indicated two methylene groups, nine methine groups and one methyl group (see Table 4.38 and Figures 4.65-4.67).

This compound is a new natural product as suggested by the NMR spectra ( $^1\text{H}$ - $^1\text{H}$  COSY,  $^1\text{H}$ - $^{13}\text{C}$  HETCOR, and NOE difference) of the acetylated compound. The structure assigned is consistent with a stereoisomer of the known (+)-5-deoxygonioppyrone previously isolated from *G. giganteus*. NOE difference spectra shows NOE enhancement between the phenyl protons and H-7 and H-8, these effects suggesting that H-7 and the phenyl group are in close proximity (see Figure 4.57). For an assumed preferential average conformation of the phenyl group in a quasi-equatorial position H-7 and H-8 will assume a transoid geometry. A coupling constant value of 10.4 Hz between H-7 and H-8 is in agreement of an almost antiparallel geometry of the two hydrogens. Similarly, a 10.0 Hz doublet for H-8 was also observed in the  $^1\text{H}$  NMR spectrum of EELA 25. In contrast, a singlet is reported for H-8 in the compound (+)-5-deoxygonioppyrone due to an almost orthogonal H-7-H-8 orientation. In the new compound, NOE enhancements were observed between H-5b and H-7 and between H-3b and H-8. Since the compound is a stereoisomer of the previously isolated (+)-5-deoxygonioppyrone, it is assigned as (-)-iso-5-deoxygonioppyrone with a 6*R*, 7*R*, 8*S* configuration.



(-)-Iso-5-deoxygoniopyrhone acetate

Figure 4. 55: Structure of (-)-iso-5-deoxygoniopyrhone



(+)-5-Deoxygoniopyrhone

Figure 4. 56: Structure of (+)-5-deoxygoniopyrhone

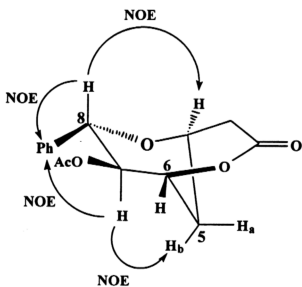
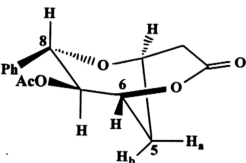


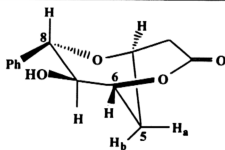
Figure 4. 57: NOE enhancements of (-)-iso-5-deoxygoniopyrhone acetate

**Table 4. 34:  $^1\text{H}$  NMR assignments for (-)-iso-5-deoxygoniopyrhone acetate (270 MHz,  $\text{CDCl}_3$ )**

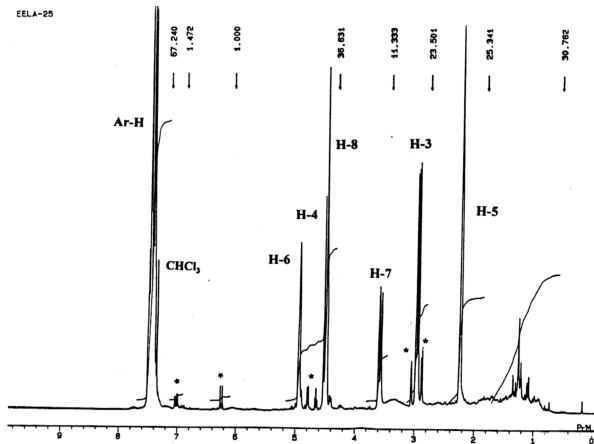
Proton	$\delta$	$J$ (Hz)	 <p>(-)-Iso-5-deoxygoniopyrhone acetate</p>
H-3a	3.06 ddd	19.5, 2.0, 2.0	
H-3b	2.95 d	19.5	
H-4	4.52 q	2.0	
H-5a	2.20 ddd	14.2, 4.4, 2.0	
H-5b	2.33 dddd	14.2, 3.9, 2.0, 2.0	
H-6	5.02 ddd	2.0, 4.4, 3.9	
H-7	4.82 dd	10.4, 2.0	
H-8	4.68 d	10.4	
OAc	1.94 s		
Ph	7.34 m		

**Table 4. 35:  $^1\text{H}$  -  $^1\text{H}$  connectivities obtained from  $^1\text{H}$  -  $^1\text{H}$  COSY experiment for (-)-iso-5-deoxygoniopyrhone acetate**

Proton resonance	Connectivity
3.06 (H-3a)	2.95 (H-3b), 4.52 (H-4), 2.33 (H-5b)
2.95 (H-3b)	3.06 (H-3a)
4.52 (H-4)	3.06 (H-3a), 2.20 (H-5a), 2.33 (H-5b)
2.20 (H-5a)	2.33 (H-5b), 4.52 (H-4), 5.02 (H-6)
2.33 (H-5b)	2.20 (H-5a), 5.02 (H-6), 3.06 (H-3a), 4.52 (H-4)
5.02 (H-6)	2.33 (H-5b), 2.20 (H-5a), 4.82 (H-7)
4.82 (H-7)	4.68 (H-8), 5.02 (H-6)
4.68 (H-8)	4.82 (H-7)

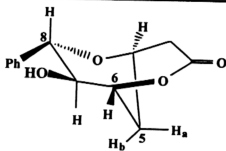


(-)-Iso-5-deoxygonioppyrone



\* = goniodiol

Figure 4. 58: <sup>1</sup>H NMR spectrum of (-)-iso-5-deoxygonioppyrone (crude) (270 MHz, CDCl<sub>3</sub>)



(-)-Iso-5-deoxygoniopyrone

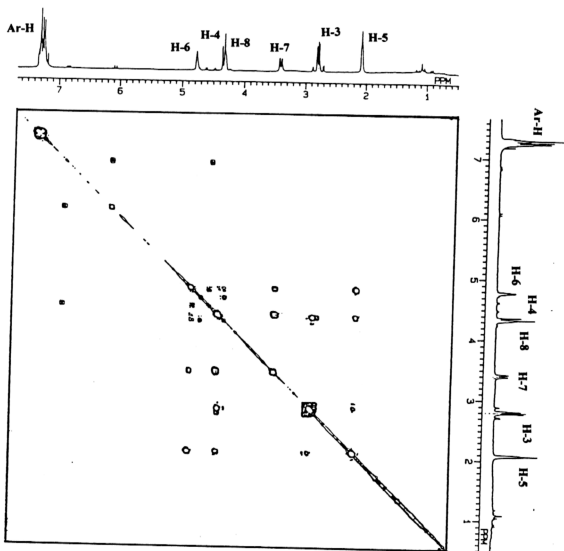
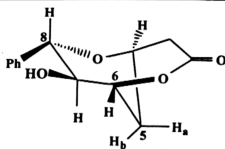


Figure 4. 59:  $^1\text{H}$ - $^1\text{H}$  COSY spectrum of (-)-iso-5-deoxygoniopyrone (crude)



(-)-Iso-5-deoxygoniopyrone

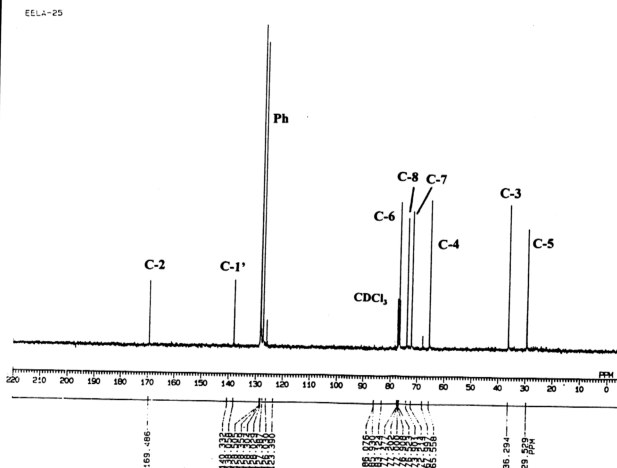
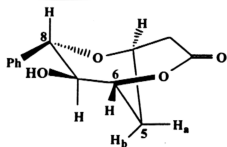


Figure 4. 60:  $^{13}\text{C}$  NMR spectrum of (-)-iso-5-deoxygoniopyrone (crude) (67.8 MHz,  $\text{CDCl}_3$ )





(-)-Iso-5-deoxygonioppyrone

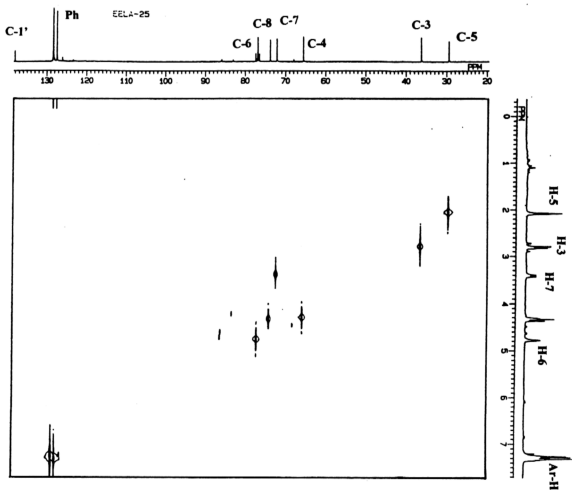
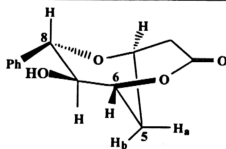
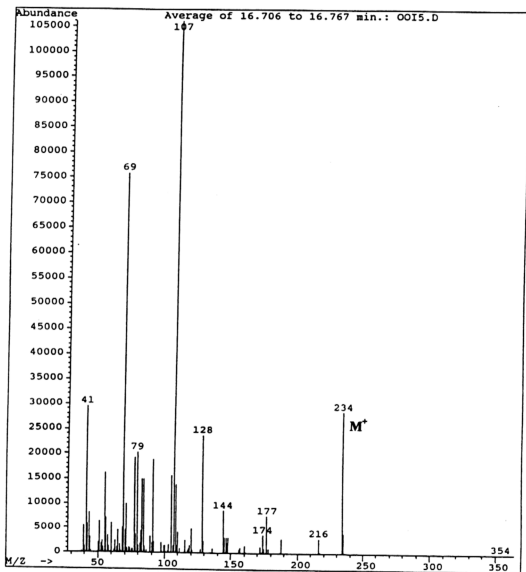


Figure 4. 61:  $^1\text{H}$ - $^{13}\text{C}$  HETCOR spectrum of (-)-iso-5-deoxygonioppyrone (crude)



**(-)-Iso-5-deoxygoniopypyrone**



**Figure 4. 62: EIMS spectrum of (-)-iso-5-deoxygoniopypyrone**

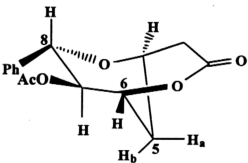
Table 4. 36:  $^1\text{H}$  NMR assignments for (-)-iso-5-deoxygoniopypyrone (270 MHz,  $\text{CDCl}_3$ )

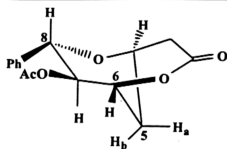
Proton	$\delta$	$J$ (Hz)
H-3a	2.78 dd	19.1, 4.8
H-3b	2.88 d	19.1
H-4	4.34 m	-
H-5a	2.10 brs	-
H-5b	2.10 brs	-
H-6	4.79 brs	-
H-7	3.41 brd	10.0
H-8	4.39 d	10.0
7-OH	3.71 brs	-
Ph	7.33 m	-

Table 4. 37:  $^1\text{H}$  -  $^{13}\text{C}$  connectivities obtained from  $^1\text{H}$  -  $^{13}\text{C}$  HETCOR experiment for (-)-iso-5-deoxygoniopypyrone acetate

Proton resonance	Connectivity
3.06 (H-3a)	36.2
2.95 (H-3b)	36.2
4.52 (H-4)	65.9
2.20 (H-5a)	29.4
2.33 (H-5b)	29.4
5.02 (H-6)	73.8
4.82 (H-7)	72.8
4.68 (H-8)	71.0
1.94 (OAc)	20.4

Table 4. 38:  $^{13}\text{C}$  NMR assignments for (-)-iso-5-deoxygoniopypyrone acetate (67.8 MHz,  $\text{CDCl}_3$ )

Carbon	$\delta$	 <p>(-)-Iso-5-deoxygoniopypyrone acetate</p>
OAc	20.4	
C-5	29.4	
C-3	36.2	
C-4	65.9	
C-8	71.0	
C-7	72.8	
C-6	73.8	
C-2', C-6'	127.0	
C-3', C-5'	128.6	
C-4'	128.3	
C-1'	136.9	
C=O	168.3	
C=O, OAc	169.4	



(-)-Iso-5-deoxygoniopypyrone acetate

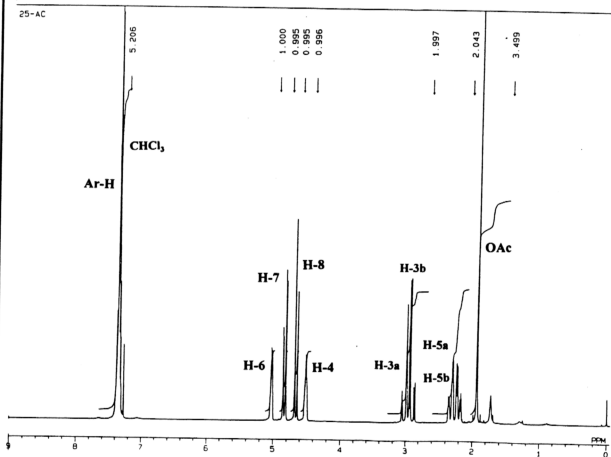
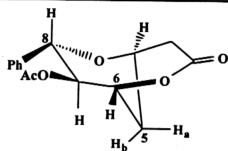


Figure 4. 63: <sup>1</sup>H NMR spectrum of (-)-iso-5-deoxygoniopypyrone acetate (270 MHz, CDCl<sub>3</sub>)



(-)-Iso-5-deoxygoniopyrone acetate

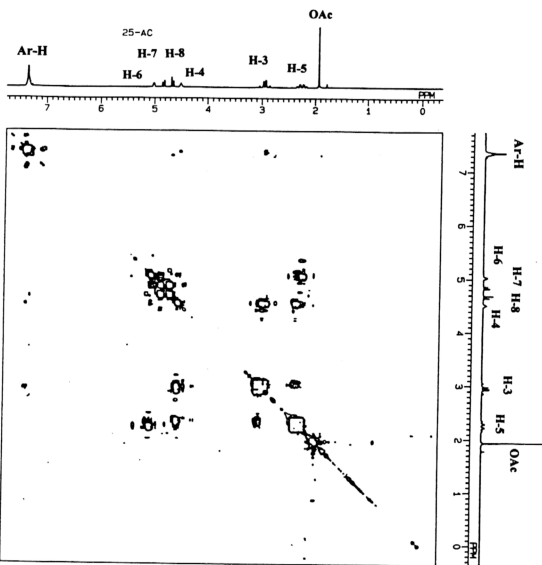
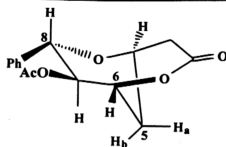
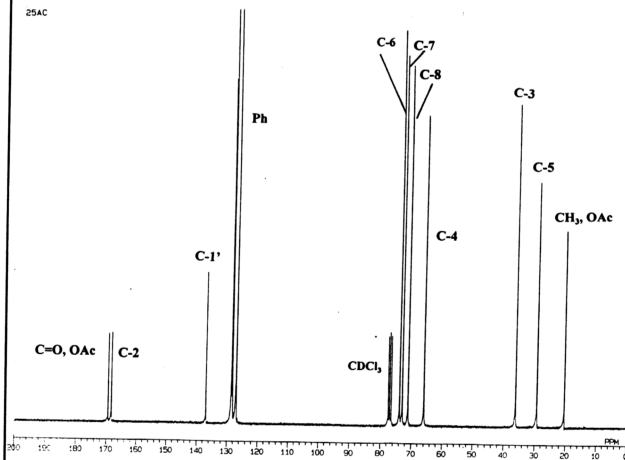


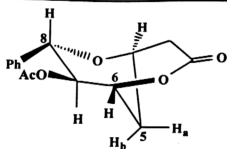
Figure 4. 64:  $^1\text{H}$ - $^1\text{H}$  COSY spectrum of (-)-iso-5-deoxygoniopyrone acetate



**(-)-Iso-5-deoxygoniopyrone acetate**



**Figure 4. 65:  $^{13}\text{C}$  NMR spectrum of (-)-iso-5-deoxygoniopyrone acetate (67.8 MHz,  $\text{CDCl}_3$ )**



(-)-Iso-5-deoxygoniopypyrone acetate

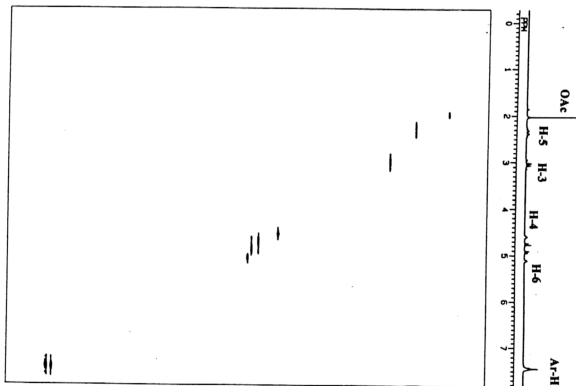
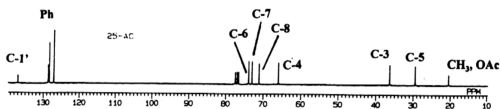
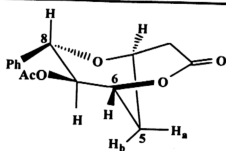


Figure 4. 66:  $^1\text{H}$ - $^{13}\text{C}$  HETCOR spectrum of (-)-iso-5-deoxygoniopypyrone acetate



(-)-Iso-5-deoxygoniopypyrone acetate

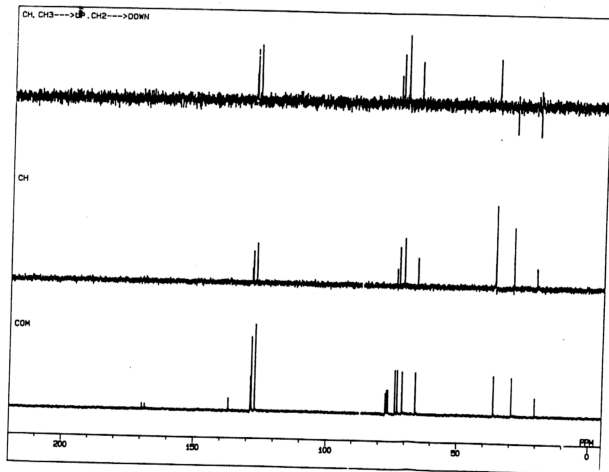


Figure 4. 67: DEPT spectra of (-)-iso-5-deoxygoniopypyrone acetate



**(-)-Iso-5-deoxygoniopyrpyrone acetate.** The EIMS spectrum for (-)-iso-5-deoxygoniopyrpyrone acetate is as follows:  $m/z$  233 (52%,  $M - \text{CH}_3\text{CO}$ ), 216 (34,  $M - \text{CH}_3\text{COOH}$ , 172 (88), 127 (32), 107 (61), 91 (37), 77 (38), 69 (19), 43 (100). IR ( $\nu_{\text{max}}$   $\text{cm}^{-1}$ ): 3678, 3542, 3026, 2967, 2889, 1736, 1457, 1376, 1228, 1198, 1087, 1065, 766, 724. UV( $\lambda_{\text{max}}$ , EtOH, nm): 206 (log  $\epsilon$  3.90).

**(-)-Iso-5-deoxygoniopyrpyrone.** The EIMS spectrum for (-)-iso-5-deoxygoniopyrpyrone is as follows:  $m/z$  234 (29%, MH), 216 (2%,  $M - \text{H}_2\text{O}$ ), 177 (8%), 144 (9%), 128 (24%), 107 (100%), 91 (19%), 79 (20%), 77 (19%). High resolution EI mass spectrum  $m/z$  234.0898 ( $\text{C}_{13}\text{H}_{14}\text{O}_4$  requires 234.0892). IR ( $\nu_{\text{max}}$   $\text{cm}^{-1}$ ): 3424, 2964, 1724, 1604, 1195, 1082, 774, 739. UV( $\lambda_{\text{max}}$ , EtOH, nm): 246 (log  $\epsilon$  3.18).

#### 4.2.15.1 Synthesis of (-)-iso-5-deoxygoniopyrpyrone

As mentioned earlier in section 2.2.11.1, Zhou and Yang (1993) were successful in synthesising (+)-goniopyrpyrone from methyl cinnamate. Hence, it was postulated that the *erythro*-goniodiol could be cyclised by a catalytic amount of DBU in THF solvent to produce the compound (-)-iso-5-deoxygoniopyrpyrone.

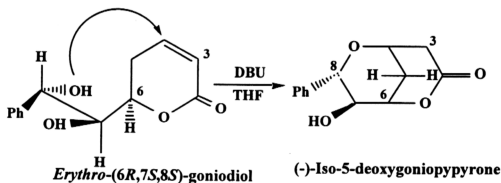
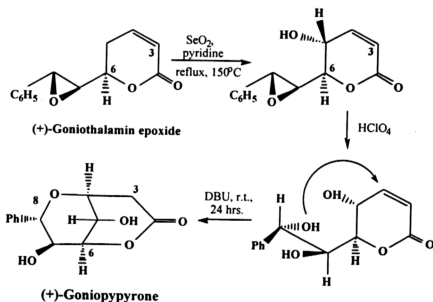


Figure 4. 68: Synthesis of (-)-iso-5-deoxygoniopyrpyrone

In relation to this postulation, the *erythro*-goniodiol (8 mg,  $3.4 \times 10^{-5}$  mol), was reacted with a catalytic amount of DBU in dry THF (25  $\mu$ l in 2 ml) under nitrogen atmosphere for 48 hours at room temperature. GC was able to detect the presence of a very minute amount of (-)-iso-5-deoxygoniopyrpyrone.

Goniothalamine was able to react with  $\text{SeO}_2$  in dioxane to give 5-hydroxygoniothalamine (see section 4.2.18.1). It was postulated that since *erythro*-goniodiol was cyclised by DBU in THF to give the (-)-iso-5-deoxygoniopyrpyrone, hence with a OH group at the C-5 position the same cyclisation would give (+)-goniopyrpyrone. An attempt was made to synthesise goniopyrpyrone using the same postulation but with goniothalamine epoxide as the starting material.



**Figure 4. 69: Postulated synthesis of goniopyrpyrone**

However,  $\text{SeO}_2$  did not attack the 5-H position as predicted to produce the 5-hydroxygoniothalamine epoxide.

#### 4.2.16 Characterisation of GMg and GV9b as (+)-goniothalenol

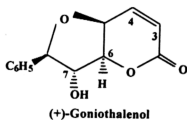
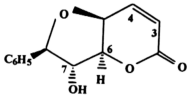


Figure 4. 70: Structure of (+)-goniothalenol

GMg and GV9b were very strongly UV active at wavelength 366 nm and gave a very bright yellowish colour on the TLC plate. This compound was isolated from *Goniothalamina malayanus* as well as *Goniothalamus velutinus*. The compound was isolated as pale yellow crystals of melting point 107-108 °C (Lit. 110 °C) and  $[\alpha]_{25}^D = +190.5$  (c 1.0, ethanol) (Lit +184.7, ethanol) (El-zayat *et al.*, 1985). The mass spectrum (EIMS) gave an  $M^+$  ion at 232 (21%). Other fragments were 170 (0.7%), 144 (1.6%), 136 (9%), 126 (8%), 107 (24%), 97 (100%), 95 (25%), 91 (14%), 79 (14%), 77 (16%) and 51 (10%) (see Figure 4.76). A molecular weight of 232 is consistent with the molecular formula  $C_{13}H_{12}O_4$ . The pair of doublet and doublet of doublet at  $\delta$  6.22 ( $J = 10.0$  Hz),  $\delta$  6.97 ( $J = 10.0$  Hz, 5.0 Hz) indicated that H-3 and H-4 of the pyrone ring are still unchanged. Moreover, the  $^{13}C$  NMR spectrum indicated signals at  $\delta$  140.5 and  $\delta$  123.8 for C-4 and C-3 at the pyrone ring. The carbonyl signal was observed at  $\delta$  161.8 which was very close to that for the carbonyl at the pyrone ring in goniothalamine. This indicated that the pyrone ring was unchanged. The disappearance of the doublet of doublet at  $\delta$  6.28 ( $J = 15.6$  Hz, 6.3 Hz) and the doublet at  $\delta$  6.73 ( $J = 15.6$  Hz) for H-7 and H-8 and the appearance of their signals at  $\delta$  4.44 (dd,  $J_{7,6} = 2.4$  Hz,  $J_{7,8} = 6.0$  Hz) for H-7 and at  $\delta$  4.73 (d,  $J_{8,7} = 6.0$  Hz) for H-8

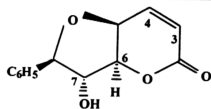
indicated, H-7 and H-8 are no longer attached to a double bond. Moreover, the H-5 signal indicated the loss of one proton and had moved from  $\delta$  2.55 to  $\delta$  4.64 (t,  $J_{5,6}$  = 5.0 Hz). Also the signal for H-6 had moved from  $\delta$  5.11 in goniothalamin to  $\delta$  4.93 in GMg. The fact that C-5 has only one proton would mean that cyclisation of C-5, C-6, C-7 and C-8 to a tetrahydrofuran ring had occurred. This carbon skeleton explains the observed signals at  $\delta$  68.2,  $\delta$  86.0,  $\delta$  83.8 and  $\delta$  86.1 for C-5, C-6, C-7 and C-8.  $^1\text{H}$  NMR assignments were carried out using  $^1\text{H}$ - $^1\text{H}$  COSY and the  $^{13}\text{C}$  assignments using  $^1\text{H}$ - $^{13}\text{C}$  HETCOR (see Tables 4.39-4.42, and Figures 4.71-4.75).

**Table 4. 39:  $^1\text{H}$  NMR ( $\delta$ ) assignments and  $J(\text{Hz})$  values for (+)-goniothalenol (270 MHz,  $\text{CDCl}_3$ )**

Proton	$\delta$	$J(\text{Hz})$	 <p>(+)-Goniothalenol</p>
H-3	6.22, d	10.0	
H-4	6.97, dd	10.0, 5.0	
H-5	4.64, t	5.0	
H-6	4.93, dd	5.0, 2.4	
H-7	4.44, dd	2.4, 6.0	
H-8	4.73, d	6.0	
Ph	7.23-7.31, m	-	
7-OH	3.64, d	2.9	

**Table 4. 40:  $^1\text{H}$ - $^1\text{H}$  connectivities ( $^1\text{H}$ - $^{13}\text{C}$  HETCOR) for (+)-goniothalenol**

Proton resonance	Connectivity
6.22 (H-3)	6.97 (H-4)
6.97 (H-4)	6.22 (H-3), 4.64 (H-5)
4.64 (H-5)	6.97 (H-4)
4.93 (H-6)	4.64 (H-5), 4.44 (H-7)
4.44 (H-7)	4.93 (H-6)
4.73 (H-8)	4.44 (H-7)



(+)-Goniothalenol

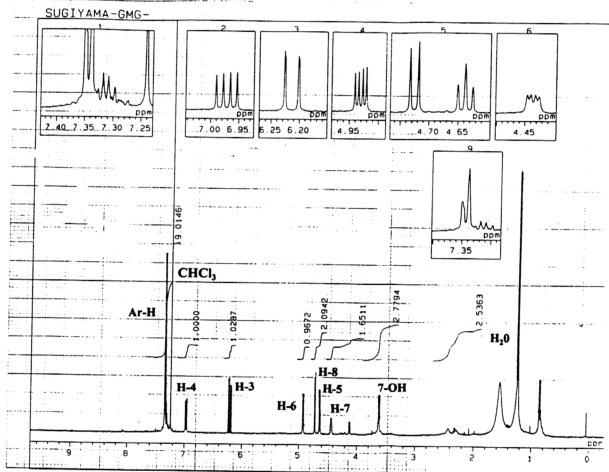
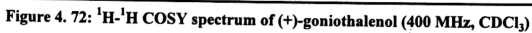
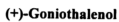


Figure 4. 71: <sup>1</sup>H NMR spectrum of (+)-goniothalenol (400 MHz, CDCl<sub>3</sub>)



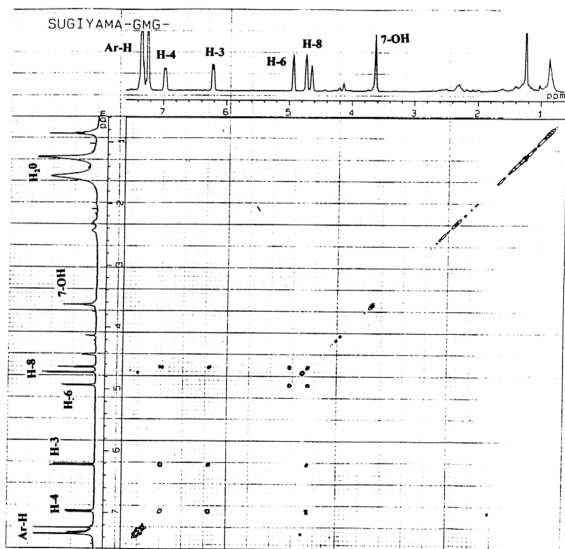
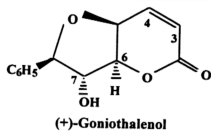
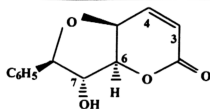


Figure 4. 73: Long-range  $^1\text{H}$ - $^1\text{H}$  COSY spectrum of (+)-goniothalenol



(+)-Goniothalenol

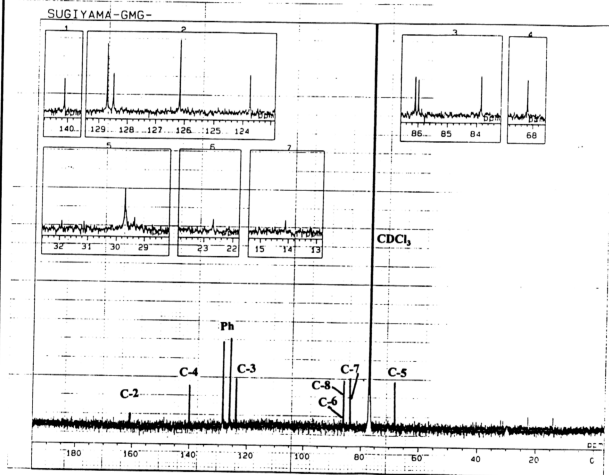
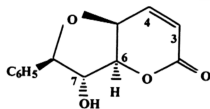


Figure 4. 74: <sup>13</sup>C NMR spectrum of (+)-goniothalenol (400 MHz, CDCl<sub>3</sub>)





(+)-Goniothalenol

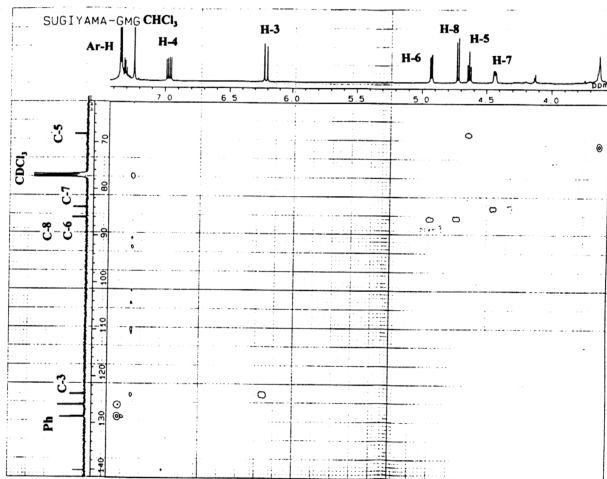
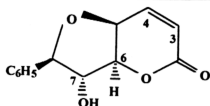


Figure 4. 75: HSQC spectrum of (+)-goniothalenol



(+)-Goniothalenol

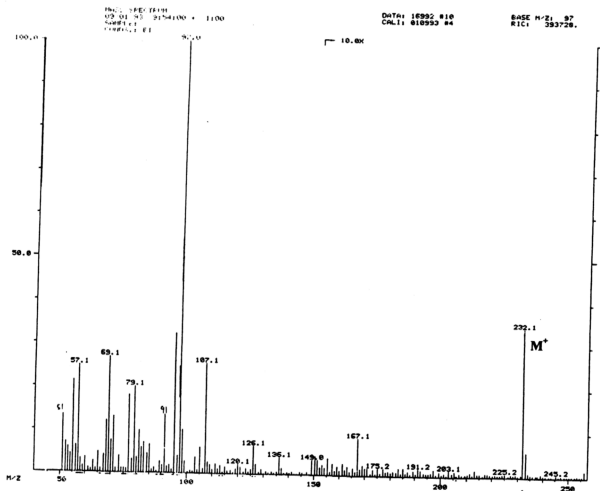
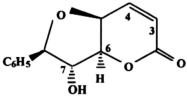


Figure 4. 76: EIMS spectrum of (+)-goniothalenol

**Table 4. 41:  $^1\text{H}$  -  $^{13}\text{C}$  connectivities obtained from  $^1\text{H}$  -  $^{13}\text{C}$  HETCOR experiment for (+)-goniothalenol**

Proton resonance	Connectivity
6.22 (H-3)	123.8
6.97 (H-4)	140.1
4.64 (H-5)	68.2
4.93 (H-6)	86.0
4.44 (H-7)	83.8
4.73 (H-8)	86.1

**Table 4. 42:  $^{13}\text{C}$  NMR ( $\delta$ ) assignments for goniothalenol (67.8 MHz,  $\text{CDCl}_3$ )**

Carbon	$\delta$	 <p>(+)-Goniothalenol</p>
C-2 (C=O)	161.8	
C-3	123.8	
C-4	140.1	
C-5	68.2	
C-6	86.0	
C-7	83.8	
C-8	86.1	
C-1'	138.1	
C-2', C-6'	126.2	
C-3', C-5'	128.7	
C-4'	128.5	

#### 4.2.16.1 Synthesis of goniiothalenol

Tadano *et al.* (1988) was able to synthesise (+)-goniiothalenol from L-arabinose.

It is postulated that (+)-goniiothalenol can be synthesised via a cyclisation of 5 $\beta$ -hydroxyisogoniiothalamine epoxide.

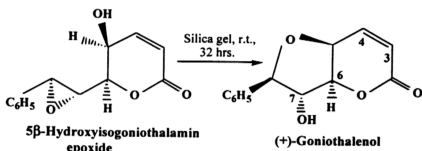


Figure 4. 77: Cyclisation of 5 $\beta$ -hydroxyisogoniiothalamine epoxide

On the other hand, cyclisation of 5 $\beta$ -hydroxygoniiothalamine epoxide could provide the stereoisomer of goniiothalenol, isoalthalactone.

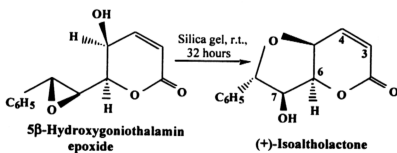
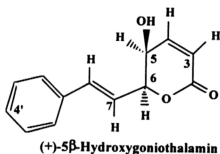


Figure 4. 78: Cyclisation of 5 $\beta$ -hydroxygoniiothalamine epoxide

An attempt was made to synthesise the iso-althalactone from goniiothalamine epoxide by first reacting the epoxide with selenium dioxide to obtain the 5 $\beta$ -

hydroxygoniothalamin epoxide. However, the reaction did not proceed as predicted and instead, the diol was formed. A second attempt was made to synthesise the 5 $\beta$ -hydroxygoniothalamin epoxide starting with 5 $\beta$ -hydroxygoniothalamin and reacting it with MCPBA on a milligram scale but epoxidation failed to occur at C-7 and C-8.

#### 4.2.17 Characterisation of LB21C1 as (+)-5 $\beta$ -hydroxygoniothalamin

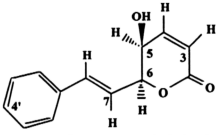


**Figure 4. 79: Structure of (+)-5 $\beta$ -hydroxygoniothalamin**

LB21C1 was isolated as a yellow oil from the ethyl acetate extract of the stem bark of *Goniothalamus dolichocarpus*. Column chromatography of 44 g of the crude ethyl acetate extract of the stem bark of *Goniothalamus dolichocarpus* through silica gel 60 (80-100 mesh) with solvent mixtures of increasing polarity (hexane, hexane-chloroform, chloroform and chloroform-methanol) gave the crude (+)-5 $\beta$ -hydroxygoniothalamin. Repeated SiO<sub>2</sub> column chromatography gave a total yield of 0.003% (140 mg) of the (+)-5 $\beta$ -hydroxygoniothalamin. This compound has an  $[\alpha]_D^{20} = +79^\circ$  (c, 0.2, CHCl<sub>3</sub>). (+)-5 $\beta$ -hydroxygoniothalamin is a new natural product (Goh *et al.*, 1995).

The EIMS gave an  $m/z$  of 216 which is consistent with the molecular formula  $C_{13}H_{12}O_3$  (see Figure 4.84). The HREIMS gave 216.0787 for  $C_{13}H_{12}O_3$  (calculated 216.0786). Other fragments in the EIMS were 198 (71.6%), 170 (35.4%), 155 (21.9%), 141 (50.5%), 128 (21.3%), 115 (100%), 105 (20.9%).

**Table 4. 43:**  $^1\text{H}$  NMR ( $\delta$ ) assignments for (+)-5 $\beta$ -hydroxygoniothalamin (270 MHz,  $\text{CDCl}_3$ )

Proton	$\delta$	$J(\text{Hz})$	 <p>(+)-5<math>\beta</math>-Hydroxygoniothalamin</p>
H-3	6.12, d	9.8	
H-4	6.97, dd	5.4, 9.8	
H-5	4.25, m	-	
H-6	5.03, ddd	2.9, 6.4, 1.5	
H-7	6.31, dd	6.4, 16.1	
H-8	6.81, brd	16.1	
5-OH	2.10, brs	-	
Ph	7.30, m	-	
Ph	7.30, m	-	

The  $^1\text{H}$  NMR assignments were carried out using  $^1\text{H}$  -  $^1\text{H}$  COSY experiment.

**Table 4. 44:**  $^1\text{H}$ -  $^1\text{H}$  connectivities obtained from  $^1\text{H}$  -  $^1\text{H}$  COSY experiment for (+)-5 $\beta$ -hydroxygoniothalamin

Proton resonance	Connectivity
6.12 (H-3)	6.97 (H-4)
6.97 (H-4)	6.12 (H-3), 4.25 (H-5)
4.25 (H-5)	6.97 (H-4), 5.03 (H-6)
5.03 (H-6)	4.25 (H-5), 6.31 (H-7)
6.31 (H-7)	5.03 (H-6), 6.81 (H-8)
6.81 (H-8)	6.31 (H-7)

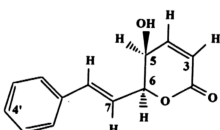
The  $^1\text{H}$  NMR (270 MHz,  $\text{CDCl}_3$ ) spectrum showed a broad doublet at  $\delta$  6.81 for H-8 and a coupling constant value of 16.1 Hz for coupling between H-8 and H-7. A doublet of doublet at  $\delta$  6.31 was assigned to H-7. This gave coupling constant values of 16.1 and 6.4 Hz for coupling with H-8 and H-6 respectively. A ddd at  $\delta$

5.03 with coupling constant values of 2.9, 6.4 and 1.5 Hz was assigned to H-6 and coupling with H-5, H-7 and H-8, respectively. H-5 gave a multiplet signal at  $\delta$  4.25. A broad singlet at  $\delta$  2.10 was assigned to the 5-OH. H-4 gave a doublet of doublet signal at  $\delta$  6.97 with a coupling constant value of 5.4 Hz for coupling with H-5 and 9.8 Hz for coupling with H-3. A doublet with a coupling constant value of 9.8 Hz at  $\delta$  6.12 was assigned to H-3. The phenyl protons gave a multiplet signal at  $\delta$  7.30 (see Tables 4.43 and 4.44 and Figure 4.80). The  $^{13}\text{C}$  assignments were obtained from  $^1\text{H}$  -  $^{13}\text{C}$  connectivities in the HETCOR experiment (see Tables 4.45 and 4.46 and Figure 4.81).

**Table 4. 45:  $^1\text{H}$  -  $^{13}\text{C}$  connectivities obtained from  $^1\text{H}$  -  $^{13}\text{C}$  HETCOR experiment for (+)-5 $\beta$ -hydroxygoniothalamin**

Proton resonance	Connectivity
6.12 (H-3)	121.5
6.97 (H-4)	144.4
4.25 (H-5)	63.1
5.03 (H-6)	80.9
6.31 (H-7)	135.3
6.81 (H-8)	123.0

**Table 4. 46:  $^{13}\text{C}$  NMR ( $\delta$ ) assignments for (+)-5 $\beta$ -hydroxygoniothalamin (67.8 MHz,  $\text{CDCl}_3$ )**

Carbon	$\delta$	 <p>(+)-5<math>\beta</math>-Hydroxygoniothalamin</p>
C-2	163.0	
C-3	121.5	
C-4	144.4	
C-5	63.1	
C-6	80.9	
C-7	135.3	
C-8	123.0	
C-1'	135.6	
C-2', C-6'	126.8	
C-3', C-5'	128.7	
C-4'	128.6	

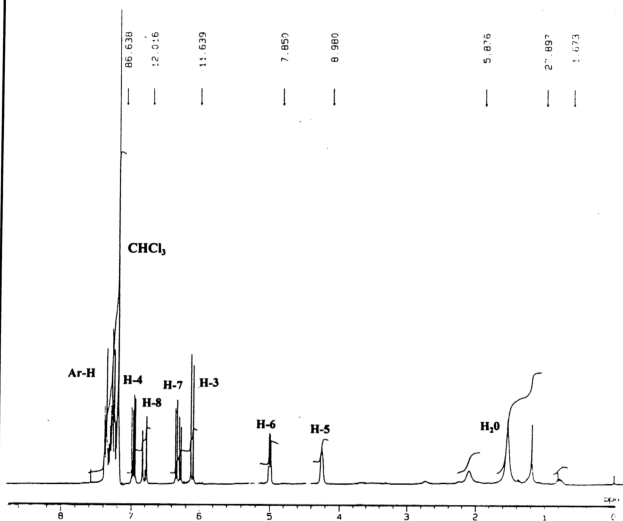
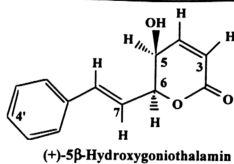


Figure 4. 80: <sup>1</sup>H NMR spectrum of (+)-5β-hydroxygoniothalamin (270 MHz, CDCl<sub>3</sub>)



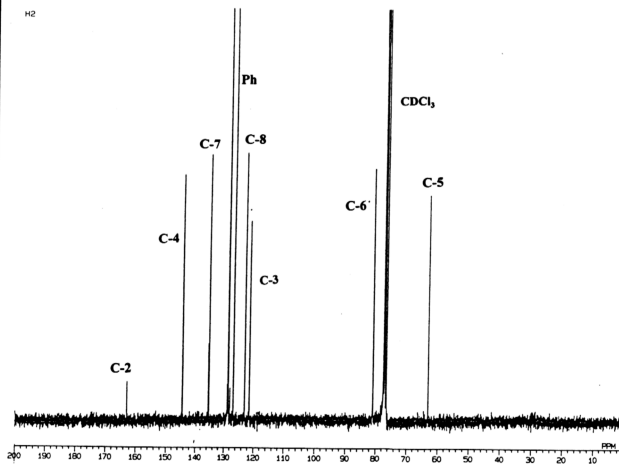
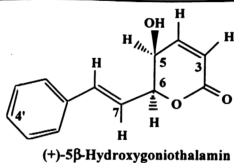
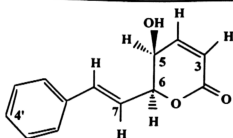


Figure 4. 81:  $^{13}\text{C}$  NMR spectrum of (+)-5β-hydroxygoniothalamin (67.8 MHz,  $\text{CDCl}_3$ )



(+)-5β-Hydroxygoniothalamin

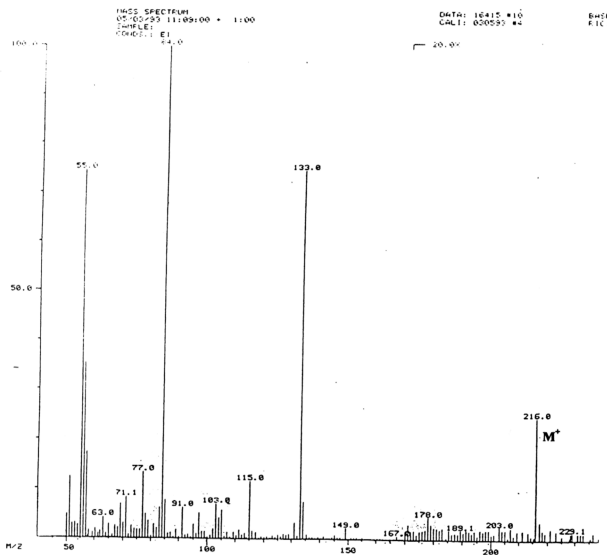


Figure 4. 82: EIMS spectrum of (+)-5β-hydroxygoniothalamin

$^1\text{H}$ - $^1\text{H}$  COSY,  $^1\text{H}$ - $^{13}\text{C}$  HETCOR and NOE difference spectra were used to assign the structure of 5 $\beta$ -hydroxygoniothalamin. A coupling constant of 2.9 Hz between H-5 and H-6 indicates a dihedral angle of approximately 50°. Moreover, the acetate derivative also shows a similar  $J_{5,6}$  coupling of 2.9 Hz. there is no NOE enhancement between H-7 and H-5. With the absolute configuration of (+)-6*R*-goniothalamin known, the absolute configuration of (+)-5 $\beta$ -hydroxygoniothalamin and its acetate can be assigned as 5*S*, 6*S*. This finding of a simple hydroxylated derivative of the more abundant goniothalamin epoxide can arise to provide (after hydroxyl attack on the epoxide) known natural products such as isoaltholactone and goniopyrpyrone reported previously from some *Goniothalamus* species (Colegate *et al.*, 1990; Fang *et al.*, 1990).

IR ( $\nu_{\text{max}}$   $\text{cm}^{-1}$ ): 3407, 1725, 1636, 1495, 1453, 1375, 1251, 970, 742. UV ( $\lambda_{\text{max}}$ , EtOH, nm): 249 (log  $\epsilon$  3.84).

#### 4.2.18 (-)-5 $\beta$ -Acetoxygoniothalamin

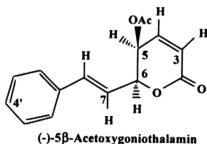
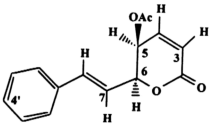


Figure 4. 83: Structure of (-)-5 $\beta$ -acetoxygoniothalamin

5 $\beta$ -Hydroxygoniothalamin was acetylated with acetic anhydride and pyridine to provide (-)-5 $\beta$ -acetoxygoniothalamin ( $[\alpha]_{\text{D}}^{20} = -372$  (c, 0.2,  $\text{CHCl}_3$ ) (Lit. - 325)

(Ahmad *et al.*, 1991). The EIMS of (-)-5 $\beta$ -acetoxyniothalamine gave an  $M^{+}$  of 258 (21.7%) which is consistent with the molecular formula  $C_{15}H_{14}O_4$ . Other observed fragments were 216 [ $M^{+} - C_2H_2O$ ] (2.8%), 198 [ $M^{+} - CH_3COOH$ ] $^{+}$  (17.5%), 175 [ $C_{11}O_{11}O_2$ ] (18.2%), 133 [ $C_9H_9O$ ] $^{+}$  (78.1%), 126 [ $C_6H_6O_3$ ] $^{+}$  (66.1%), 115 [ $C_9H_7$ ] $^{+}$  (24.6%), 84 [ $C_3H_4O_2$ ] $^{+}$  (98.8%), 77 ( $C_6H_5$ ) $^{+}$  (23.4%) and 42 ( $C_2H_2O$ ) $^{+}$  (100%). The  $^1H$  NMR (270 MHz,  $CDCl_3$ ) gave a doublet of doublet at  $\delta$  7.01 with coupling constant values of 9.8 and 5.4 Hz. This signal was assigned to H-4 ( $J_{4,3} = 9.8$  Hz,  $J_{4,5} = 5.4$  Hz). H-3 gave a signal at  $\delta$  6.27 as a doublet, with a coupling constant value of 9.8 Hz. This is for coupling between H-3 and H-4. A doublet of doublet at  $\delta$  5.37 was assigned to H-5. A coupling constant value of 2.9 Hz for coupling between H-5 and H-6 is consistent with the 2.9 Hz for coupling between H-5 and H-6 in the 5 $\beta$ -hydroxyniothalamine. This confirms the dihedral angle of approximately 50 $^{\circ}$  between H-5 and H-6. The  $J$  value of H-4 and H-5 was calculated to be 5.4 Hz. A doublet of doublet at  $\delta$  5.19 with coupling constant values of 2.9 and 6.3 Hz was assigned to H-6. ( $J_{6,5} = 2.9$  Hz,  $J_{6,7} = 6.3$  Hz). H-7 gave a doublet of doublet as well at  $\delta$  6.22. The coupling constant values of 6.3 and 15.6 Hz were for coupling between H-7 and H-6 and between H-7 and H-8 which are *trans* to each other. H-8, however, gave a doublet of doublet at  $\delta$  6.83 with  $J$  values of 15.6 and 1.0 Hz for coupling with H-7 and long range coupling with H-6, respectively. The phenyl protons gave a multiplet at  $\delta$  7.36. The acetate protons gave a singlet at  $\delta$  2.07. The  $^1H$  and  $^{13}C$  values are shown below (see Tables 4.47 and 4.50, Figures 4.84 and 4.85).

**Table 4. 47:**  $^1\text{H}$  NMR ( $\delta$ ) assignments and  $J(\text{Hz})$  values for (-)-5 $\beta$ -acetoxygoniothalamin (270 MHz,  $\text{CDCl}_3$ )

Proton	$\delta$	$J(\text{Hz})$	 <p>(-)-5<math>\beta</math>-Acetoxygoniothalamin</p>
H-3	6.27, d	9.8	
H-4	7.01, dd	9.8, 5.4	
H-5	5.37, dd	2.9, 5.4	
H-6	5.17, dd	2.9, 6.3	
H-7	6.22, dd	6.3, 15.6	
H-8	6.83, dd	15.6, 1.0	
Ph	7.36, m		
OAc	2.07, s		

**Table 4. 48:**  $^1\text{H}$  -  $^1\text{H}$  connectivities obtained from  $^1\text{H}$  -  $^1\text{H}$  COSY experiment for (-)-5 $\beta$ -acetoxygoniothalamin

Proton resonance	Connectivity
6.27 (H-3)	7.01 (H-4)
7.01 (H-4)	6.27 (H-3), 5.37 (H-5)
5.37 (H-5)	7.01 (H-4), 5.19 (H-6)
5.19 (H-6)	5.37 (H-5), 6.22 (H-7)
6.22 (H-7)	5.19 (H-6), 6.83 (H-8)
6.83 (H-8)	6.22 (H-7), 5.19 (LR) (H-6)

LR refers to long range coupling

**Table 4. 49:**  $^1\text{H}$  -  $^{13}\text{C}$  connectivities obtained from  $^1\text{H}$  -  $^{13}\text{C}$  HETCOR experiment for (-)-5 $\beta$ -acetoxygoniothalamin

Proton resonance	Connectivity
6.27 (H-3)	121.0
7.01 (H-4)	140.6
5.37 (H-5)	63.9
5.19 (H-6)	79.1
6.22 (H-7)	134.8
6.83 (H-8)	124.7

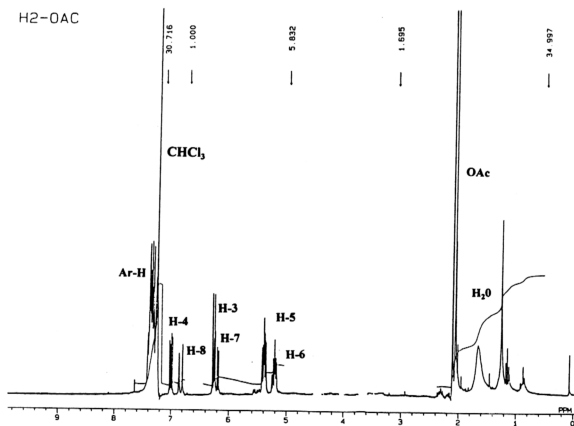
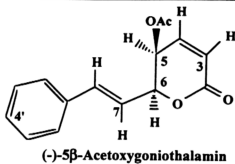


Figure 4. 84:  $^1\text{H}$  NMR spectrum of (-)-5 $\beta$ -acetoxygoniothalamine (270 MHz,  $\text{CDCl}_3$ )

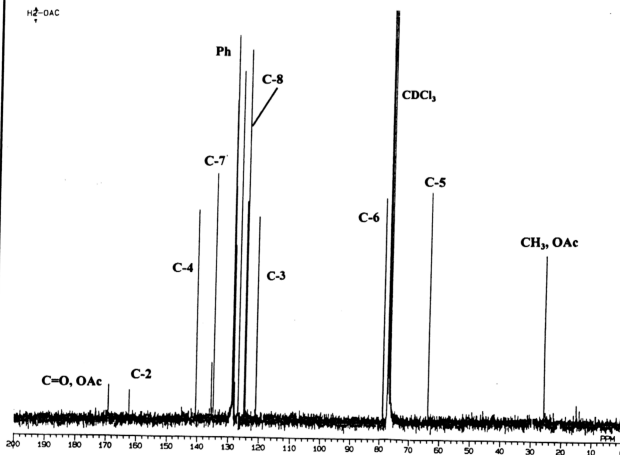
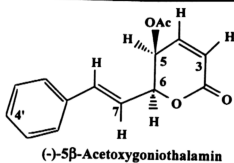
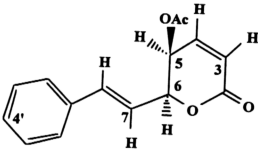


Figure 4. 85:  $^{13}\text{C}$  NMR spectrum of (-)-5β-acetoxygoniothalamine (67.8 MHz,  $\text{CDCl}_3$ )

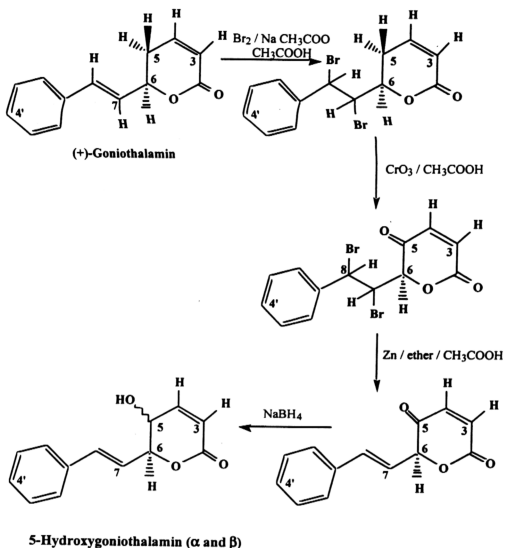
**Table 4. 50:**  $^{13}\text{C}$  NMR assignments for (-)-5 $\beta$ -acetoxygoniothalamine (67.8 MHz,  $\text{CDCl}_3$ )

Carbon	$\delta$	
C-2	162.3	 <p style="text-align: center;">(-)-5<math>\beta</math>-Acetoxygoniothalamine</p>
C-3	121.0	
C-4	140.6	
C-5	63.9	
C-6	79.1	
C-7	134.8	
C-8	124.7	
C-1'	135.6	
C-2', C-6'	126.7	
C-3', C-5'	128.7	
C-4'	128.5	
Methyl, OAc	20.5	
C = O, OAc	169.9	

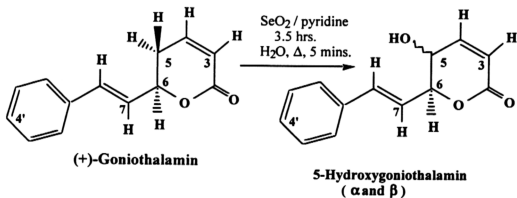
#### 4.2.18.1 Syntheses of 5 $\beta$ -hydroxygoniothalamine and 5 $\alpha$ -hydroxygoniothalamine

Several unsuccessful attempts were carried out to synthesise the 5-hydroxygoniothalamine based on the assumption that the following pathways would lead to the required compound.





(1)



(2)

Figure 4. 86: Attempted syntheses of 5-hydroxygoniothalamin (Smith, 1994)

Bromination had occurred at the styryl double bond as was observed by the disappearance of the H-7 doublet of doublet at  $\delta$  6.28 and the H-8 doublet at  $\delta$  6.73. This indicated the disappearance of the styryl double bond. Instead H-7 appeared at  $\delta$  4.66 as a broad doublet and H-8 at  $\delta$  5.61 as another broad double with coupling constant values of 11.5 Hz. H-3 and H-4 signals remain unchanged at  $\delta$  6.18 and  $\delta$  7.06 with  $J$  values of 9.8 Hz and 1.9 Hz for H-3 and 9.8 Hz and 4.2 Hz for H-4.

(+)-5 $\beta$ -Hydroxygoniothalamin and its diastereomer (+)-5 $\alpha$ -hydroxygoniothalamin were finally synthesised by reacting goniothalamin with selenium dioxide and refluxing in dioxane in a 0.6% and 6.8% yield respectively. (+)-5 $\alpha$ -hydroxygoniothalamin crystallised from dichloromethane-cyclohexane as plates.

#### 4.2.19 (+)-5 $\alpha$ -Hydroxygoniothalamin

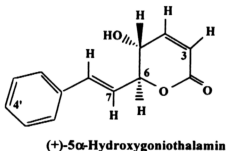
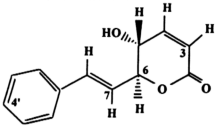


Figure 4. 87: Structure of (+)-5 $\alpha$ -hydroxygoniothalamin

(+)-5 $\alpha$ -Hydroxygoniothalamin crystallised as plates with a melting point of 98 °C from dichloromethane-cyclohexane  $[\alpha]_D^{20} = +18^{\circ}$  (c, 0.3, CHCl<sub>3</sub>). The EIMS of (+)-5 $\alpha$ -hydroxygoniothalamin gave an  $M^{+}$  of 216 (9.8%) which is consistent with the

molecular formula  $C_{13}H_{12}O_3$ . The HREIMS gave 216.0785 for  $C_{13}H_{12}O_3$  (calculated 216.0786). Other fragments were 198 (62.0%), 170 (43.0%), 155 (43.2%), 154 (40.2%), 141 (40.2%), 128 (48.2%), 115 (10.0%) and 105 (50.4%).

**Table 4. 51:**  $^1\text{H}$  NMR ( $\delta$ ) assignments and  $J$  values for (+)-5 $\alpha$ -hydroxygoniothalamin (270 MHz,  $\text{CDCl}_3$ )

Proton	$\delta$	$J(\text{Hz})$	 <p>(+)-5<math>\alpha</math>-Hydroxygoniothalamin</p>
H-3	5.97, dd	9.8, 2.0	
H-4	6.83, dd	9.8, 2.0	
H-5	4.36, m	-	
H-6	4.80, ddd	8.0, 7.3, 1.5	
H-7	6.17, dd	7.3, 15.6	
H-8	6.74, brd	15.6	
5-OH	2.35, d	4.4	

**Table 4. 52:**  $^1\text{H}$ - $^1\text{H}$  connectivities obtained from  $^1\text{H}$ - $^1\text{H}$  COSY experiment for (+)-5 $\alpha$ -hydroxygoniothalamin

Proton resonance	Connectivity
5.97 (H-3)	6.83 (H-4), 4.36 (LR) (H-5)
6.83 (H-4)	5.97 (H-3), 4.36 (H-5)
4.36 (H-5)	6.83 (H-4), 4.80 (H-6)
4.80 (H-6)	4.36 (H-5), 6.17 (H-7), 6.74 (LR) (H-8)
6.17 (H-7)	4.80 (H-6), 6.74 (H-8)
6.74 (H-8)	6.17 (H-7)
2.35 (5-OH)	4.36 (H-5)

LR refers to long range coupling

The  $^1\text{H}$  NMR (270 MHz,  $\text{CDCl}_3$ ) gave a doublet of doublet at  $\delta$  5.97 with coupling constant values of 9.8 and 2.0 Hz for H-3 and another doublet of doublet at  $\delta$  6.83 with coupling constant values of 9.8 and 2.0 Hz for H-4. H-5 gave a multiplet signal at  $\delta$  4.36 while the 5-OH appeared as a doublet at  $\delta$  2.35 with a coupling constant value of 4.4 Hz for coupling of the proton of the OH with H-5. A ddd at  $\delta$  4.80 with  $J$  values of 8.0 Hz ( $J_{5,6}$ ), 7.3 Hz ( $J_{7,6}$ ) and 1.5 Hz ( $J_{6,8}$ ) was assigned to H-6.

A coupling constant value of 8.0 Hz between H-5 and H-6 in this compound indicates the two protons to be approximately of diaxial orientation (see Tables 4.51 and 4.52, Figures 4.89 and 4.90). Similarly, a relatively large value of 6 Hz was observed for the acetate derivative of the compound. There is NOE enhancement between H-7 and H-5 in this compound as well as in its acetate derivative (see Figure 4.93). H-5 and H-7 thus assumes the diaxial geometry. There is also observed a long range coupling ( $J = 2.0$  Hz) between H-3 and H-5. This was also seen in the  $^1\text{H}$  NMR of the acetate derivative ( $J = 1.0$  Hz). With the absolute configuration of (+)-6*R*-goniothalamine known, the absolute configuration of 5 $\alpha$ -hydroxygoniothalamine is 5*R*, 6*S*. The  $^{13}\text{C}$  NMR values were assigned with the help of  $^1\text{H}$ - $^{13}\text{C}$  HETCOR experiment and by comparing with the  $^{13}\text{C}$  values for (+)-5 $\beta$ -hydroxygoniothalamine (see Tables 4.53 and 4.54, Figures 4.91 and 4.92).

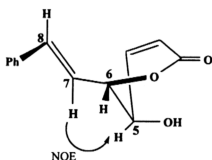
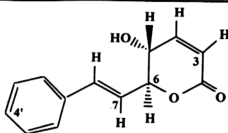


Figure 4. 88: NOE enhancement for 5 $\alpha$ -hydroxygoniothalamine

Table 4. 53:  $^1\text{H}$  - $^{13}\text{C}$  connectivities obtained from  $^1\text{H}$  - $^{13}\text{C}$  HETCOR experiment for (+)-5 $\alpha$ -hydroxygoniothalamine

Proton resonance	Connectivity
5.97 (H-3)	120.8
6.83 (H-4)	148.0
4.36 (H-5)	66.0
4.80 (H-6)	83.3
6.17 (H-7)	135.3
6.74 (H-8)	123.0



(+)-5 $\alpha$ -Hydroxygoniothalamin

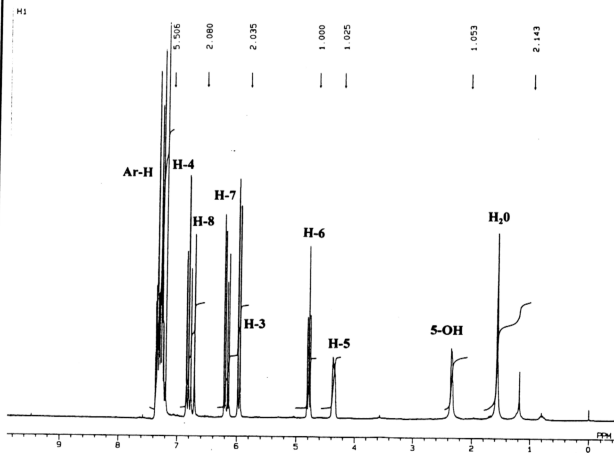
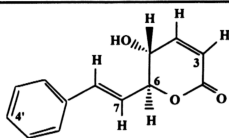


Figure 4. 89:  $^1\text{H}$  NMR spectrum of (+)-5 $\alpha$ -hydroxygoniothalamin (270 MHz,  $\text{CDCl}_3$ )



(+)-5 $\alpha$ -Hydroxygoniothalamin

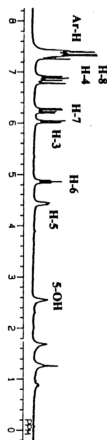
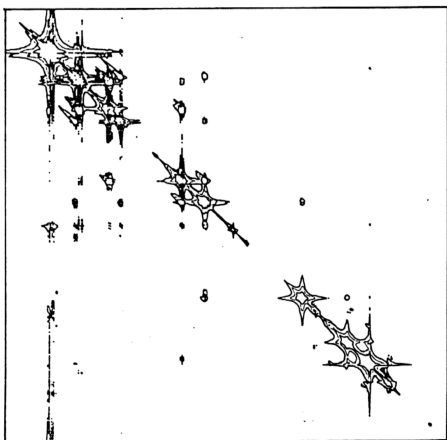
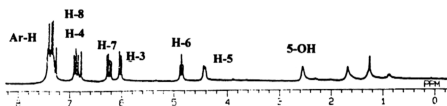
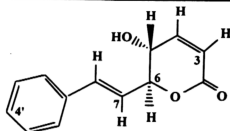


Figure 4. 90:  $^1\text{H}$ - $^1\text{H}$  COSY spectrum of (+)-5 $\alpha$ -hydroxygoniothalamin



(+)-5 $\alpha$ -Hydroxygoniothalamin

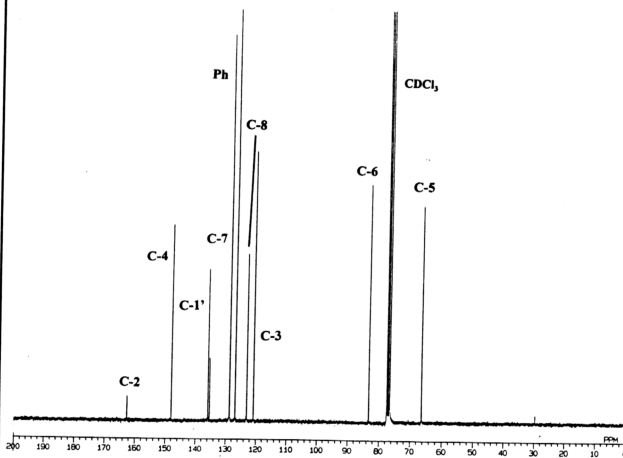
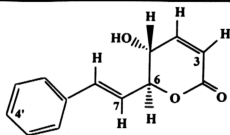


Figure 4. 91:  $^{13}\text{C}$  NMR spectrum of (+)-5 $\alpha$ -hydroxygoniothalamin (67.8 MHz,  $\text{CDCl}_3$ )



(+)-5 $\alpha$ -Hydroxygoniothalamin

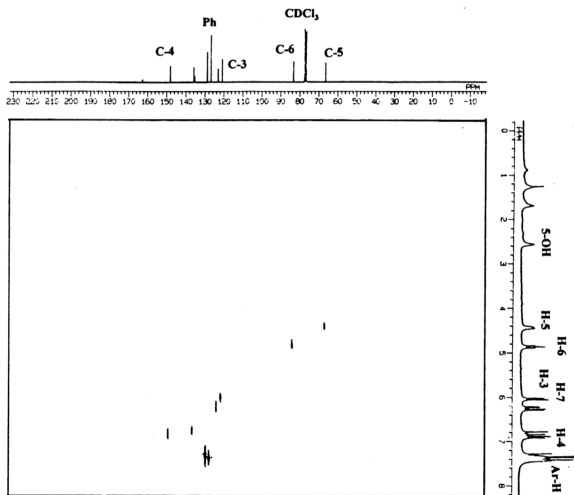
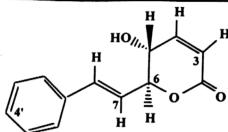


Figure 4. 92:  $^1\text{H}$ - $^{13}\text{C}$  HETCOR spectrum of (+)-5 $\alpha$ -hydroxygoniothalamin





(+)-5 $\alpha$ -Hydroxygoniothalamin

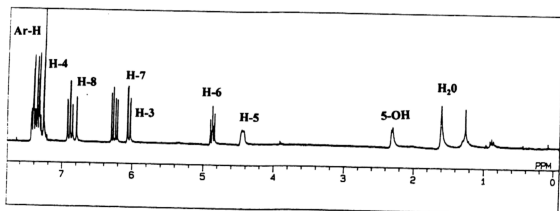
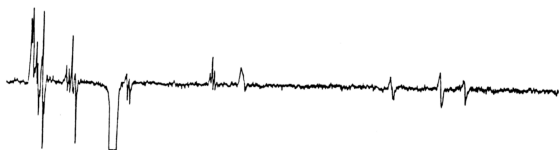
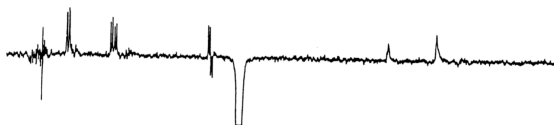
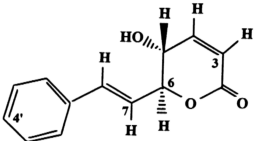


Figure 4. 93: NOE difference spectra of (+)-5 $\alpha$ -hydroxygoniothalamin

**Table 4. 54:**  $^{13}\text{C}$  NMR ( $\delta$ ) assignments for (+)-5 $\alpha$ -hydroxygoniothalamin (67.8 MHz,  $\text{CDCl}_3$ )

Carbon	$\delta$	
C-2	162.6	
C-3	120.8	
C-4	148.0	
C-5	66.0	
C-6	83.3	
C-7	135.3	
C-8	123.0	
C-1'	135.8	
C-2', C-6'	126.8	
C-3, C-5'	128.8	
C-4'	128.7	<p><b>(+)-5<math>\alpha</math>-Hydroxygoniothalamin</b></p>

(+)-5 $\alpha$ -Hydroxygoniothalamin crystals were subjected to single crystal X-ray crystallography for stereochemical determination. The crystal system is orthorhombic, crystal size, 0.20 x 0.30 x 0.50 mm<sup>3</sup> and the intensities were measured with MoK $\alpha$  graphite-monochromatised radiation ( $\lambda = 0.71073$  Å). The group is P2<sub>1</sub>2<sub>1</sub>2<sub>1</sub> (No. 19),  $M_r$  216.2,  $a = 4.838(1)$  Å,  $b = 5.959(1)$ ,  $c = 39.023(8)$ ,  $V = 1124.9(4)$  Å<sup>3</sup>,  $z = 4$ ,  $F(000) = 456$ ,  $R_f = 0.045$ ,  $D_c = 1.28$  gcm<sup>-3</sup>. The scan type was  $\omega$ -scan; 3.00-30.00 deg min<sup>-1</sup>. 1018 unique data was measured, observed data with  $|F_o| > 4\sigma(|F_o|)$ .  $n = 702$ ,  $wR = [\sum w(|F_o| - |F_c|)^2 / \sum w|F_o|^2]^{1/2} = 0.044$  (Figure 4.94 and Appendix 5). Raw intensities were collected on a Siemens P4/PC four-circle diffractometer at room temperature (291 °K). The crystal structure was solved by direct phase determination. All non-hydrogen atoms were subjected to anisotropic refinement. The hydrogen atom of the hydroxy group was located on a different Fourier map, and the other hydrogen atoms were generated geometrically (C-H bonds fixed at 0.96 Å) and allowed to ride on their respective parent C atoms; they were assigned the same

isotropic temperature factors ( $U = 0.08 \text{ \AA}^2$ ) and included in the structure-factor calculations. Computation were performed using the SHELTXL PC program package (Sheldrick, 1989; Sheldrick, 1990) on a PC486 computer. Analytic expressions of atomic scattering factors were employed, and anomalous dispersion corrections were incorporated.

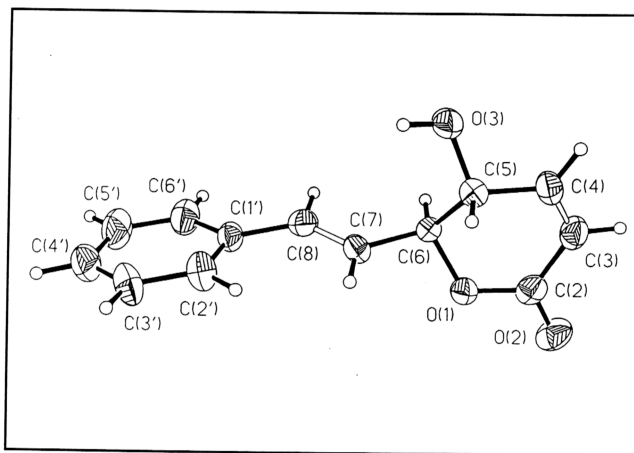


**Figure 4. 94: A perspective view of (+)-5 $\alpha$ -hydroxygoniothalamin**

The configuration of (+)-5 $\alpha$ -hydroxygoniothalamin is hence 5*R*, 6*S*. An intermolecular hydrogen bond is formed between O(3) and O(2a) ( $a = -1 + x, 1 + y, z$ )

with  $O(3) \cdots O(2a) = 2.833 \text{ \AA}$ ,  $H(30) \cdots O(2a) = 1.962 \text{ \AA}$ .  $C(5) - O(3) \cdots O(2a) = 123.7^\circ$ ,  $C(2a) - O(2a) \cdots O(3) = 136.4^\circ$ , and  $O(3) - H(30) \cdots O(2a) = 158.6^\circ$ .

IR ( $\nu_{\max} \text{ cm}^{-1}$ ): 3400, 1728, 1490, 1370, 1243, 970, 740. UV ( $\lambda_{\max}$ , EtOH, nm):

251 (log  $\epsilon$  4.13).

### 3.2.19.1 Mechanism of reaction

This reaction involved the oxidation of an allylic C-H fragment to the corresponding allylic alcohol (Smith, 1994). The reaction of  $\text{SeO}_2$  and allylic molecule proceeds via an initial Ene reaction. A 2,3-sigmatropic shift gives the selenol.

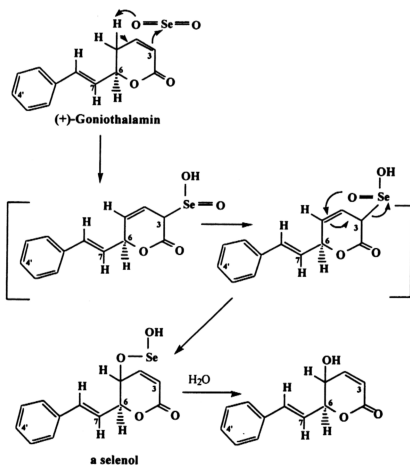


**Figure 4. 95: Mechanism for the oxidation of goniothalamin to (+)-5β-hydroxygoniothalamin**

#### 4.2.20 (-)-5 $\alpha$ -Acetoxygoniothalamin

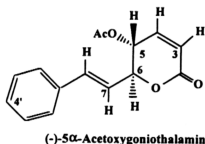


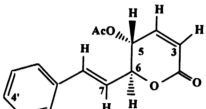
**Figure 4. 96: Structure of(-)-5 $\alpha$ -acetoxygoniothalamin**

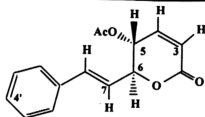
5 $\alpha$ -Hydroxygoniothalamin was acetylated by acetic anhydride and pyridine to (-)-5 $\alpha$ -acetoxygoniothalamin. Recrystallised (-)-5 $\alpha$ -acetoxygoniothalamin (chloroform) has a melting point of 88 °C and  $[\alpha]_D^{20}$  - 150° (c, 0.2; CHCl<sub>3</sub>). The EIMS gave a  $m/z$  = 198 (77%) which is a loss of a molecule of acetic acid from C<sub>15</sub>H<sub>14</sub>O<sub>4</sub> (258). Other fragments were 133 (33%), 126 (31%), 115 (13%), 84 (100%), 77 (14%) and 44 (79%). The <sup>1</sup>H NMR (270 MHz, CDCl<sub>3</sub>) gave a doublet of doublet at  $\delta$  6.05 for H-3 with coupling constant values of 10.0 Hz for coupling of H-3 to H-4 and 1.0 Hz for long range coupling between H-3 and H-5. A dd at  $\delta$  6.75 with coupling constant values of 10.0 Hz ( $J_{3,4}$ ) and 3.0 Hz ( $J_{4,5}$ ) was assigned to H-4. H-5 gave a ddd signal at  $\delta$  5.39 with coupling constant values of 1.0, 3.0 and 6.0 Hz for long range coupling between H-5 and H-3, coupling between H-5 and H-4, and between H-5 and H-6, respectively. This small long range coupling 1.0 Hz between H-3 and H-5 is consistent with that found in the hydroxy compound. A 3-proton singlet at  $\delta$  2.05 was assigned to the methyl of the acetate group. A ddd at  $\delta$  5.05

(coupling constant values 6.0, 6.4 and 1.0 Hz) was assigned to H-6. The coupling between H-6 and H-5 with a relatively large value of 6 Hz is consistent with the observation of a large coupling constant value between H-6 and H-5 in the original compound again indicating the two protons to be approximately of diaxial orientation. There was also an NOE interaction between H-5 and H-7. H-5 and H-7 thus assumes a diaxial geometry. H-7 gave a signal at  $\delta$  6.11 (doublet of doublet) with coupling constant values of 6.4 Hz ( $J_{6-7}$ ) and 16.0 Hz ( $J_{7-8}$ ). Lastly, the doublet of doublet at  $\delta$  6.67 with coupling constant values of 16.0 Hz ( $J_{7-8}$ ) and 1.0 Hz ( $J_{6-8}$ ) was assigned to H-8. The aromatic protons gave a multiplet signal at  $\delta$  7.28 (see Tables 4.55 and 4.56, Figure 4.97).

IR ( $\nu_{\max}$   $\text{cm}^{-1}$ ): 1735, 1660, 1580, 1495, 1374, 1233, 966, 741. UV ( $\lambda_{\max}$ , EtOH, nm): 251 (log  $\epsilon$  4.15).

**Table 4. 55:  $^1\text{H}$  NMR ( $\delta$ ) assignments and  $J(\text{Hz})$  values for (-)-5 $\alpha$ -acetoxygoniothalamine**

Proton	$\delta$	$J(\text{Hz})$	 <p>(-)-5<math>\alpha</math>-Acetoxygoniothalamine</p>
H-3	6.05, dd	10.0, 1.0	
H-4	6.75, dd	10.0, 3.0	
H-5	5.39, ddd	1.0, 3.0, 6.0	
H-6	5.05, ddd	6.0, 6.4, 1.0	
H-7	6.11, dd	6.4, 16.0	
H-8	6.67, dd	16.0, 1.0	
OAc	2.05, s	-	
Ph	7.28, m	-	



(-)-5 $\alpha$ -Acetoxygoniothalamin

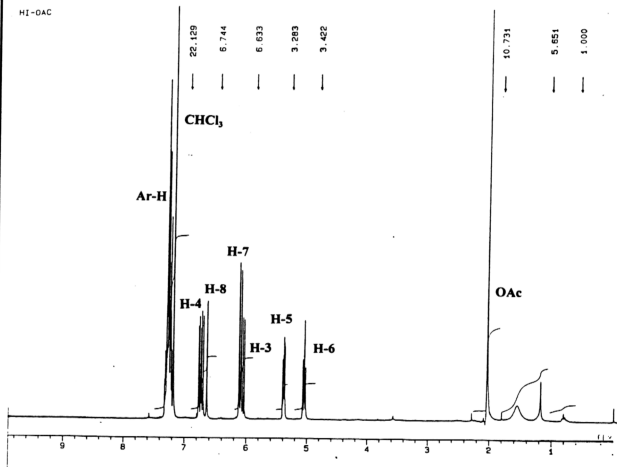
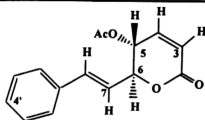


Figure 4. 97:  $^1\text{H}$  NMR spectrum of (-)-5 $\alpha$ -acetoxygoniothalamin (270 MHz,  $\text{CDCl}_3$ )



(-)-5 $\alpha$ -Acetoxygoniothalamine

H1-OAC

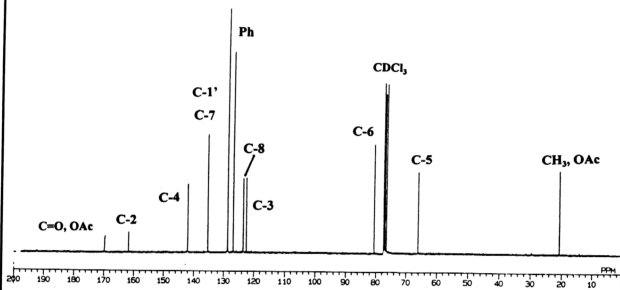
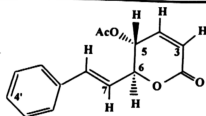


Figure 4. 98:  $^{13}\text{C}$  NMR spectrum of (-)-5 $\alpha$ -acetoxygoniothalamine (67.8 MHz,  $\text{CDCl}_3$ )





(-)-5 $\alpha$ -Acetoxygoniothalamin

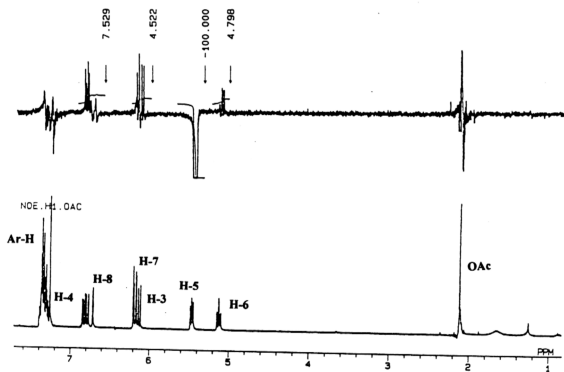


Figure 4. 99: NOE difference spectrum of (-)-5 $\alpha$ -acetoxygoniothalamin

**Table 4. 56:  $^1\text{H}$ - $^1\text{H}$  connectivities obtained from  $^1\text{H}$ - $^1\text{H}$  COSY experiment for (-)-5 $\alpha$ -acetoxygoniothalamin**

Proton resonance	Connectivity
6.05 (H-3)	6.75 (H-4), 5.39 (LR) (H-5)
6.75 (H-4)	6.05 (H-3), 5.39 (H-5)
5.39 (H-5)	6.75 (H-4), 5.05 (H-6), 6.05 (LR) (H-3)
5.05 (H-6)	5.39 (H-5), 6.11 (H-7), 6.67 (LR) (H-8)
6.11 (H-7)	5.05 (H-6), 6.67 (H-8)
6.67 (H-8)	6.11 (H-7), 5.05 (LR) (H-6)

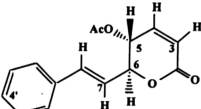
LR refers to long range coupling

The  $^{13}\text{C}$  NMR assignments were carried out using  $^1\text{H}$ - $^{13}\text{C}$  HETCOR and by comparing with previous assignments for (-)-5 $\beta$ -acetoxygoniothalamin. The  $^{13}\text{C}$  NMR values are shown in Table 4.58 (see Figure 4.98).

**Table 4. 57:  $^1\text{H}$ - $^{13}\text{C}$  connectivities obtained from  $^1\text{H}$ - $^{13}\text{C}$  HETCOR experiment for (-)-5 $\alpha$ -acetoxygoniothalamin**

Proton resonance	Connectivity
6.05 (H-3)	122.5
6.75 (H-4)	142.1
5.39 (H-5)	66.2
5.05 (H-6)	80.6
6.11 (H-7)	135.3
6.67 (H-8)	123.6
2.05 (OAc)	20.8

**Table 4. 58:  $^{13}\text{C}$  NMR ( $\delta$ ) assignments for (-)-5 $\alpha$ -acetoxygoniothalamin (67.8 MHz,  $\text{CDCl}_3$ )**

Carbon	$\delta$	 <p>(-)-5<math>\alpha</math>-Acetoxygoniothalamin</p>
C-2	161.7	
C-3	122.5	
C-4	142.1	
C-5	66.2	
C-6	80.6	
C-7	135.3	
C-8	123.6	
C-1'	135.4	
C-2', 6'	126.8	
C-3', C-5'	128.5	
C-4'	128.6	
$\text{CH}_3$ of OAc	20.8	
C=O, OAc	170.0	

#### 4.2.21 Characterisation of LBMF 8b, GMC, KHP13b and GV260R as (+)-annonacin

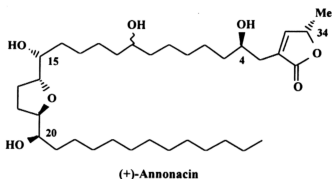


Figure 4. 100: Structure of (+)-annonacin

(+)-Annonacin was isolated as a wax from the methanol soluble fraction of the ethanol extract of *Goniothalamus dolichocarpus*, *Goniothalamus malayanus*, *Goniothalamus velutinus* and *Mezzetia umbellata*. It gave a melting point of 54-56 °C (Lit. 57 °C) (McCloud *et al.*, 1987) and  $[\alpha]_D^{20} + 2.4$  (c, 1.0, CHCl<sub>3</sub>) (Lit. +1.4) (McCloud *et al.*, 1987). The structure was elucidated using NMR and mass spectroscopy and by comparing with the literature values. The EIMS did not display a recognizable molecular ion peak but a peak at  $m/z$  523 ( $M^+ - 4 \times 18 - 1$ ) (5%) was observed. Other peaks which were observed were 449 (485 - 2 x 18) (15%), 379 (397 - 18) (18%), 361 (397 - 2 x 18) (80%), 343 (397 - 3 x 18) (30%), 309 (327 - 18) (20%), 291 (327 - 2 x 18) (7%) and 273 (327 - 3 x 18) (5%) (see Figures 4.101 and 4.110). This implied that the molecule had four hydroxyl groups. The molecular weight was conclusively established from its chemical-ionisation MS spectrum (NH<sub>3</sub>) as 596 and its molecular formula as C<sub>35</sub>H<sub>64</sub>O<sub>7</sub>. Other fragments which were observed were 579 (M + 1 - 18) (50%), 561 (M + 1 - 2 x 18) (100%), 543 (M + 1 - 3 x 18)

(60%) and 525 ( $M + 1 - 4 \times 18$ ) (10%). The fragments 379 ( $397 - H_2O$ ), 361 ( $397 - 2 \times 18$ ) (15%), 343 ( $397 - 3 \times 18$ ) (10%) which resulted from the fragmentation between C-19 and C-20 and losses of one, two and three molecules of water, respectively implied the presence of three hydroxyl group in the chain before C-20. The fragmentation between C-15 and C-16 gave the fragments 309 ( $327 - 18$ ) (40%), 291 ( $327 - 2 \times 18$ ) (25%), 273 ( $327 - 3 \times 18$ ) (15%) and 269 (10%).

The fragmentation between C-10 and C-11 gave fragments 241 (10%), 223 ( $241 - 18$ ) (5%), 205 ( $223 - 18$ ) (5%) and 355 (10%). The fragmentation between C-9 and C-10 gave fragments 193 which resulted from loss of a water molecule from 211 and 367 which also resulted from the loss of one water molecule from fragment 385. Fragmentations also occurred between C-3 and C-4 to give two fragments 111 (10.5%) and 467 ( $485 - 18$ ) (~1%), 449 ( $485 - 2 \times 18$ ) (~1%), 431 ( $485 - 3 \times 18$ ) (5%), 413 ( $485 - 4 \times 18$ ) (5%) and 111 (12%). The fragmentation between C-4 and C-5 gave fragments 141 (5%), and 123 (8%) which resulted from the loss of a molecule of  $H_2O$  from 141 (see Figure 4.109).

These fragments clearly indicated the presence of four hydroxyl groups in the molecule. The compound was silylated using BSTFA. The EIMS for the silylated compound gave a base peak at 73 and indicated an  $M^+$  of 884 (16%). This is consistent with the molecular formula  $C_{47}H_{96}O_7Si_4$  indicating four OTMS group and implying four hydroxyls in the parent molecule. Other observed fragments in the EIMS were 883 ( $M^+ - 1$ ) (16%), 882 ( $M^+ - 2$ ) (18%), 869 ( $M^+ - 15$ ) (46%), 794 ( $M^+ - TMSOH$ ) (30%), 779 ( $M^+ - CH_3 - TMSOH$ ) (56%) and 687 ( $M^+ - 15 - 2TMSOH$ ) (45%). Fragmentation between C-19 and C-20 gave the fragments 613 (2.6%) and

271 (16%). The fragmentation between C-20 and C-21 gave the fragment 169 (14%). This indicated that C-20 contains a hydroxyl group. A loss of a molecule of TMSOH from 613 gave the fragment 523 (7%) which was also observed. A further loss of two water molecules from 523 gave 343 (11%). The fragmentation between C-15 and C-16 gave two fragments 543 (22%) and 341 (10%); the former loses a molecule of TMSOH to give 453 (11%). Hence a hydroxyl group is located at C-15 (see Figures 4.102 and 4.111).

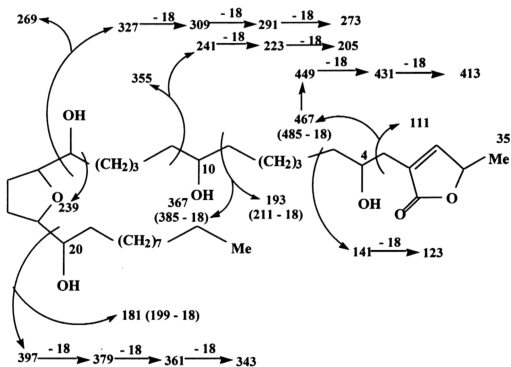
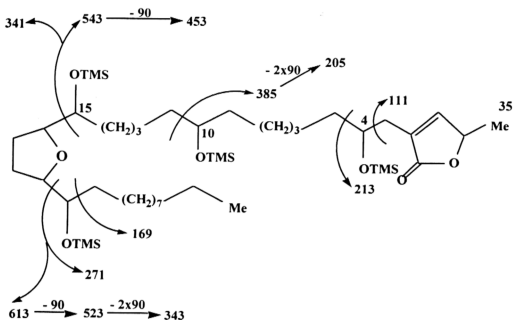


Figure 4. 101: EIMS and CIMS for (+)-annonacin



**Figure 4.102: EIMS for the silylated derivative of (+)-annonacin**

The cleavage of the bond between C-10 and C-11 resulted in the fragment 385 (27%). The fragment 385 loses two molecules of TMSOH to give 205 (4.4%). This confirmed the presence of two hydroxyl groups at C-4 and C-15. The fragment 213 which resulted from fragmentation between C-4 and C-5 and the fragment 111 which was due to the cleavage of the bond between C-3 and C-4 was indicative of the presence of the  $\alpha,\beta$ -unsaturated  $\gamma$ -lactone ring.

The <sup>1</sup>H NMR (270 MHz, CDCl<sub>3</sub>) confirmed the structure of the following fragment which contained the lactone ( $\alpha,\beta$ -unsaturated) and one of the hydroxyl functions (Figure 4.103). The <sup>1</sup>H NMR gave a doublet with a coupling constant value of 6.8 Hz at  $\delta$  1.44 for H-35, a doublet at  $\delta$  7.18 ( $J$  = 1.5 Hz) for H-33, a doublet of

quartet at  $\delta$  5.04 with coupling constant values of 6.8 Hz ( $J_{34-35}$ ) and 1.5 Hz ( $J_{34-33}$ ) for H-34.

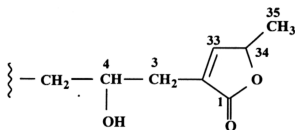
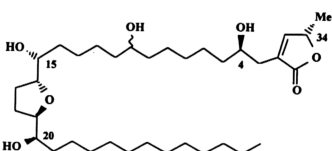


**Figure 4. 103: Structure of the  $\alpha,\beta$ -unsaturated lactone**

A doublet of doublet at  $\delta$  2.40 with coupling constant values of 14.0 Hz ( $J_{3a-3b}$ ) and 8.3 Hz ( $J_{3a-4}$ ) was assigned to H-3a; another doublet of doublet at  $\delta$  2.51 with coupling constant values of 14.0 Hz ( $J_{3b-3a}$ ) and 3.4 Hz ( $J_{3b-4}$ ) was assigned to H-3b. A multiplet at  $\delta$  3.81 was assigned to H-4. These assignments were made from the  $^1\text{H}$ - $^1\text{H}$  COSY spectrum. H-5, H-6, H-7, H-8 and H-9 lie within the methylene envelop at  $\delta$  1.2 -  $\delta$  1.7. A multiplet at  $\delta$  3.58 was assigned to H-10, H-11, H-12, H-13 and H-14 also appeared within the methylene envelop at  $\delta$  1.2 to  $\delta$  1.7. A two-proton multiplet at  $\delta$  3.39 was assigned to H-15 and H-20. Another two-proton multiplet at  $\delta$  3.77 was assigned to H-16 and H-19. H-17 gave a multiplet signal at  $\delta$  1.97 while H-18 also gave a multiplet signal but at  $\delta$  1.67. H-21 up to H-31 also lie within the methylene envelop at  $\delta$  1.2 to  $\delta$  1.7. A triplet at 0.85 with a coupling constant value of 6.6 Hz was assigned to the terminal methyl proton at C-32.  $^1\text{H}$  NMR values are shown in Table 4.59 (see also Figure 4.104).

Table 4. 59:  $^1\text{H}$  NMR ( $\delta$ ) assignments and  $J(\text{Hz})$  values for (+)-annonacin (270 MHz,  $\text{CDCl}_3$ )

Proton	$\delta$	$J(\text{Hz})$
H-3a	2.40, dd	14.0, 8.3
H-3b	2.51, dd	14.0, 3.4
H-4	3.81, m	-
H-5 - H-9	1.2 - 1.7, s	-
H-10	3.58, m	-
H-11 - H-14	1.2 - 1.7, s	-
H-15	3.39, m	-
H-16	3.77, m	-
H-17	1.97, m	-
H-18	1.67, m	-
H-19	3.77, m	-
H-20	3.39, m	-
H-21 - H-31	1.2 - 1.7, s	-
H-32	0.85, t	6.6
H-33	7.18, d	1.5
H-34	5.04, dq	6.8, 1.5
H-35	1.44, d	6.8



(+)-Annonacin

Table 4. 60:  $^1\text{H}$  -  $^1\text{H}$  connectivities obtained from  $^1\text{H}$  -  $^1\text{H}$  COSY experiment for (+)-annonacin

Proton resonance	Connectivity
2.40 (H-3a)	2.51 (H-3b)
	3.81 (H-4)
3.81 (H-4)	2.51 (H-3b)
	1.2 - 1.7 (H-5)
1.2 - 1.7 (H-9)	3.58 (H-10)
3.58 (H-10)	1.2 - 1.7 (H-11)
3.39 (H-15)	3.77 (H-16)
3.77 (H-16)	1.97 (H-17)
1.97 (H-17)	1.67 (H-18)
1.67 (H-18)	3.77 (H-19)
3.77 (H-19)	3.39 (H-20)
3.39 (H-20)	1.2 - 1.7 (H-21)
7.18 (H-33)	5.04 (H-34)
5.04 (H-34)	1.44 (H-35)



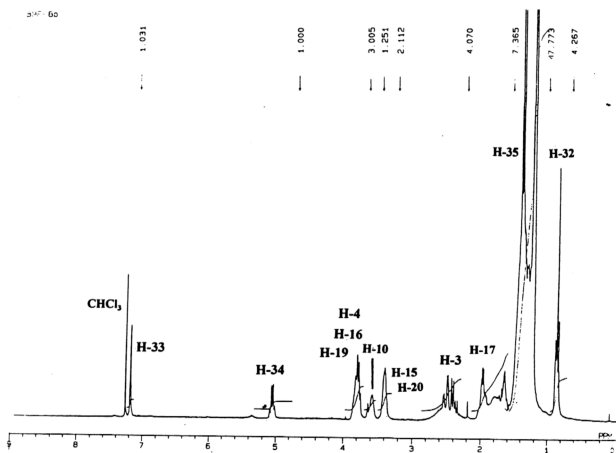
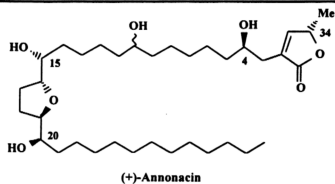


Figure 4. 104: <sup>1</sup>H NMR spectrum of (+)-annonacin (270 MHz, CDCl<sub>3</sub>)

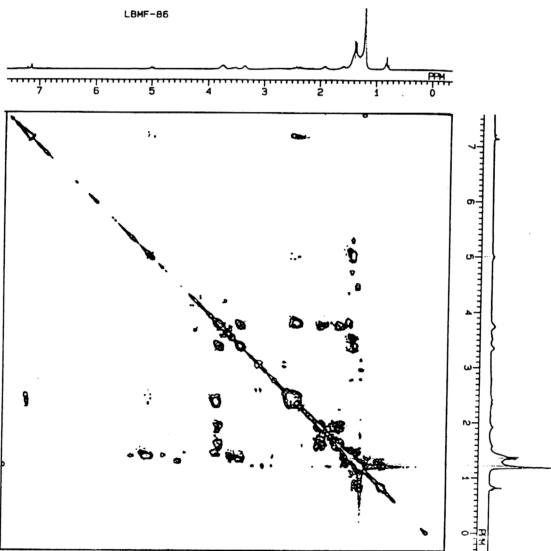
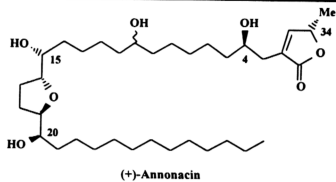
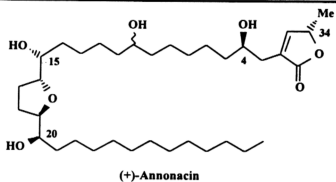


Figure 4. 105:  $^1\text{H}$ - $^1\text{H}$  COSY spectrum of (+)-annonacin



LBMF-86

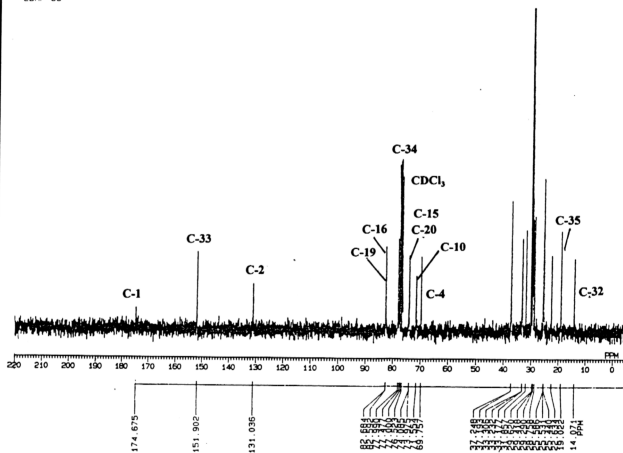
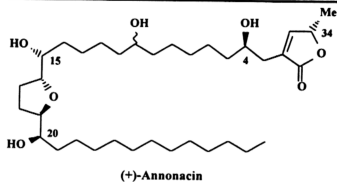


Figure 4. 106:  $^{13}\text{C}$  NMR spectrum of (+)-annonacin (67.8 MHz,  $\text{CDCl}_3$ )



CH, CH<sub>3</sub>--->UP, CH<sub>2</sub>--->DOWN



CH



COM

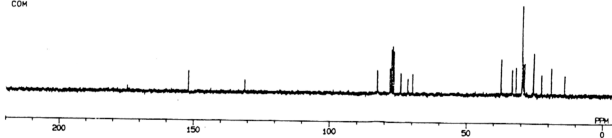


**Figure 4. 107: DEPT spectra of (+)-annonacin**

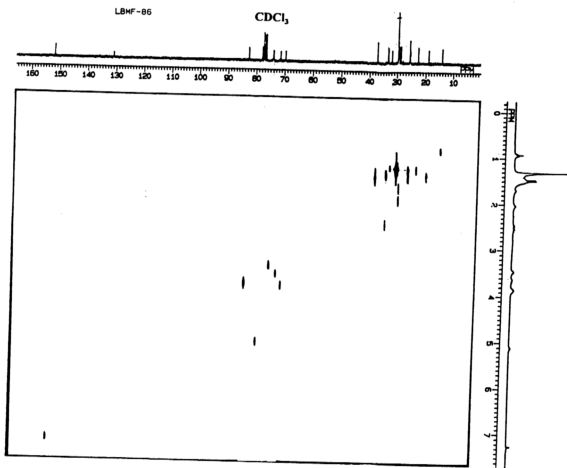
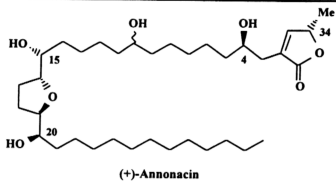
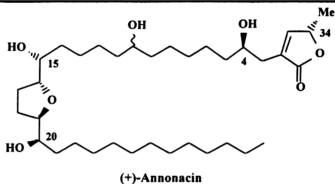


Figure 4. 108:  $^1\text{H}$ - $^{13}\text{C}$  HETCOR spectrum of (+)-annonacin



266





File:001255 Ident:29\_33 Win 1000PPM Acq:23-AUG-1993 11:09:14 +4:13 Cal:082293  
 ZAB-SEQ EI+ Magnet BpM:271 BpI:49299456 TIC:1239640320 Flags:HALL

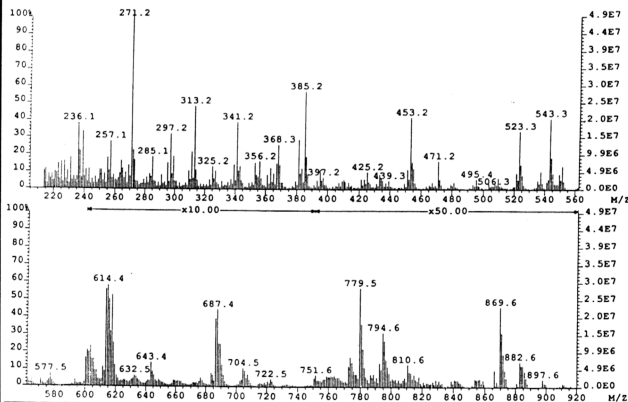


Figure 4. 111: EIMS spectrum of the silylated derivative of (+)-annonacin

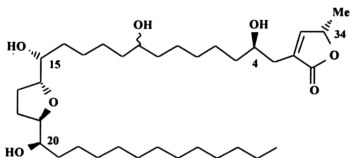


The  $^{13}\text{C}$  NMR and DEPT experiment indicated a total of 35 carbons. The  $^{13}\text{C}$  assignments were carried out using the  $^1\text{H}$ - $^{13}\text{C}$  HETCOR experiment.

(+)-Annonacin was also isolated from the stem bark of *Goniiothalamus malayanus*, *G. velutinus* and *Mezzetia umbellata*.

**Table 4. 61: Structure and  $^1\text{H}$  -  $^{13}\text{C}$  connectivities obtained from  $^1\text{H}$  -  $^{13}\text{C}$  HETCOR experiment for (+)-annonacin**

Proton resonance	Connectivity
2.40 (H-3a)	33.3
3.81 (H-4)	69.8
1.2 - 1.7 (H-5 - H-9)	22.6 - 37.2
3.58 (H-10)	71.6
1.2 - 1.7 (H-11 - H-14)	22.6 - 37.2
3.39 (H-15)	73.9
3.77 (H-16)	82.6
1.97 (H-17)	28.1
1.67 (H-18)	28.7
3.77 (H-19)	82.7
3.39 (H-20)	74.1
1.2 - 1.7 (H-21 - H-31)	22.6 - 37.2
0.85 (H-32)	14.1
7.18 (H-33)	151.9
5.04 (H-34)	77.9
1.44 (H-35)	19.0



**(+)-Annonacin**

Table 4. 62:  $^{13}\text{C}$  NMR ( $\delta$ ) assignments for (+)-annonacin (67.8 MHz,  $\text{CDCl}_3$ )

Carbon	$\delta$
C-1	174.7
C-2	131.0
C-3	33.2
C-4	69.8
C-5 - C-9	22.6 - 37.2
C-10	71.6
C-11 - C-14	22.6 - 37.2
C-15	73.9
C-16	82.6
C-17	28.1
C-18	28.7
C-19	82.7
C-20	74.1
C-21 - C-31	22.6 - 37.2
C-32	14.1
C-33	151.9
C-34	77.9
C-35	19.0

#### 4.2.22 Characterisation of F7 as a new acetogenin, disepalin

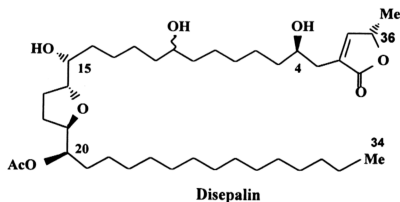


Figure 4. 112: Structure of disepalin

The new acetogenin was isolated as a whitish wax with  $[\alpha]_D +19.6$  (c, 1.0,  $\text{CHCl}_3$ ). CIMS gave an  $\text{MH}^+$  at 667 (4%). Also observed were peaks at 649 ( $\text{MH}^+ - \text{H}_2\text{O}$ ) (4%), 631 ( $\text{MH}^+ - 2\text{H}_2\text{O}$ ) (1%), 613 ( $\text{MH}^+ - 3\text{H}_2\text{O}$ ) (1%), 607 ( $\text{MH}^+ - \text{CH}_3\text{COOH}$ ) (11%), 589 ( $\text{MH}^+ - \text{CH}_3\text{COOH} - \text{H}_2\text{O}$ ) (13%), 571 ( $\text{MH}^+ - \text{CH}_3\text{COOH} - 2\text{H}_2\text{O}$ ) (4%) and 553 ( $\text{MH}^+ - \text{CH}_3\text{COOH} - 3\text{H}_2\text{O}$ ) (1%). This indicates the presence of three hydroxyl and one acetoxy groups and a molecular formula of  $\text{C}_{39}\text{H}_{70}\text{O}_8$ . FAB MS gave the following fragments: 667 ( $\text{MH}^+$ ) (10%), 607 ( $\text{MH}^+ - 60$ ) (21%), 589 ( $\text{MH}^+ - 60 - 18$ ) (13%), 571 ( $\text{MH}^+ - 60 - 2 \times 18$ ) (4%), 397 (12%), 309 (18%), 291 (8%), 279 (7%), 269 (16%), 197 (9%), 179 (8%), 141 (11%), 123 (33%) and 111 (26%). This molecular weight was further confirmed by the FAB which gave a HRMS of 667.5137 (calculated for  $\text{M}+1$  [ $\text{C}_{39}\text{H}_{71}\text{O}_8$ ], 667.5148). The FAB mass spectrometry of the acetyl derivative obtained by reacting the acetogenin with acetic anhydride in pyridine exhibited an  $\text{MH}^+$  of 793 (3%) suggesting a tetraacetate derivative of the original compound. Moreover, fragments 733 ( $\text{MH}^+ - \text{CH}_3\text{COOH}$ ) (35%), 673 ( $\text{MH}^+ - 2\text{CH}_3\text{COOH}$ ) (44%), 613 ( $\text{MH}^+ - 3\text{CH}_3\text{COOH}$ ) (15%) and 553 ( $\text{MH}^+ - 4\text{CH}_3\text{COOH}$ ) (18%) clearly shows the derivative to contain four acetyl groups. The FAB mass spectrometry of the silylated derivative gave an  $\text{MH}^+$  of 823 (883 - 60). This was due to a loss of a molecule of acetic acid ( $\text{CH}_3\text{COOH}$ ) from the silylated molecule. HRMS FAB gave an  $\text{MH}^+$  of 823.6136 (calculated for  $\text{C}_{46}\text{H}_{91}\text{Si}_3\text{O}_6$ , 823.6126). The LRMS FAB for the silylated derivative indicated 3 OTMS group in the molecule. This was obvious from the fragments 733 (823 - 90), 643 (823 -  $2 \times 90$ ) and 553 (823 -  $3 \times 90$ ). The LREIMS of the silylated derivative did not give a recognizable  $\text{M}^+$  but gave a base peak at 73 (100%). Fragments 732 (882

- 60 - 90) (0.2%), 642 (882 - 60 - 2x90) (0.3%) and 552 (882 - 60 - 3x90) (0.8 %) as well as 612 (882 - 3x90) (0.4%) were also observed. These clearly indicated three OTMS to be present in the derivative, hence three hydroxyl groups in the parent molecule. The presence of the  $\alpha,\beta$ -unsaturated  $\gamma$ -lactone ring was obvious from fragment 213 (28%) (fragmentation at C-4 and C-5 bond) and a loss of a molecule of TMSOH (213 - 90) to give the fragment 123 (5%). The fragments 269 (2%) and 197 (3%) which resulted from fragmentations between C-19 and C-20 and between C-20 and C-21 respectively clearly indicated C-20 to contain an acetoxy group. Moreover, the fragment 209 (1%) resulting from the loss of a molecule of acetic acid was also observed. Other fragments observed were: 509 (0.8%), resulting from cleavage of the bond between C-9 and C-10, a loss of TMSOH from it to give the fragment 419 (0.1%) indicating the OH group to be at C-10; 295 (0.6%) resulting from the cleavage of C-10/C-11 bond; 543 (0.4 %) and 339 (0.5%) which resulted from cleavage of the C-15/C-16 bond. A loss of a molecule of acetic acid from the fragment 339 to give fragment 279 (0.4%) is again confirmatory of the position of the acetoxy group at C-20. Other fragments are shown in Figure 4.114. The FAB gave fragment 111 which confirmed the presence of the  $\alpha,\beta$ -unsaturated  $\gamma$ -lactone and a hydroxyl group at C-4. This 4-OH group location was obvious from the fragments 141 and 123 which was a result of the loss of a water molecule. Also detected in the FAB were fragments 309 for cleavage of the C-15/C-16 bond followed by a loss of a water molecule, 291 from the loss of another water molecule and 279 from the loss of a molecule of acetic acid from 339. The other fragments which were observed are 397 and 269 which resulted from the cleavage of the C-19 and C-20 bond. The cleavage of the C-20/C-21 bond

gave the fragment 197 which indicated and confirmed the acetoxy group to be at C-20  
(see Figures 4.113 and 4.114).

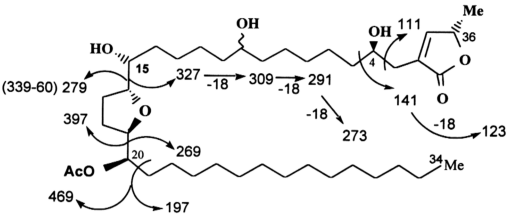


Figure 4. 113: FAB MS of disepalin

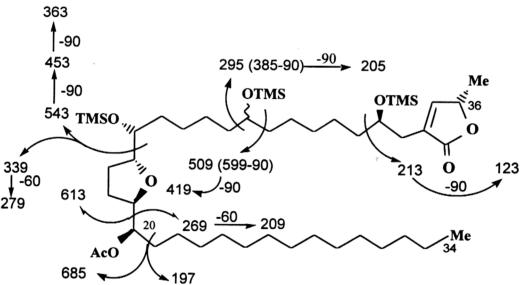
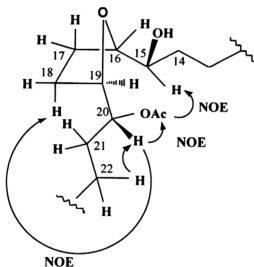


Figure 4. 114: FAB MS and EIMS for the silylated derivative of disepalin

$^1\text{H}$  and  $^{13}\text{C}$  NMR values are consistent with the presence of an  $\alpha,\beta$ -unsaturated  $\gamma$ -lactone ring with a methyl group at C-36, three hydroxyls at C-4, C-10 and C-15 (see Tables 4.63 and 4.66). The positions of these three hydroxyl groups were confirmed by  $^1\text{H}$  NMR values for H-3a and H-3b at  $\delta$  2.40 and  $\delta$  2.51 respectively; for H-4 at  $\delta$  3.82 and for H-10 and H-15 which overlap at  $\delta$  3.40. These values are consistent with those also assigned for annonacin (McCloud *et al.*, 1987) which possesses three hydroxyl groups at C-4, C-10 and C-15. The  $^1\text{H}$ - $^1\text{H}$  COSY experiment further confirmed the presence of the  $\gamma$ -lactone ring (see Table 4.64). The  $\text{CH}_3$  at  $\delta$  1.43 is coupled to the proton at  $\delta$  5.05 and the proton at  $\delta$  7.18. The olefinic proton at  $\delta$  7.18 is in turn coupled to the proton at  $\delta$  5.05 (H-36). The presence of a  $\text{C}=\text{O}$  bond in the  $^{13}\text{C}$  NMR at  $\delta$  174.5 and two signals at  $\delta$  151.8 and  $\delta$  131.0 is indicative of the unsaturated lactone ring.  $^{13}\text{C}$  NMR values for this new compound are similar to those of C-1 to C-15 in annonacin indicating that this portion of the molecule is identical to that of annonacin. The  $^{13}\text{C}$  NMR values for C-4 appears at  $\delta$  70.0, C-10 at  $\delta$  71.6 and C-15 at  $\delta$  74.1. The presence of one THF ring is clearly indicated by two  $^{13}\text{C}$  signals at  $\delta$  82.2 and  $\delta$  83.0 which were assigned to C-16 and C-19 through the  $^1\text{H}$  -  $^{13}\text{C}$  HETCOR experiment. The  $^1\text{H}$  NMR signals for H-16 and H-19 overlap at  $\delta$  3.82 as shown by  $^1\text{H}$ - $^{13}\text{C}$  HETCOR relationship. These chemical shift values are reasonably consistent with those for the THF portion of the known uvaricin. The 3H-singlet of the acetoxy group appeared at  $\delta$  2.07. The  $^1\text{H}$  -  $^{13}\text{C}$  HETCOR correlation indicated the acetoxy group to be bonded to C-20 at  $\delta$

78.0. There is NOE interaction between the acetoxy group at  $\delta$  2.07 and  $\delta$  5.09 (H-20) as well as  $\delta$  3.40 (H-15). There was also an observed NOE enhancement between  $\delta$  5.05 (H-36) and  $\delta$  1.43 (proton of the methyl group at C-37). There was also NOE interaction between protons at  $\delta$  5.09 (H-20) and  $\delta$  1.66 apart from a long range W-coupling of H-20 with one of the H-18 protons. Also observed was an NOE interaction between  $\delta$  5.09 (H-20) and  $\delta$  1.26 -  $\delta$  1.3 (one of the protons at C-22) (see Figures 4.115, 4.120 and 4.121). The HMBC experiment indicated  $^2J$  correlations between H-3 and  $\delta$  131.0 (C-2) and  $\delta$  70.0 (C-4) and  $^3J$  correlations between H-3 and  $\delta$  151.8 (C-35),  $\delta$  174.5 (C-1) and  $\delta$  37.4 (C-5). Meanwhile, there was also observed a  $^3J$  correlation between H-15 and  $\delta$  28.5 (C-17). Other obvious correlations were a  $^2J$  between H-35 and  $\delta$  131.0 (C-2);  $^3J$  between H-35 and  $\delta$  33.3 (C-3);  $^2J$  between H-35 and  $\delta$  78.0 (C-36) and  $^3J$  between H-35 and  $\delta$  174.5 (C-1). Finally, the observation of  $^2J$  correlations between H-36 ( $\delta$  5.05) and  $\delta$  19.1 (C-37) and between  $\delta$  151.8 (C-35) and H-36 were recorded (see Table 4.65 and Figure 4.122).



**Figure 4. 115: NOE enhancements observed for disepalin**

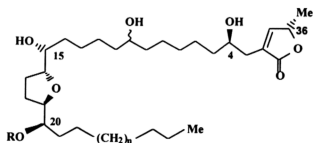
The Hoye and Suhadolnik proton chemical shift correlation methodology was used to propose the relative stereochemistry in the THF part of this compound (Hoye and Suhadolnik, 1987; Hoye and Zhuang, 1988). The diagnostic proton chemical shifts values of F7 were compared with those in the Hoye and Suhadolnik model compounds. The presence of one 3H-singlet at  $\delta$  2.07 for the acetoxy group at C-20 suggests a *threo* relationship for C-19/C-20 (Hoye and Suhadolnik, 1987; Hoye and Zhuang, 1988). Different chemical shifts values for H-15 ( $\delta$  3.40) and H-16 ( $\delta$  3.82) would suggest a *threo* relationship for C-15/C-16 (Fang *et al.*, 1993). The identical chemical shifts values for H-16 and H-19 at  $\delta$  3.95 in the acetylated compound and chemical shift values of  $\delta$  3.82 strongly suggests a *trans* configuration for the THF ring (Cortes *et al.*, 1993) (See Table 4.67). Hence, the relative stereochemistry of the THF part can be described as *threo/trans/threo* going from C-15 to C-20. Hence, the molecule has the configuration of 15*R*, 16*R*, 19*R*, 20*R*, assuming a similar biosynthetic origin as that for (+)-annonacin and uvaricin.

IR ( $\nu_{\max}$   $\text{cm}^{-1}$ ): 3471, 2913, 2840, 1741, 1650, 1463, 1375, 1320, 1195, 1079, 957, 845, 741. UV ( $\lambda_{\max}$ , EtOH, nm): 209 ( $\log \epsilon$  4.18).



**Table 4. 63: Structure and proton NMR spectral data for disepalin (CDCl<sub>3</sub>, 500 MHz) and annonacin (CDCl<sub>3</sub>, 470 MHz) (McCloud *et al.*, 1987)**

Proton	F7 ( $\delta$ )	$J(\text{Hz})$	Annonacin ( $\delta$ )	$J(\text{Hz})$
H-3a	2.40, dd	$J_{3a-4} = 8.3$ $J_{3a-3b} = 14.0$	2.38, dddd	$J_{3a-3b} = 14.0$ $J_{3a-4} = 8.0$ $J_{3a-4OH} = 1.0$ $J_{3a-33} = 0.5$
H-3b	2.51, dd	$J_{3b-4} = 3.4$ $J_{3b-3a} = 14.0$	2.51, dddd	$J_{3b-3a} = 14.0$ $J_{3b-4} = 3.4$ $J_{3b-4OH} = 0.5$ $J_{3b-33} = 0.5$
H-4	3.82, m		3.88, tt	
H-5	1.55, m		1.2 - 1.7	
H-6 - H-9	1.3, m		H-6 -H-9, 1.2-1.7	
H-10	3.40, m		3.56, m	
H-11 - H-14	1.3, m		1.2 - 1.7	
H-15	3.40, m		3.38, dt	$J_{15-16} = 11.6$
H-16	3.82, m		3.77, dt	$J_{14-15} = 5.8$ $J_{15-16} = 11.6$ $J_{16-17} = 6.9$
H-17	1.98, m		1.97, m	
H-18	1.66, m		1.67, m	
H-19	3.82, m		3.77, dt	$J_{19-20} = 11.6$
H-20	5.09, m		3.38, dt	$J_{19-18} = 6.9$ $J_{20-19} = 11.6$ $J_{20-21} = 5.8$
H-21	1.55, m			
H-22 - H-33	1.26 - 1.3, m		H-21-H-31, 1.2-1.7	
H-34	0.88, t	$J_{34-33} = 6.8$	H-32 0.85, t	$J_{31-32} = 7.0$
H-35	7.18, d	$J_{35-36} = 1.5$	H-33 7.16, d	$J_{33-34} = 1.4$
H-36	5.05, dq	$J_{36-37} = 6.8$ $J_{36-35} = 1.5$	H-34 5.04, q	$J_{34-33} = 1.4$ $J_{34-35} = 6.8$
H-37	1.43, d	$J_{37-36} = 6.8$	H-35 1.40, d	$J_{35-34} = 6.6$
OAc	2.07, s			



Disepalin n=9, R=Ac  
Annonacin n=7, R=H

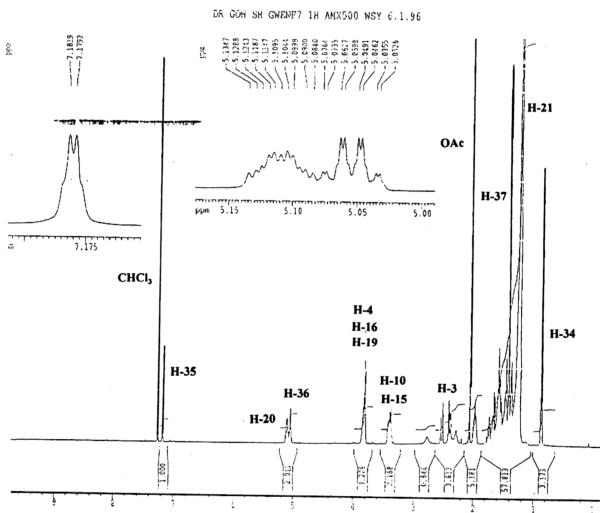
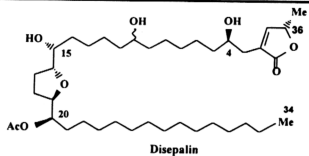
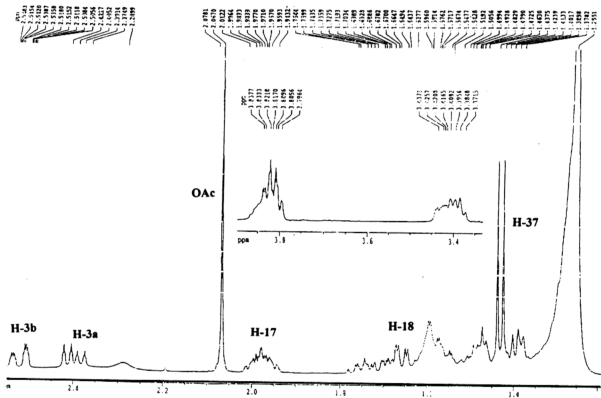
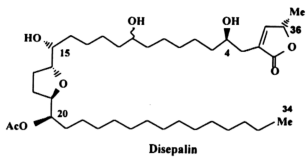


Figure 4. 116:  $^1\text{H}$  NMR spectrum of disepalin (500 MHz,  $\text{CDCl}_3$ )



**Figure 4. 117:  $^1\text{H}$  NMR spectrum of disepalin (500 MHz,  $\text{CDCl}_3$ ) (expanded)**

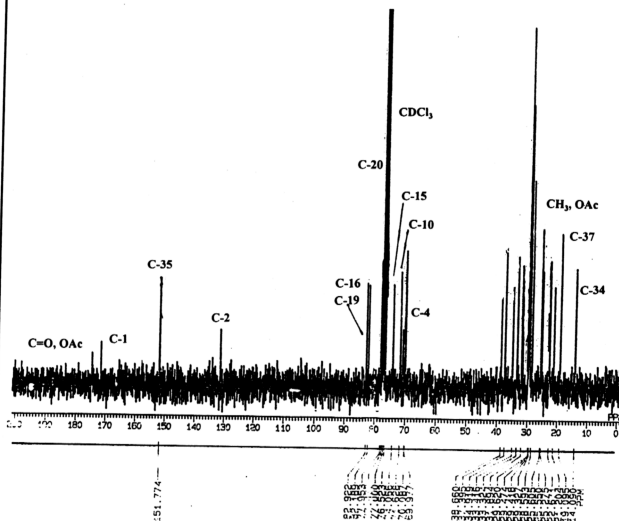
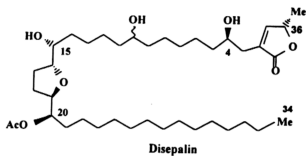
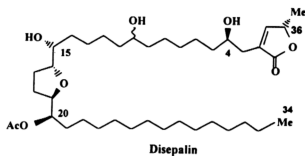


Figure 4. 118:  $^{13}\text{C}$  NMR spectrum of disepalin (67.8 MHz,  $\text{CDCl}_3$ )



DR 60H GNE#7 1H COSYQTP AXI500 WSY HS-32X512 (512X512) WSY 15.2.96

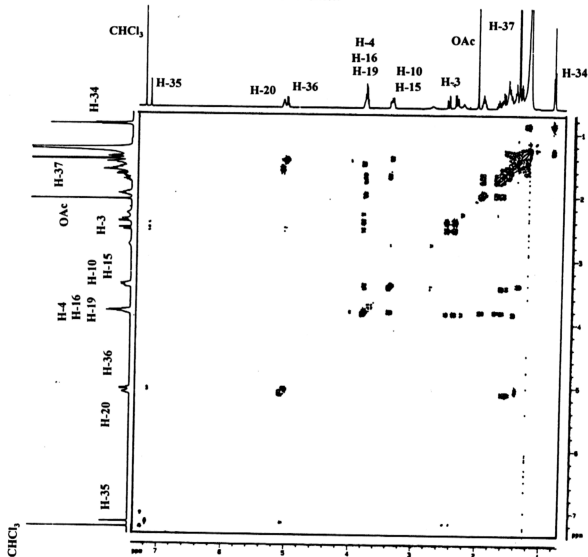


Figure 4. 119:  $^1\text{H}$ - $^1\text{H}$  COSY spectrum of disepalin (500 MHz,  $\text{CDCl}_3$ )

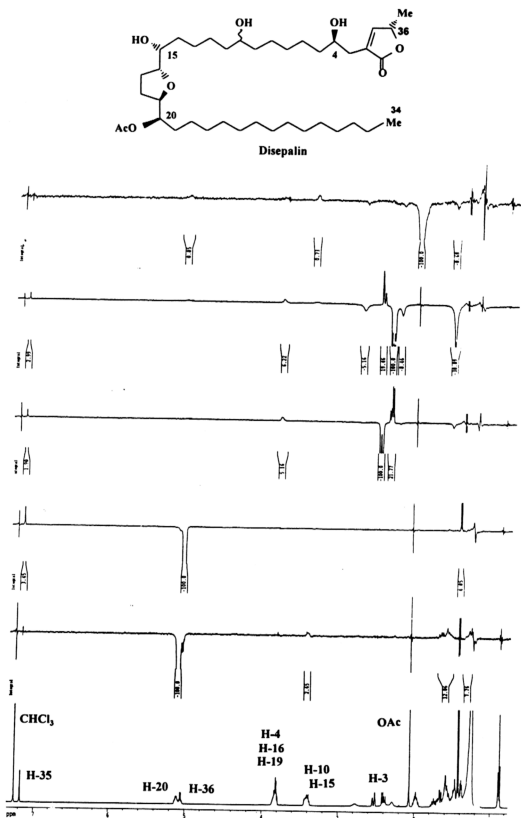


Figure 4. 120: NOE difference spectrum of disepalin

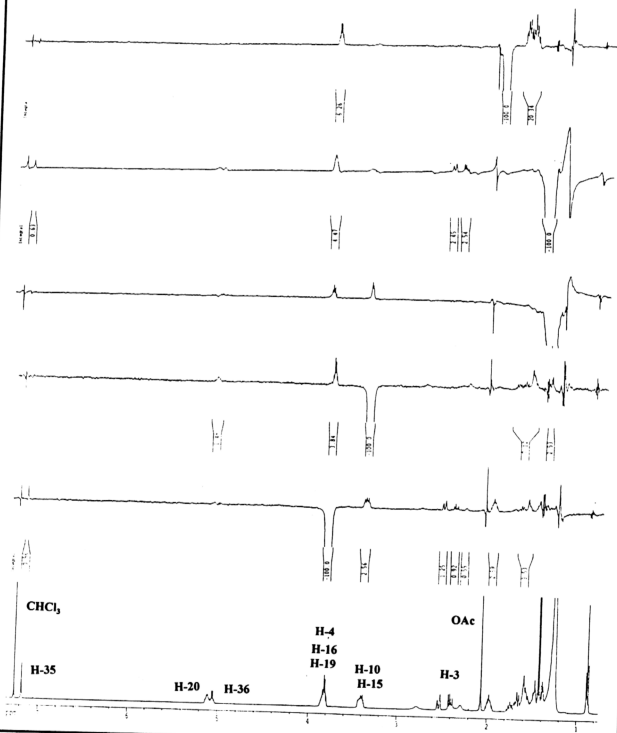
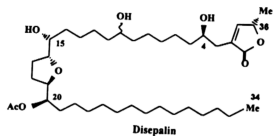


Figure 4. 121: NOE difference spectra of disepalin (500 MHz, CDCl<sub>3</sub>)

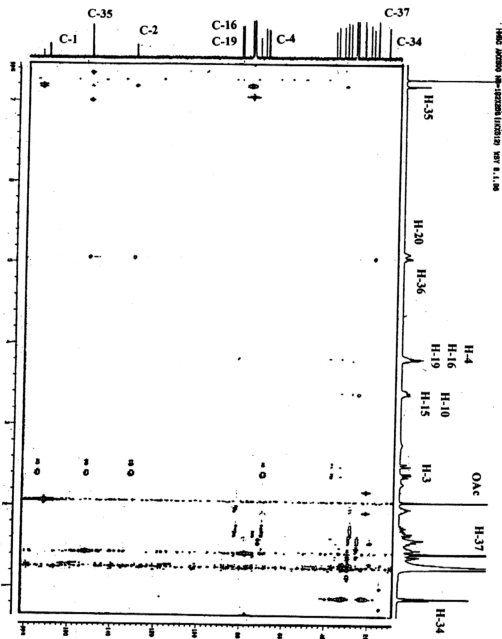
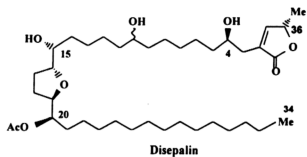
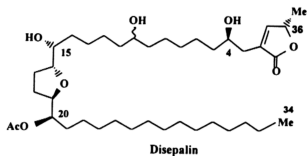
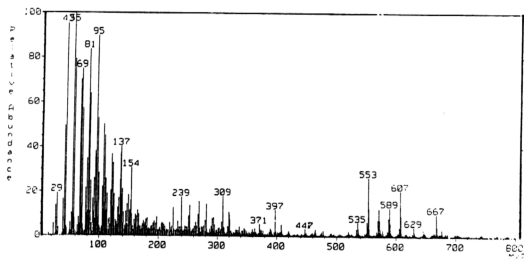


Figure 4. 122: HMBC spectrum of disepalin (500 MHz, CDCl<sub>3</sub>)

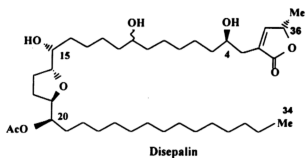




MASS SPECTRUM Data File: CH04727 27-APR-95 13:51  
 Sample: F 7  
 0.000 FAB(Pos.) GC-21474B400.0c BP: m/z 55.0625 Int. 40.0268 Lv 0.00  
 Scan (1)



**Figure 4. 123: FAB MS spectrum of disepalin**



MASS SPECTRUM Data File: CH04730 27-APR-95 15:33  
 Run Date: 27-51  
 Ret. Time: 0.00 FAB(Pos.) GC 0.4c BP: m/z 129.0798 Int. 131.6834 Lv 0.00  
 Scan# (1)

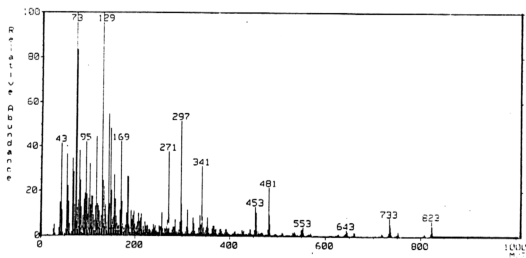


**Figure 4. 124: FAB MS spectrum of the silylated derivative of disepalin**

Table 4. 64: Proton-proton connectivities obtained from <sup>1</sup>H-<sup>1</sup>H COSY experiment for disepalin

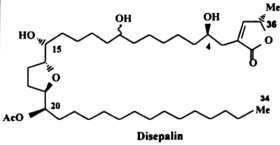
Proton resonance	Connectivity	
2.40 (H-3a)	2.51 (H-3b)	
3.82 (H-4)	3.82 (H-4)	
	2.51 (H-3b)	
	1.55 (H-5)	
3.40 (H-15)	3.82 (H-16)	
3.82 (H-16)	1.98 (H-17)	
1.98 (H-17)	1.66 (H-18)	
1.66 (H-18)	3.82 (H-19)	
3.82 (H-19)	5.09 (H-20)	
5.09 (H-20)	1.55 (H-21)	
5.05 (H-36)	1.43 (H-37)	
5.09 (H-20)	3.82 (H-19), 1.55 (H-21)	

Table 4. 65: Proton and carbon connectivities and their <sup>2</sup>J and <sup>3</sup>J interactions obtained from <sup>1</sup>H - <sup>13</sup>C HETCOR and HMBC experiments for disepalin

Proton resonance	Connectivity	<sup>2</sup> J	<sup>3</sup> J
2.40 (H-3a)	174.5 (C-1) 131.0 (C-2) 33.3 (C-3)	131.0 (C-2) 70.0 (C-4)	151.8 (C-35) 174.5 (C-1) 37.4 (C-5)
3.82 (H-4)	70.0 (C-4)		
1.55 (H-5)	37.4 (C-5)		
1.3 (H-6 - H-9)	22.7 - 38.0 (C-6 - C-9)		
4.40 (H-10)	71.6 (C-10)		
1.3	22.7 - 38.0		
H-11 - H-14)	(C-11 - C-14)		
4.40 (H-15)	74.1 (C-15)		28.5 (C-17)
.82 (H-16)	82.2 (C-16)		
.98 (H-17)	28.5 (C-17)		
.66 (H-18)	34.9 (C-18)		
.82 (H-19)	83.0 (C-19)		
.09 (H-20)	78.0 (C-20)		
.55 (H-21)	37.4 (C-21)		
.26 - 1.3	22.7 - 38.0		
H-22 - H-33)	(C-22 - C-33)		
.88 (H-34)	14.1 (C-34)		
18 (H-35)	151.8 (C-35)	131.0 (C-2) 78.0 (C-36) 151.8 (C-35) 19.1 (C-37)	33.3 (C-3) 174.5 (C-1) 131.0 (C-2)
05 (H-36)	78.0 (C-36)		
43 (H-37)	19.1 (C-37)		
07 (OAc)	171.5 (C=O, OAc) 21.2 (CH <sub>3</sub> , OAc)		

Table 4. 66:  $^{13}\text{C}$  NMR spectral data for disepalin ( $\text{CDCl}_3$ , 67.8 MHz) and annonacin (McCloud *et al.*, 1987)

Carbon	Disepalin	Carbon	Anonacin
C-1	174.5	C-1	174.7
C-2	131.0	C-2	131.1
C-3	33.3	C-3	33.2
C-4	70.0	C-4	69.8
C-5	37.4	C-5 - C-9	22.0 - 38.0
C-6 - C-9	22.7 - 38.0		
C-10	71.6	C-10	71.6
C-11 - C-14	22.7 - 38.0	C-11 - C-14	22.0-38.0
C-15	74.1	C-15	74.0
C-16	82.2	C-16	82.6
C-17	28.5	C-17 - C-18	22.0-38.0
C-18	34.9		
C-19	83.0	C-19	82.7
C-20	78.0	C-20	74.1
C-21	37.4		
C-22 - C-33	22.7 - 38.0	C-21 - C-31	22.0-38.0
C-34	14.1	C-32	14.1
C-35	151.8	C-33	151.8
C-36	78.0	C-34	78.0
C-37	19.1	C-35	19.0
C=O, OAc	171.5		
$\text{CH}_3$ , OAc	21.2		

Table 4. 67: Structure and comparison of  $^1\text{H}$  NMR values of the acetate derivatives of disepalin and annonacin

Compound	$^1\text{H}$			$^{13}\text{C}$ NMR			$^1\text{H}$ NMR of acetate		
Carbon #	15	16	19	15	16	19	15	16	19
Disepalin	3.40	3.82	3.82	74.1	82.2	83.0	4.84	3.95	3.95
Annonacin	3.38	3.77	3.77	74.0	82.6	82.7	4.83	3.94	3.94

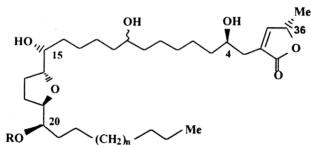
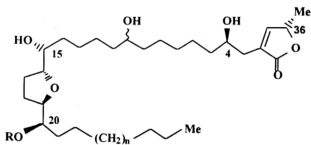


Table 4. 66:  $^{13}\text{C}$  NMR spectral data for disepalin ( $\text{CDCl}_3$ , 67.8 MHz) and annonacin (McCloud *et al.*, 1987)

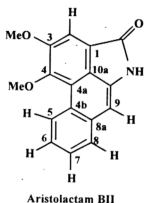
Carbon	Disepalin	Carbon	Anonacin
C-1	174.5	C-1	174.7
C-2	131.0	C-2	131.1
C-3	33.3	C-3	33.2
C-4	70.0	C-4	69.8
C-5	37.4	C-5 - C-9	22.0 - 38.0
C-6 - C-9	22.7 - 38.0		
C-10	71.6	C-10	71.6
C-11 - C-14	22.7 - 38.0	C-11 - C-14	22.0-38.0
C-15	74.1	C-15	74.0
C-16	82.2	C-16	82.6
C-17	28.5	C-17 - C-18	22.0-38.0
C-18	34.9		
C-19	83.0	C-19	82.7
C-20	78.0	C-20	74.1
C-21	37.4		
C-22 - C-33	22.7 - 38.0	C-21 - C-31	22.0-38.0
C-34	14.1	C-32	14.1
C-35	151.8	C-33	151.8
C-36	78.0	C-34	78.0
C-37	19.1	C-35	19.0
C=O, OAc	171.5		
$\text{CH}_3$ , OAc	21.2		

Table 4. 67: Structure and comparison of  $^1\text{H}$  NMR values of the acetate derivatives of disepalin and annonacin

Compound	$^1\text{H}$			$^{13}\text{C}$ NMR			$^1\text{H}$ NMR of acetate		
Carbon #	15	16	19	15	16	19	15	16	19
Disepalin	3.40	3.82	3.82	74.1	82.2	83.0	4.84	3.95	3.95
Annonacin	3.38	3.77	3.77	74.0	82.6	82.7	4.83	3.94	3.94



#### 4.2.23 Characterisation of GM5-7 and GV3b-2 as aristolactam BII



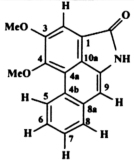
**Figure 4. 125: Structure of aristolactam BII**

GM 5-7 and GV 3b-2 were isolated as yellow solids from the methanol soluble fraction of the ethanol extracts of the stem bark of *Goniothalamus malayanus* and *G. velutinus*, respectively. This solid was insoluble in most organic solvents. After numerous purification via preparative layer chromatography both gave needles of melting point 244-246 °C (Lit 247-250 °C) (Crohare *et al.*, 1974). The EIMS gave an  $M^+$  of 279 and the FAB gave an  $M+1$  of 280. This implied a molecular formula of  $C_{17}H_{13}NO_3$ . These two compounds were concluded to be similar from their NMR spectra and to be aristolactam BII.

The  $^1H$  NMR (270 MHz,  $CDCl_3$ ) indicated two methoxy groups ( $^1H/^{13}C$  peaks at  $\delta$  4.07/56.3 and  $\delta$  4.13/60.3) which are located at C-3 ( $\delta$  154.5) and C-4 ( $\delta$  152.0), respectively. A broad singlet at  $\delta$  8.20 was assigned to the proton attached to the nitrogen. Two other singlets at  $\delta$  7.10 and  $\delta$  7.80 consisting of one proton each were assigned to H-9 and H-2 respectively. The very downfield doublet of doublet signal at  $\delta$  9.24 ( $J = 1.1$  Hz, 9.8 Hz) was assigned to H-5. A single- proton broad doublet at

$\delta$  7.81 ( $J = 9.8$  Hz) was assigned to H-8. Finally, a two proton multiplet at  $\delta$  7.57 was assigned to H-7 and H-8. These assignments were deduced from the  $^1\text{H} - ^1\text{H}$  COSY experiment (Table 4.69 and Figure 4.127). The  $^1\text{H}$  NMR values are shown in Table 4.68 (see also Figure 4.126).

**Table 4. 68:**  $^1\text{H}$  NMR assignments ( $\delta$ ) and  $J$  values (Hz) for aristolactam BII (270 MHz,  $\text{CDCl}_3$ )

Proton	$\delta$	$J(\text{Hz})$	 Aristolactam BII
H-2	7.80, s	-	
H-5	9.24, dd	9.8, 1.1	
H-6	7.57, m	-	
H-7	7.57, m	-	
H-8	7.81, brd	9.8	
H-9	7.10, s	-	
OMe-3	4.07, s	-	
OMe-4	4.13, s	-	
N-H	8.20, s	-	

**Table 4. 69:**  $^1\text{H} - ^1\text{H}$  connectivities obtained from  $^1\text{H} - ^1\text{H}$  COSY experiment for aristolactam BII

Proton resonance	Connectivity
9.24 (H-5)	7.57 (H-6) 7.57 (H-7)
7.57 (H-6)	9.24 (H-5) 7.81 (H-8)
7.57 (H-7)	7.81 (H-8) 9.24 (H-5)
7.81 (H-8)	7.57 (H-7) 7.57 (H-6)

The  $^{13}\text{C}$  NMR spectrum indicated a total of seventeen carbons (Figure 4.128).

DEPT experiment indicated six CH groups, two methoxy groups, one carbonyl group and six quaternary carbons. The  $^{13}\text{C}$  assignments are in agreement with the literature values (Crohare *et al.*, 1974.) (see Table 4.71).

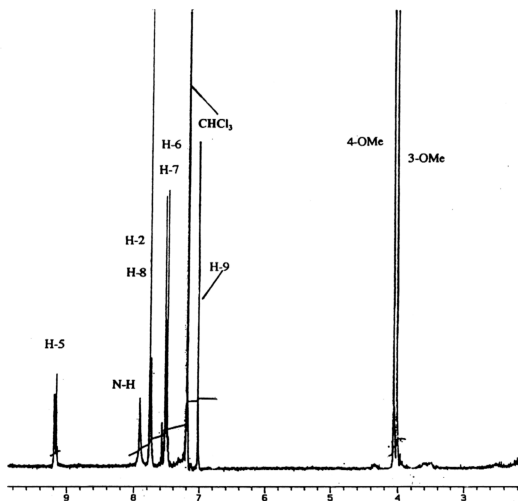
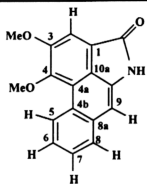
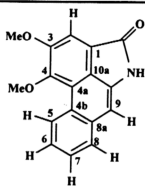


Figure 4. 126:  $^1\text{H}$  NMR spectrum of aristolactam BII (270 MHz,  $\text{CDCl}_3$ )





Aristolactam BII

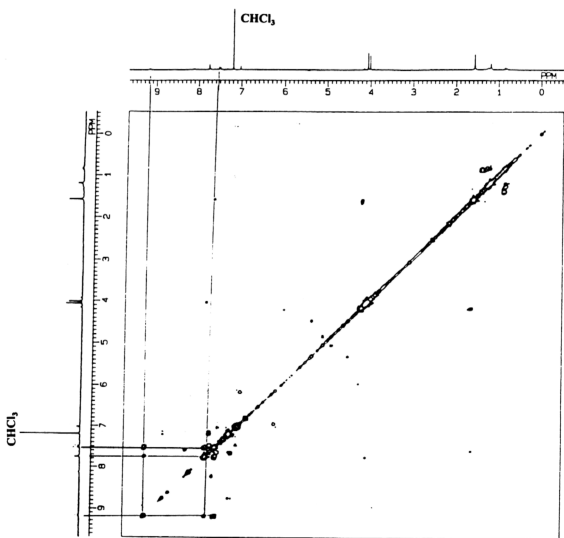


Figure 4. 127:  $^1\text{H}$ - $^1\text{H}$  COSY spectrum of aristolactam BII

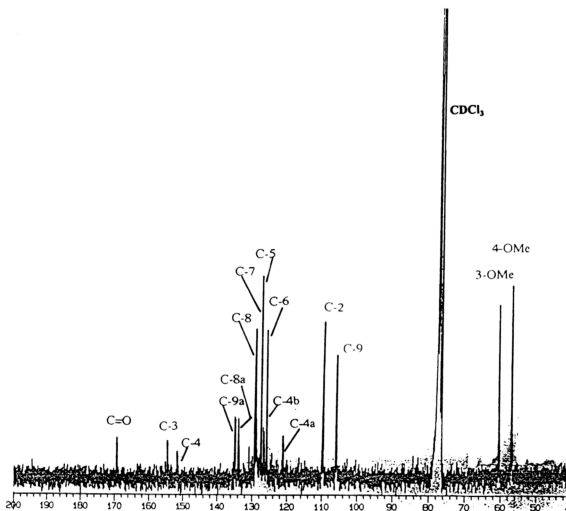
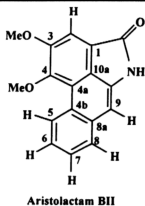
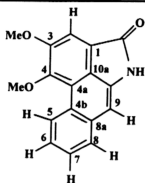


Figure 4. 128:  $^{13}\text{C}$  NMR spectrum of aristolactam BII (67.8 MHz,  $\text{CDCl}_3$ )



Aristolactam BII

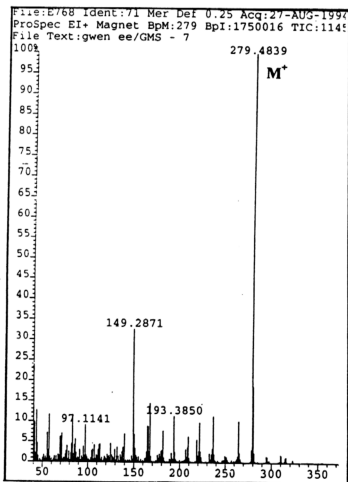
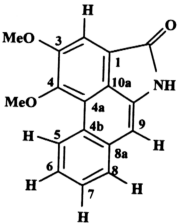


Figure 4. 129: EIMS spectrum of aristolactam BII

**Table 4. 70:  $^1\text{H}$  -  $^{13}\text{C}$  connectivities obtained from  $^1\text{H}$  -  $^{13}\text{C}$  HETCOR experiment for aristolactam BII**

Proton resonance	Connectivity
7.80 (H-2)	109.5
9.24 (H-5)	127.6
7.57 (H-6)	126.0
7.57 (H-7)	127.6
7.81 (H-8)	129.0
4.07 (OMe-3)	56.9
4.13 (OMe-4)	60.3
7.10 (H-9)	105.7

**Table 4. 71:  $^{13}\text{C}$  NMR ( $\delta$ ) assignments for aristolactam BII (67.8 MHz,  $\text{CDCl}_3$ )**

Carbon	$\delta$ ( $\text{CDCl}_3$ )	 <p><b>Aristolactam BII</b></p>
C-1	124.0	
C-2	109.5	
C-3	154.3	
C-4	152.0	
C-4a	121.1	
C-4b	127.0	
C-5	127.6	
C-6	126.0	
C-7	127.6	
C-8	129.0	
C-8a	133.9	
C-9	105.7	
C-10	134.7	
C-10a	121.0	
C=O	170.0	
OMe-3	56.9	
OMe-4	60.3	

#### 4.2.24 Characterisation of LS13-4y-13 as liriodenine

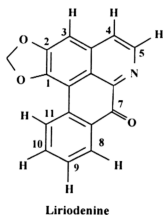


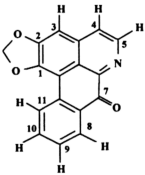
**Figure 4. 130: Structure of liriodenine**

The methanol soluble fraction of the ethanol extract of the stem bark of *Disepalum anomalum* after multiple separations via preparative layer chromatography gave a minor amount of a yellow compound. This compound crystallised as yellow needles from chloroform, m.p. 277-279 °C (Lit. 278-280 °C) (Yang and Chen, 1979). EIMS gave an  $M^+$  of 275 suggesting the molecular formula  $C_{17}H_9O_3N$ . From the  $^1H$  and  $^{13}C$  NMR spectra of LS13-4y-13, it was concluded that the compound was liriodenine.

The  $^1H$  NMR (270 MHz,  $CDCl_3$ ) indicated the presence of an  $O-CH_2-O$  group in the molecule. This was assigned to C-1 and C-2. A pair of doublets at  $\delta$  7.78 and  $\delta$  8.89 with a coupling constant value of 5.4 Hz is typical of the pair of protons at the C-4 and C-5 positions of oxoaporphine. Hence the pair of doublets was assigned to C-4 and C-5, respectively. A singlet at  $\delta$  7.20 was assigned to H-3. A doublet at  $\delta$  8.59 with a coupling constant value of 8.8 Hz was assigned to H-8 while the other

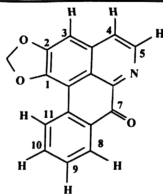
doublet at  $\delta$  8.66 with a coupling constant value of 8.8 Hz was assigned to H-11. A triplet at  $\delta$  7.78 with a coupling constant value of 8.8 Hz was assigned to H-9 while another triplet at  $\delta$  7.58 with a coupling constant value of 8.8 Hz was assigned to H-10. These proton assignments were made based on the  $^1\text{H}$ - $^1\text{H}$  COSY spectrum. The  $^1\text{H}$  NMR values are listed in Table 4.72 (see Figure 4.131).

**Table 4. 72:**  $^1\text{H}$  NMR ( $\delta$ ) assignments and  $J(\text{Hz})$  values for liriodenine (270 MHz,  $\text{CDCl}_3$ )

Proton	$\delta$	$J(\text{Hz})$	 <p>Liriodenine</p>
H-3	7.20, s	-	
H-4	7.78, d	5.4	
H-5	8.89, d	5.4	
H-8	8.59, d	8.8	
H-9	7.78, t	8.8	
H-10	7.58, t	8.8	
H-11	8.66, d	8.8	

**Table 4. 73:**  $^1\text{H}$  -  $^1\text{H}$  connectivities ( $^1\text{H}$  -  $^1\text{H}$  COSY) for liriodenine

Proton resonance	Connectivity
7.78 (H-4)	8.89 (H-5)
8.89 (H-5)	7.78 (H-4)
8.59 (H-8)	7.78 (H-9)
7.78 (H-9)	8.59 (H-8)
	7.58 (H-10)
7.58 (H-10)	7.78 (H-9)
	8.66 (H-11)
8.66 (H-11)	7.58 (H-10)



Liriodenine

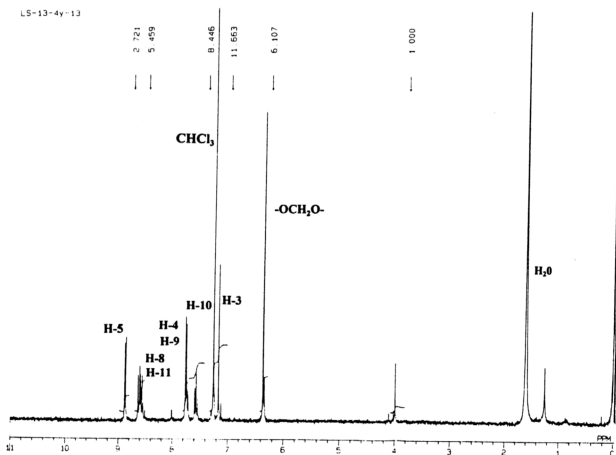
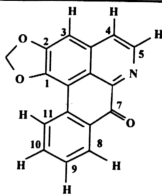


Figure 4. 131: <sup>1</sup>H NMR spectrum of liriodenine (270 MHz, CDCl<sub>3</sub>)



Liriodenine

LS-13L4Y-13

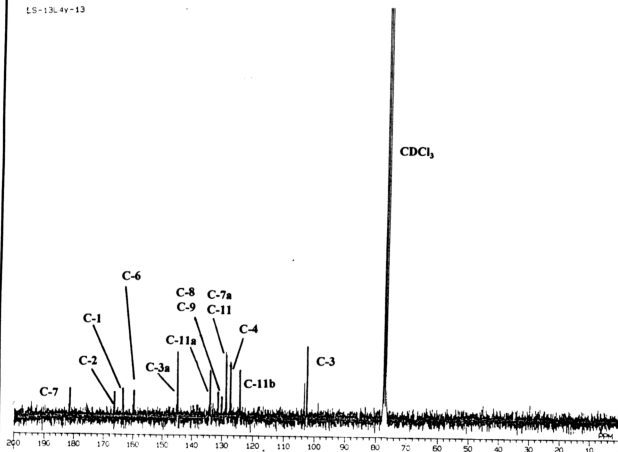
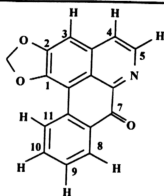


Figure 4.  $^{13}\text{C}$  NMR spectrum of liriodenine (67.8 MHz,  $\text{CDCl}_3$ )





Liriodenine

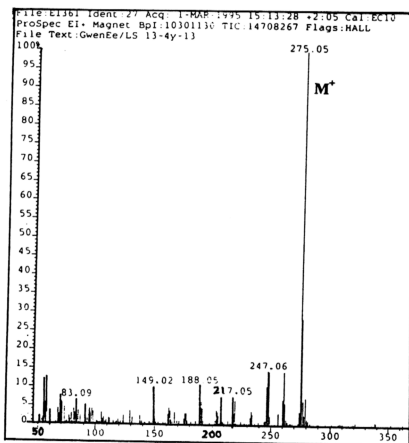
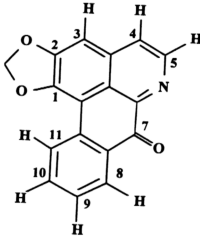


Figure 4. 133: EIMS spectrum of liriodenine

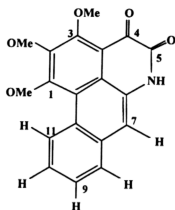
The  $^{13}\text{C}$  NMR assignments were made by comparing with literature values (Guinaudeau *et al.*, 1983). The  $^{13}\text{C}$  NMR values are shown in Table 4.74.

**Table 4. 74:**  $^{13}\text{C}$  NMR ( $\delta$ ) assignments for liriodenine (67.8 MHz,  $\text{CDCl}_3$ )

Carbon	$\delta$	
C-1	163.0	 <p style="text-align: center;"><b>Liriodenine</b></p>
C-2	167.0	
C-3	103.2	
C-4	127.3	
C-5	140.5	
C-6	160.5	
C-7	182.0	
C-7a	128.6	
C-8	131.3	
C-9	132.8	
C-10	135.7	
C-11	128.8	
C-11a	135.7	
C-11b	124.2	
C-6a	139.5	
C-3a	144.9	

#### 4.2.25 Characterisation of GV26SF2 and GMf as ouregidione

Fraction 26 from the  $\text{SiO}_2$  column chromatography of the methanol soluble fraction of *Goniothalamus velutinus* bark extract gave a mixture of (+)-annonacin and GV26SF2. The latter crystallised from chloroform as orange needles. This compound was characterised and identified as ouregidione from 1-D and 2-D NMR spectra. The same compound was isolated from the bark extract of *Goniothalamus malayanus*.



Ouregidione

Figure 4. 134: Structure of ouregidione

Ouregidione, insoluble in most common organic solvents crystallised as fine orange needles (from chloroform) which immediately turned red and opaque upon removal from the mother liquor. The crystals melted at 274-276 (Lit. > 280 °C) (Cortes *et al.*, 1968). The EIMS gave an  $M^+$  of 337 indicating a molecular formula of  $C_{19}H_{15}NO$ . Other peaks observed in the EIMS were 336 (25%), 309 (75%) and 281 (7%). The IR ( $CHCl_3$ ) spectrum showed peaks at 3019, 1211, 773, 672 and 477  $cm^{-1}$  and the UV (EtOH) spectrum showed peaks at 211, 241, 305 and 417 nm. The  $^1H$  NMR (270 MHz,  $CDCl_3$ ) gave three methoxy signals at  $\delta$  4.10,  $\delta$  4.17 and  $\delta$  4.21. By comparing with reported compounds, it is possible to assign the methoxy signals. OMe-1 signal always appears at a higher field than OMe-2 signal (Achenbach *et al.*, 1991). Hence, the signal at  $\delta$  4.10 was assigned to OMe-1,  $\delta$  4.17 to OMe-2 and  $\delta$  4.21 to OMe-3. Again, from the literature, it is known that among the four hydrogens in ring D, H-11 is always most shielded and has a very low field chemical shift value. Hence the signal at  $\delta$  9.51 which is a dd with  $J$  values of 9.0 and 2.0 Hz was assigned to H-11. Other observed signals were two singlets at  $\delta$  11.75 (broad singlet) and  $\delta$

7.70. The very downfield broad singlet at  $\delta$  11.75 was assigned to the hydrogen attached to the nitrogen. The other singlet at  $\delta$  7.70 was assigned to H-7. There is NOE interaction between the singlet signal at  $\delta$  7.70 and the broad singlet at  $\delta$  11.75 (N-H), hence implying the proton to be at C-7 and not C-3 (see Figure 4.138). Again from the literature, among the three protons H-8, H-9 and H-10, H-8 always appears at the lowest field (Achenbach *et al.*, 1991). Hence, the doublet of doublet at  $\delta$  7.90 with  $J$  values of 9.0 and 2.0 Hz, the latter coupling was due to H-8, while the two protons at  $\delta$  7.66 (ddd) with  $J$  values of 9.0, 9.0 and 2.0 Hz were assigned to H-9 and H-10. The  $^1\text{H}$  NMR values are shown in Table 4.75 (see also Figure 4.135).

**Table 4. 75: Structure and  $^1\text{H}$  NMR ( $\delta$ ) assignments and  $J(\text{Hz})$  values for ouregidione in different solvents (270 MHz)**

Proton	$\text{CDCl}_3$	$\text{CF}_3\text{COOD}$	$\text{C}_5\text{D}_5\text{N}$
OMe-1	4.10, s	4.20, s	4.03, s
OMe-2	4.17, s	4.59, s	4.16, s
OMe-3	4.21, s	4.61, s	4.20, s
N-H	11.75, br s	-	-
H-7	7.70, s	8.29, s	7.89, s
H-8	7.90, dd (9.0, 2.0)	8.14, br d (9.0)	8.03, dd (7.0, 2.0)
H-9	7.66, ddd (9.0, 9.0, 2.0)	7.86 td (9.0, 2.0)	7.72, ddd (7.0, 7.0, 2.0)
H-10	7.66, ddd (9.0, 9.0, 2.0)	7.95 td (9.0, 2.0)	7.71 ddd (7.0, 7.0, 2.0)
H-11	9.51, dd (9.0, 2.0)	9.57 br d (9.0)	9.70 br d (7.0)

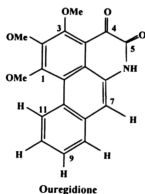


**Table 4. 76:  $^1\text{H}$  -  $^1\text{H}$  connectivities obtained from  $^1\text{H}$  -  $^1\text{H}$  COSY experiment for ouregidione**

Proton resonance	Connectivity
7.90 (H-8)	7.66 (LR) (H-10), 7.66 (H-9)
7.66 (H-9)	7.90 (H-8), 7.66 (H-10), 9.51 (LR) (H-11)
7.66 (H-10)	7.66 (H-9), 9.51 (H-11), 7.90 (LR) (H-8)
9.51 (H-11)	7.66 (H-10), 7.66 (LR) (H-9)

LR refers to long range coupling.

The  $^{13}\text{C}$  NMR spectrum showed a total of 19 carbons. Two carbonyl signals appeared at  $\delta$  175.4 and 157.6. These two signals are typical for the C-4 and C-5 carbonyl carbons of the 4,5-dioxoaporphine. Three OMe signals appeared at  $\delta$  147.5, 159.0 and 160.5. The HMBC experiment showed the  $^2\text{J}$  correlation between the  $\delta$  4.10 - OMe signal with  $\delta$  147.5, the  $\delta$  4.17-OMe signal with  $\delta$  159.0 and the  $\delta$  4.21-OMe signal with  $\delta$  160.5. Hence,  $\delta$  147.5 was assigned to C-1,  $\delta$  159.0 to C-2 and  $\delta$  160.5 to C-3. The HMQC experiment showed the correlation between the singlet at  $\delta$  7.70 and  $\delta$  116.0, hence  $\delta$  116.0 was assigned to C-7.  $^{13}\text{C}$  NMR values are shown in Table 4.78. Other HMQC correlations are between the proton at  $\delta$  9.51 (H-11) and  $\delta$  127.3 and between the proton at  $\delta$  7.90 (H-8) and  $\delta$  128.3. Hence, the peak  $\delta$  127.3 was assigned to C-11 and  $\delta$  128.3 to C-8. HMQC also showed correlations between the protons at  $\delta$  7.66 (H-9 and H-10) and  $\delta$  127.3 and  $\delta$  127.5. Hence, these two carbon chemical shift values were assigned to C-9 and C-10, respectively. HMBC was used to assign the quaternary carbons. HMBC showed correlations ( $^3\text{J}$ ) between the NH proton and  $\delta$  120.3 and between the proton at  $\delta$  7.7 (H-7) and  $\delta$  120.3. Hence,  $\delta$  120.3 was assigned to carbon C-11c. There is  $^2\text{J}$  correlation between the  $\delta$  127.6-C and  $\delta$  9.51-H and a  $^3\text{J}$  correlation between the  $\delta$  9.51- proton and  $\delta$  121.3-C. Hence  $\delta$

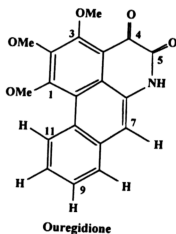
and  $\delta$  9.51-H and a  $^3J$  correlation between the  $\delta$  9.51- proton and  $\delta$  121.3-C. Hence  $\delta$  127.6 and  $\delta$  121.3 were assigned to carbons C-11a and C-11b respectively. HMBC also gave a  $^2J$  correlation between the OMe-3 signal ( $\delta$  4.21) and  $\delta$  128.5. Hence  $\delta$  128.5 was assigned to C-3a (see Table 4.77).

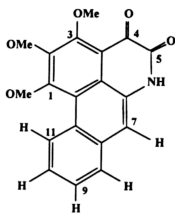
**Table 4. 77: Proton and carbon connectivities and their  $^2J$  and  $^3J$  interactions obtained from HMQC and HMBC experiments for ouregidione(CDCl<sub>3</sub>, 270 MHz and 67.8 MHz)**

Proton resonance	Connectivity	$^2J$	$^3J$
4.10 (OMe-1)	61.8	128.5	147.5
4.17 (OMe-2)	61.2		159.0
4.12 (OMe-3)	62.1		160.5
7.70 (H-7)	116.0		120.3
7.90 (H-8)	128.3		
7.66 (H-9)	127.3		
7.66 (H-10)	127.5	127.6	
9.51 (H-11)	127.3		121.3
11.75 (N-H)			120.3

**Table 4. 78:  $^{13}C$  NMR ( $\delta$ ) assignments for ouregidione**

Carbon	CDCl <sub>3</sub>	Pyridine-d <sub>5</sub>
C-1	147.5	147.9
C-2	159.0	158.4
C-3	160.5	159.9
C-3a	128.5	123.0
C-4	175.4	176.8
C-5	157.6	157.2
C-6a	131.7	131.3
C-7	116.0	114.3
C-7a	131.7	132.8
C-8	128.3	128.7
C-9	127.3	127.8
C-10	127.5	127.2
C-11	127.3	127.8
C-11a	127.6	127.2
C-11b	121.3	122.0
C-11c	120.3	119.0
OMe-1	61.8	61.2
OMe-2	61.2	61.8
OMe-3	62.1	62.0





Ouregidione

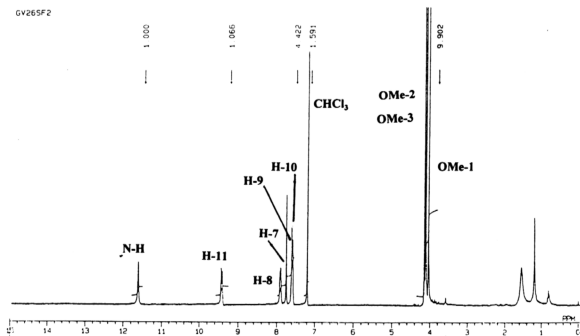
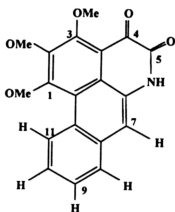


Figure 4. 135:  $^1\text{H}$  NMR spectrum of ouregidione (270 MHz,  $\text{CDCl}_3$ )



Ouregidione

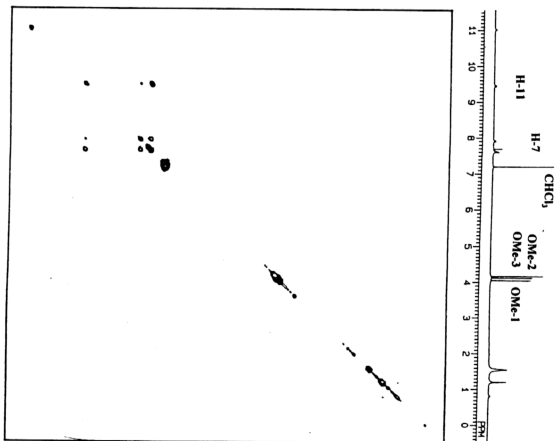
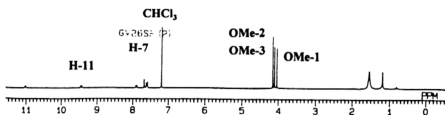
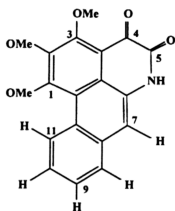


Figure 4. 136:  $^1\text{H}$ - $^1\text{H}$  COSY spectrum of ouregidione





Ouregidione

GV26SF (2)

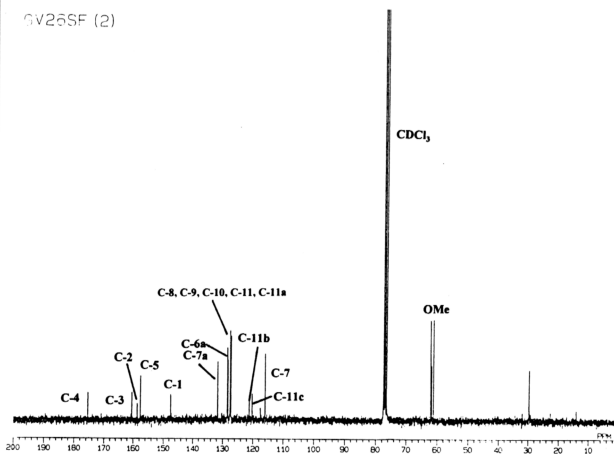


Figure 4. 137:  $^{13}\text{C}$  NMR spectrum of ouregidione (67.8 MHz,  $\text{CDCl}_3$ )

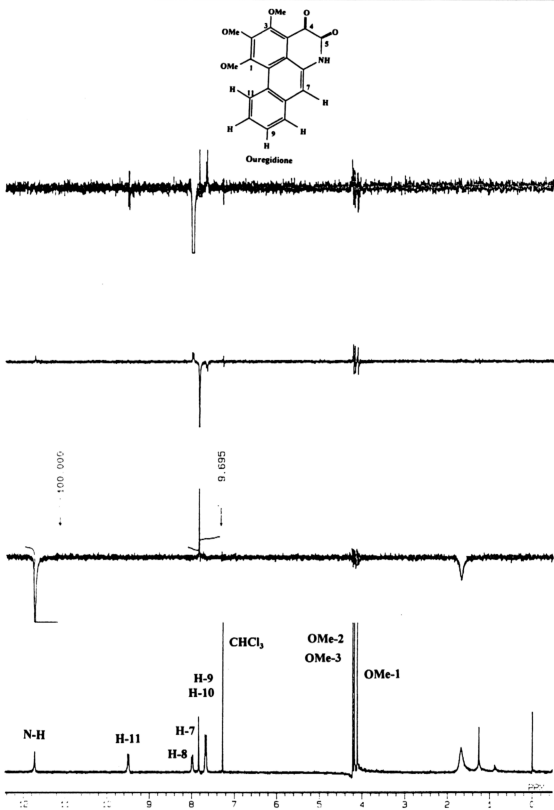
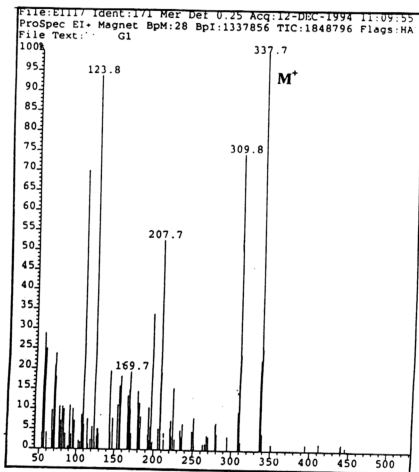
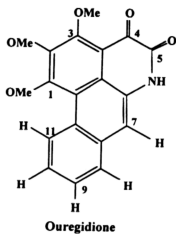


Figure 4. 138: NOE difference experiments for ouregidione



**Figure 4. 139: EIMS spectrum of ouregidione**